STUDIES RELATED TO THE EVOLUTION OF THE LUNAR SOIL MATERIALS

J. L. Carter

Principal Investigator

The University of Texas at Dallas

P. O. Box 30365

Dallas, Texas 75230

(A/C 214) 231-1471

Progress Report

31 July 1973

Sponsored by

National Aeronautics and Space Administration

Grant No.: NGR 44-004-116, Suppl. #2

The attached five reprints (1-5), four papers in press (6-9) and two abstracts (10-11) cover the areas of research completed and some of those that are in progress. Completed projects using scanning electron microscope, electron microprobe and energy dispersive x-ray techniques include a study that involved the chemistry and surface morphology of six glass spheres and five glass-bonded agglutinates from Luna 20 LRL sample 22003 (1). The presence of fragments of plagioclase in the centers of some of the impact features and the non-random distribution and nature of the craters suggest that most of the glass spheres were probably derived locally by meteoritic impact processes and that most craters on their surfaces may have occurred from impacts of relatively high velocity particles in the impact debris cloud while the glass sphere was at elevated temperatures. Fragments of $CaCO_3$ were found on the surfaces of two spheres, and masses of chlorides rich in Ca, Al, Fe and K (first time reported on the moon) were observed on two other spheres. The $CaCO_3$ and complex chlorides may be the result of lunar volcanism or fusion of components of carbonaceous chondrites.

A second completed project involved the discovery of proposed VLS (Vapor-Liquid-Solid)-type whisker growth of metallic iron needles on the surface of breccia 15015,36 (5, 6, 9, 11) which is the first documentation of this process occurring in nature, and provides a growth mechanism which could have been significant in the early accretionary history of the Earth. Since the metallic iron needles are either signle domain or pseudo-single domain due to shape anisotropy, they may affect strongly the magnetic properties of rock 15015, and contribute to its hard magnetic component. Soil breccias containing these needles could have a large magnetically hard component.

A study of Apollo 16 samples from the less than 1 mm fines 68841,11 (light-colored ray ejecta) and 69941,13 (dark-colored ejecta) from South Ray Crater focussed on some unusual types of metallic particles and silicate spheres with textured surfaces. The metallic particles consist of two types: rounded forms with euhedral crystals of schreibersite intergrown with metallic iron FeS and chemically defined bornite (first time reported occurring on the moon)., and irregularly-shaped forms with low contents of schreibersite intergrown with plagioclase laths and olivine, and also containing well-developed crystals of hydrated iron oxide, possibly lepidocrocite, on their surfaces. It was suggested that this material formed in a hot impact ejecta blanket or in an igneous environment and later exposed by meteoritic impact. The silicate spheres with textured surfaces consist of interlocking plagioclase laths, that formed during quenching of melts of essentially highland basalt composition, and have attached spherules and hemispheres of the same composition as the host sphere on their surfaces. The original melt could be either impact-produced or volcanic in origin. The volcanic hypothesis is favored because of homogeneity in composition between spheres, general lack of surface debris and shocked debris, and the lack of metallic iron of meteoritic composition.

A study of the morphology and chemistry of particles from Apollo 17 less than 1 mm fines 74220, 74241 and 75081 (4) suggested that particles from these fines formed in a cloud of siliceous vapors. A volcanic origin similar to a volcanic fire fountain on earth is favored because of the lack of shocked material and complex flow structures, the low content of metallic iron of meteoritic composition, the complex chemical zoning on a micron scale in the minerals and the composite silicate glass forms with low velocity-type impact features and less than 0.1 micron in diameter spherules on their surfaces.

The lack of hypervelocity-type impacts and the old age of the orange fines (74220) suggest that it was laid down, rapidly covered, and more recently exposed. Material from the dark mantle fines (75081), in contrast, has numerous impact-produced craters primarily less than 1 micron in diameter on their surfaces which suggests that sample 75081 was exposed for a longer period to micrometeoritic bombardment or that it has been in the high velocity portion of an impact-produced debris cloud. The presence of highly vesicular particles generally less than 150 microns in diameter suggest that one component of the dark mantle could be pyroclastic in nature. A particle consisting of a core containing only Ca and S surrounded by a zone consisting of only K and S (first time reported on the moon), as shown by energy dispersive techniques, is present on one of the composite glass spheres. The origin of this material is unknown.

A study of silicate mineral chemistry of the less than 1 mm size fraction of Apollo fines 15501, 15411, 66081 and 69941 was completed (3,8). The fine fraction of sample 15411 consists primarily of gabbroic-anorthosite components, whereas the fine fraction of sample 15501 consists primarily of mare-type basaltic components. From these data it was suggested that downslope transport under the influence of gravity or electrostatic effects may be more important at least locally than transport of fine particles of meteoritic impact phenomena. The Apollo 16 fine fraction of sample 66081 shows only ANT components whereas the fine fraction of sample 69941 from South Ray Crater has a major ANT component together with a possible minor KREEP and ultramafic component.

Scanning electron microscope and electron microprobe studies involving the use of montages of glass sphere fragment 65016.6, which contains large metallic iron mounds with laths of schreibersite, reveals a lack of impact

features and the presence of silicate mounds admixed with the metallic mounds. This is similar to metallic mounds formed by reduction with hydrogen. Also present in the metallic mounds are patches consisting primarily of aluminum as shown by energy dispersive techniques. This type of relationship has not been reported previously on lunar materials. If these patches are metallic aluminum, it is significant in that it means a much lower oxygen fugacity for the formation of these metallic mounds than for mounds consisting only of metallic iron. The exact nature of these mounds is being studied. Morphological and chemical studies of selected particles of other Apollo 17 less than 1 mm fines are in progress using the approach of first rapidly scanning large numbers of fragments for purposes of cataloguing, then selecting those which merit further detailed scanning, energy dispersive x-ray and electron microprobe analyses. A three dimensional structural analysis of breccia 14318 is in progress with 27X optical montages completed for 6 of the 8 thin sections. Surface reduction experiments on glass spheres of simulated lunar composition and impact studies on targets of simulated lunar composition at various temperatures and with various projectile velocities are also in progress.

ATTACHMENTS

1) Carter, J. L. (1973) "Chemistry and surface morphology of soil particles from Lunar 20 LRL sample 22003", Geochim. Cosmochim. Acta, Vol. 37, pp. 795-803.

2) Carter, J. L. and E. R. Padovani (1973) "Genetic implications of Apollo 16 soil particles", Lunar Science IV (eds., J. W. Chamberlain and C. Watkins), The Lunar Sci. Inst., Houston, Texas, pp. 121-123.

3) Taylor, H. C. Jim and J. L. Carter (1973) "Silicate mineral chemistry of Apollo soil 66081,5", Lunar Science IV (eds., J. W. Chamberlain and C. Watkins), The Lunar Sci. Inst., Houston, Texas, pp. 713-714.

4) Carter, J. L., H. C. Jim Taylor and E. Padovani (1973) "Morphology and chemistry of particles from Apollo 17 soils 74220, 74241 and 75081", EOS, Vol. 54, No. 6, pp. 582-584.

5) Carter, J. L. and D. L. Crosthwait, Jr. (1973) "Vapor-Liquid-Solid whisker growth on lunar breccia 15015", 31st. Ann. Proc. Electron Microscopy Soc. Amer., New Orleans, La., (ed., C. J. Arcenaeux).

6) Carter, J. L. (1973) "VLS (Vapor-Liquid-Solid): A newly discovered growth mechanism on the lunar surface?", Science, in press.

7) Carter, J. L. and E. Padovani (1973) "Genetic implications of some unusual particles in Apollo 16 less than 1 mm fines 68841,11 and 69941,13", Proc. Fourth Lunar Sci. Conf., Geochim. Cosmochim. Acta, in press.

8) Taylor, H. C. Jim and J. L. Carter (1973) "Silicate mineral chemistry of Apollo soils 15501, 15411, 66081 and 69941", Proc. Fourth Lunar Sci. Conf., Geochim. Cosmochim. Acta, in press.

9) Carter, J. L. (1973) "Morphology and chemistry of VLS (Vapor-Liquid-Solid)-type of whisker structures and other features on the surface of breccia 15015,36", Proc. Fourth Lunar Sci. Conf., Geochim. Cosmochim. Acta, in press.

10) Padovani, E. R. and J. L. Carter (1973) "Unusual particles in Apollo 16 soils", Trans. A.G.U. (abstract).

11) Carter, J. L. (1973) "VLS (Vapor-Liquid-Solid) growth on the surface of rock 15015", Trans. A.G.U. (abstract).

CHEMISTRY AND SURFACE MORPHOLOGY OF SOIL PARTICLES FROM LUNA 20 LRL SAMPLE 22003

James L. Carter

The University of Texas at Dallas,
The Institute for Geological Sciences
P. O. Box 30365
Dallas, Texas 75230

PREPRINT

Contribution No. 227, The University of Texas at Dallas, The Institute for Geological Sciences, P. O. Box 30365, Dallas, Texas 75230

ABSTRACT

Six siliceous glass spheres, five siliceous glass-bonded agglutinates and one breccia fragment from Luna 20 LRL sample number 22003 were analyzed by optical microscope, scanning electron microscope, scanning electron microprobe and energy-dispersive techniques. The data suggest that most of the glass spheres were probably derived locally by meteoritic impact processes and that most craters on their surfaces may have occurred from impacts of relatively high velocity particles in the impact-produced debris cloud while the glass sphere was at elevated temperatures. This is suggested by the nature of the craters, the partially buried fragments of plagioclase surrounded by radiating fractures and by the apparent absence of craters on the glass surfaces of the glass-bonded agglutinates. One glass sphere has a surface suggestive of a complex multiple impact origin involving liquid siliceous material and numerous siliceous spherules from 0.1 μm to 1 μm in diameter that may have formed from vaporization and condensation processes possibly in a relatively large scale meteoritic impact event.

The surfaces of the siliceous glass spheres have several different types of materials. Concentration of metallic iron spherules on the surfaces of the glass spheres is generally lower than for similar Apollo 11 and 12 glass spheres. This is consistent with reduction processes being of primary importance in the formation of this metallic iron. Surface material composed only of Ca, C and O_2, possibly $CaCO_3$, is probably derived from carbonaceous chondrites. Splashes of material rich in Ca, Al, Fe, K and Cl occur. The origin of the relatively low temperature chlorine-bearing melt is unknown but it may be related to vaporization and condensation processes, possibly volcanic in nature, or possibly to partial fusion of components of carbonaceous chondrites. Siliceous surface material rich in potassium may represent either fused splash material of granitic composition or material enriched by vaporization and condensation processes.

INTRODUCTION

Six siliceous glass spheres, five siliceous glass-bonded agglutinates and one breccia fragment from Luna 20 soil sample LRL number 22003 were ultrasonically cleaned and analyzed by optical microscope, scanning electron microscope, scanning electron microprobe and energy-dispersive techniques. Photomosaics were made of the entire surface of each particle at 900X and 3,000X to study the morphology, chemistry and relationships of the surface material in detail. The results of the studies of each particle will be discussed separately.

Siliceous Glass Spheres

Figs. 1 to 17 are scanning electron microscope photographs of the glass spheres and their selected surface features. The shape of the glass spheres shows that they have been at temperatures high enough to allow surface tensional forces to contract the material into a spherical shape while in free flight. The glass spheres in Figs. 1, 4 and 7 show the least amount of surface debris and those in Figs. 1 and 4 are similar to the Type-II Apollo 11 glass spheres (Carter and MacGregor, 1970), whereas those in Figs. 9, 12 and 14 show the most surface debris and are similar to the Type-I Apollo 11 glass spheres (Carter and MacGregor, 1970). In comparison to the Apollo 11 and 12 glass spheres, the glass spheres shown in Figs. 9, 12 and 14 have less crystalline surface material. Carter and MacGregor (1970), McKay et al. (1970) and Carter (1971) described Type-I glass spheres as those whose surfaces show a constructional history that is characterized by firmly attached crystalline and glass debris of variable grain size, numerous siliceous splashes and FeS mounds, whereas Type-II glass spheres generally have a smooth surface that shows a destructional history as a result of bombardment by relatively high velocity projectiles,and FeNi mounds. The Type-I glass spheres are generally opaque to translucent and brown to black in color, whereas the Type-II glass spheres are transparent to translucent and colorless to brown in color.

Sphere number 22003,C-3 (Fig. 1) is 235 μm in diameter, transparent, and light brown in color. It has the least amount of surface debris of the glass spheres studied. It has more impact craters over 1 μm in diameter than the other five glass spheres (Table 1), but it apparently has no craters less than 1 μm in diameter on its surface. The largest crater on its surface is approximately 7 μm in diameter. Table 1 lists all craters (number versus pit diameter in μm) present on the surface of the glass spheres studied at 3,000X

with a spatial resolution of 0.3 μm. Fig. 2, which is an enlarged view of the central upper right area of Fig. 1, shows a feature that is rich in K, Ca and Cl and it has minor Mg but no other elements as shown by energy-dispersive techniques. There are other masses of material similar in composition on this surface. Potassium chloride has been found on an Apollo 15 glass sphere (Carusi et al., 1972) and siliceous material rich in potassium has been found on numerous Apollo samples (e.g., Carter and MacGregor, 1970; McKay et al., 1970; McKay et al., 1972), but chlorides of the other elements have not been reported previously.

Fig. 3 is an enlarged view of the feature seen in the central area of Fig. 1. Energy-dispersive and scanning electron microprobe techniques show that this feature is composed of Ca, C and O_2, which suggests that it is probably $CaCO_3$. If it is $CaCO_3$, its presence raises the question of its origin. $CaCO_3$ on Earth is usually formed by precipitation processes from water or by organisms. It is produced to a very minor extent by igneous processes. This feature is probably not an Earth contaminant because a) the samples were cleaned ultrasonically three times before coating to remove all particles not stuck to the surface, b) there are hemispherical concentration of iron on its surface and c) its edges are rounded. Most likely it is a fragment of a carbonaceous chondrite. This is consistent with the findings of pure carbon material and carbon-bearing siliceous splashes on Apollo 11 materials (Carter and MacGregor, 1970).

Sphere number 22003,C-2 (Fig. 4) is 215 μm in diameter, translucent to transparent, and brown in color. Its surface is covered with metallic iron spherules that average 0.5 μm in diameter. Its surface has the highest concentration of metallic iron of any of the glass spheres studied. Fig. 5, which is an enlarged view of the central portion of Fig. 4, shows blebs of siliceous material with protrusions at their contact with the surface of the glass sphere. These protrusions may have resulted from vapor deposition and growth by surface tension. Asunmaa et al. (1970) describe a similar widespread bridging structure for the attachment of particles to the surface of Apollo 11 rock 10017,20. They suggested that this widespread bridging structure phenomena may be the result of preferred silicate vapor growth below particle edges. Fig. 6, an enlargement of the central bottom of Fig. 4, shows an area that has an unique feature that consists of a thin coating of material that is surrounded by what

appears to be an etched surface. The chemical nature of this coating material is unknown and the origin of the feature can not be ascertained because the glass sphere dislodged while in the scanning electron microprobe.

Sphere number 22003,C-1 (Fig. 7) is 280 μm in diameter, transparent, and green in color. The surface of the glass sphere is coated with dark brown siliceous material. Its surface (Figs. 7 and 8) has features suggestive of a multiple impact constructional history. The surface may have been impacted by angular debris which was then partially melted (Fig. 8), possibly by passage through a high temperature portion of an impact-produced debris cloud, and impacted with relatively large masses of molten vesiculating siliceous material (Fig. 7) and very fluid siliceous material (Fig. 8). Vapor deposition of siliceous materials may have contributed also to the constructional and welded nature of the surface of this glass sphere. This is indicated by the rounded nature of the surface blebs, the lack of splashed rays, the welded nature of the blebs, the relatively large vesicular areas of siliceous surface material, the numerous 0.1 μm to 1 μm in diameter siliceous spherules and the glazed appearance of the surface of the glass sphere. Alternatively, the surface of the glass sphere was struck by hot, partially molten, siliceous material at velocities low enough not to produce splashed rays, then impacted by relatively large masses of molten vesiculating siliceous material (Fig. 7), very fluid siliceous material (Fig. 8) and numerous 0.1 μm to 1 μm in diameter siliceous spherules (Fig. 8).

Energy-dispersive techniques show that many of the surface blebs are similar in composition to the glass sphere. However, some of the siliceous blebs are rich in potassium while others contain titanium and are lower in calcium and aluminum and higher in magnesium and iron than the glass sphere. This is similar to the surfaces of some Apollo 11 glass spheres (Carter and MacGregor, 1970). The surface also has a few metallic iron spherules (2 wt. % to 3 wt. % Ni) that are partially buried and range in diameter from 0.1 μm to 1 μm with an average diameter of 0.6 μm (Fig. 8).

Fig. 9 is a scanning electron microscope photograph of a 185 μm diameter glass sphere (number 22003,C-5) that has a brown transparent core surrounded by colorless transparent glass. Its surface has been impacted repeatedly with masses of crystalline material, mostly plagioclase (Figs. 9, 10 and 11). The surface of the glass sphere was essentially solidified, whereas its interior was capable of plastic deformation when impacted because the fragments of

plagioclase are partially buried in the glass sphere with radiating fractures extending outward from the point of impact (Figs. 10 and 11). Similar features have been described by Carter and MacGregor (1970) and Tolansky (1971) for some Apollo 11 glass spheres. The surface of the glass sphere also has metallic iron spherules (2 wt. % to 3 wt. % Ni) that range in diameter from 0.15 μm to 1.5 μm with an average diameter of 0.7 μm.

Sphere number 22003,C-7 is 140 μm in diameter, translucent, and dark brown in color with a surface of numerous siliceous splashes and out-gassing pores (Fig. 12). This glass sphere has the largest number of impact-produced craters less than 1 μm in diameter of any of the glass spheres studied (Table 1; Fig. 13). The left side of the glass sphere has been caved-in (Fig. 12) either because of impact in free flight or from impacting the lunar surface. Similar features on Apollo 11 glass spheres, which probably resulted when a glass sphere impacted the lunar surface while the glass sphere was still capable of deforming plastically, have been described by Carter and MacGregor (1970). However, splashes of siliceous material across the boundary of the caved-in area favors a debris cloud impact origin. If the caved-in area resulted from impact into the lunar soil, the craters probably originated by micrometeoritic bombardment because the craters occur primarily on the right side of this glass sphere, which would be the side that was exposed to micrometeoritic bombardment, if the glass sphere remained in its impact position on the lunar surface.

Sphere number 22003,C-6 (Fig. 14) is 160 μm in diameter, opaque, dark brown in color and heterogeneous in composition. Its surface has the most debris of the six glass spheres studied. The surface of this glass sphere shows a complex history of impact by angular siliceous debris and fluid siliceous material. The composition of the splashed material on the central bottom of the glass sphere is similar to the low iron basaltic portion of the glass sphere. The large mass of debris on the top left side of the glass sphere (Fig. 14) may have impacted the glass sphere when it was partially solidified, broken through the crust and allowed the still fluid interior to spew out onto the surface as splashed rays of iron-rich basaltic composition between the mass of angular solid particles and the glass sphere (Figs. 14 and 15). Alternatively, it impacted as a mixture of solid particles and liquid, or the splash occurred before the impact of debris. This later view is incon-

sistent with Fig. 15 which shows a continuity of some splashed rays that extend from the debris mass. Since the debris material is primarily a mixture of plagioclase fragments and siliceous glass that is rich in aluminum and calcium, impacting into a glass sphere with a solidified crust but an interior that is still fluid is favored. This is also consistent with the nature of the holes in the glass sphere as shown by Fig. 14 (lower left and top), especially the hole in the lower left in which the lip is turned inward.

A calcium-rich particle was found also in this debris mass (Fig. 16, center right). This particle is very similar morphologically to the one shown in Fig. 3, which it was suggested is a fragment of carbonaceous chondrite.

Three types of metallic mounds are present in small numbers on the surface of glass sphere number 22003,C-6. They are: metallic iron, iron sulfide and mixtures of nickel-rich metallic iron and iron sulfide. The metallic iron spherules are 1 μm or less in diameter. The iron sulfide spherules occur up to 0.6 μm in diameter. The mixtures of metallic iron, which contain 5 wt. % nickel, and iron sulfide occur as irregular blebs from 1 μm to 3 μm in diameter. These irregular blebs probably represent remelted components of meteorites (Goldstein et al., 1972).

An unusual and previously unreported type of splash is seen on the surface of this glass sphere (Fig. 17). Other smaller splashes of material of similar composition occur on the surface of this glass sphere. Thin rays that extend outwards and upwards from a heterogeneous mass of material that is rich in Ca, Al, K, Fe and Cl as shown by energy-dispersive techniques suggest that the material was very fluid when it struck the surface of the glass sphere. The main mass of material is composed of Ca, Al, Fe and Cl, whereas the smaller mass on the left side of the main mass is composed of Ca, Al, K, Fe and Cl with minor Si. The Si is possibly due to a X-ray signal from the substrate. As discussed above, KCl has been found on an Apollo 15 sphere (Carusi et al., 1972) and siliceous material rich in potassium has been found on numerous Apollo samples (e.g., Carter and MacGregor, 1970; McKay et al., 1970; McKay et al., 1972), but chlorides of the other elements have not been reported previously. The nature of the chlorine-bearing relatively low temperature melt is unknown, but it may be related to vaporization and condensation processes, possibly volcanic in nature. Alternatively, it may be partially fused components of carbonaceous chondrites.

Siliceous Glass-bonded Agglutinates

Five glass-bonded agglutinates were photographed with the scanning electron microscope (Figs. 18 to 21). No hypervelocity-type craters were noted on their surfaces at a 0.3 μm spatial resolution. This is consistent with the observations of Carter (1971) and Carter and McKay (1971) that hypervelocity-type craters occur primarily on the smooth surfaced Type-II Apollo siliceous glass spheres. This is further support for the hypothesis of Carter and MacGregor (1970), McKay et al. (1970) and Frondel et al. (1970) that the impact-produced debris cloud plays an important role in the formation of craters on glass spheres and that the substrate temperature is an important parameter in crater formation (Carter and MacGregor, 1970) as confirmed by the laboratory experiments of Carter and McKay (1971) on heated glass targets.

The glass-bonded agglutinates have very few metallic iron or iron sulfide mounds on their surfaces. This is consistent with the findings of lower metallic iron concentrations on the Luna 20 siliceous glass spheres than for Apollo 11 and 12 materials (Carter and MacGregor, 1970; Carter, 1971). This is also consistent with the absence of hypervelocity-type craters suggesting that these materials have never been in the high velocity portion of an impact-produced debris cloud. Fig. 19, an enlarged view of the upper central portion of Fig. 18 (sample number 22003,C-10, brown translucent siliceous glass), shows the largest (13 μm in diameter) iron sulfide mound found on the five glass-bonded agglutinates examined and shows the stringer nature of the metallic iron mounds which is typical of this type of occurrence (Carter and MacGregor, 1970; Carter and McKay, 1972). No single mound of metallic iron larger than 1 μm in diameter was noted.

The extreme debris-welded nature of sample number 22003,C-11, grayish translucent siliceous glass, is shown by Fig. 20. Fig. 21, an enlarged view of the central right portion of Fig. 20, shows stringers of siliceous material that appear to be part of the framework that holds the material together.

Breccia Fragment

Sample number 22003,C-12 is a fragment of plagioclase-rich breccia (Fig. 22). As shown by Fig. 23, which is an enlarged view of the right center of Fig. 22, the fragment is very vesicular or frothy, apparently because of partial fusion. The surface of the particle has been heated to the point where sharp

edges such as the edges of cleavage surfaces have been rounded (Fig. 24). The debris on its surface is metallic iron and siliceous materials. Some of the metallic iron spherules contain up to 5 wt. % nickel as shown by energy-dispersive techniques. The surface has no hypervelocity-type craters on it.

DISCUSSION AND CONCLUSIONS

The presence of siliceous splashes rich in Ca and Al (essentially anorthositic in composition) and the high percentage of plagioclase fragments that penetrate the surfaces of some of the glass spheres (Figs. 9 to 12, 14 and 15) suggest that the glass spheres examined were derived locally from relatively small scale meteoritic events, with the possible exception of glass sphere number 22003,C-1 (Figs. 7 and 8), and not, for example, from an adjacent maria and later splashed with anorthositic material. Reid et al. (1973) and Glass (1973) suggest from chemical analyses of glasses that there is a minor contribution of mare rocks to the Luna 20 soil. The surface of the glass sphere number 22003,C-1 (Fig. 8), as discussed above, suggest a complex multiple impact origin involving liquid siliceous material. The numerous siliceous spherules that are 0.1 μm to 1 μm in diameter, the glazed appearance of the surface and the lack of angular crystalline debris suggest that vaporization and condensation processes may have been involved in the formation of this complex surface. The particle possibly formed in a relatively large scale meteoritic impact event and not from a relatively small scale local micrometeoritic impact event.

The nature of the metallic iron (2 wt. % to 3 wt. % Ni) mounds and their low concentrations with respect to Apollo 11 and 12 siliceous glass spheres (e.g., Carter and MacGregor, 1970; Carter, 1971) suggest that reduction processes played an important role in the formation of these mounds (Carter, 1971; Carter and McKay, 1972; Carter, 1972 a,b). The minor irregularly-shaped metallic iron blebs with 5 wt. % nickel content and with minor sulfur may be remelted fragments of meteoritic origin (Goldstein et al., 1972). These interpretations are consistent with the Luna 20 soil having a much lower total iron content than the Apollo 11 or 12 soils (Vinogradov, 1972; LSPET, 1969, 1970).

The surface materials rich in Ca, C and O_2 may be fragments of carbonaceous chondrites. This interpretation is consistent with the findings of carbon-

bearing compounds in Apollo 11 material (Carter and MacGregor, 1970). The origin of the splashes and debris that are rich in Ca, Al, Fe, K and Cl is unknown. It may be related to vaporization and condensation processes, possibly volcanic in nature. Alternatively, they may be partially fused components of carbonaceous chondrites. Their relative abundance argues against a meteoritic origin. The siliceous material rich in potassium may represent either splash material of granitic composition or enrichment by vaporization and condensation processes.

The nature and distribution of craters on the glass spheres (Table 1) and their apparent absence from the glass-bonded agglutinates suggest that the cratering events occurred mainly in an impact-produced debris cloud and not by random micrometeoritic bombardment while the particle was at rest on the lunar surface. This interpretation is consistent with the following data:

1) Reid et al. (1973, Table 1) give agglutinates as the most abundant particle type in the less than 125 μm size fraction, whereas Glass (1973, Table 1) gives agglutinates in the 125 μm to 250 μm size fraction as about 1/5 the abundance shown by Reid et al. (1973). McKay et al. (1971) and Clanton et al. (1972) showed that the percentage of glass-bonded agglutinates in a lunar soil provides a relative index of maturity or residence time on the lunar surface. Therefore, if the cratering events occurred from random micrometeoritic bombardment while the particle rested on the lunar surface, the surfaces of the abundant glass-bonded agglutinates should record these impacts.

2) The surface of glass sphere 22003,C-3 (Figs. 1 to 3) apparently has no impact craters smaller than 1 μm in diameter even though its surface has the largest number of craters larger than 1 um in diameter of any of the glass spheres studied (Table 1). This does not appear to be consistent with a micrometeroritic origin for these craters because of the large number of submicron size craters that should be present (Hörz et al., 1971) but are not.

3) The large number of less than 1 μm in diameter craters on the surface of the glass sphere 22003,C-7 (Figs. 12 and 13) and of the glass sphere 22003,C-6 (Fig. 14) is consistent with the findings of Carter and MacGregor (1970) and Carter (1971) for Type-I Apollo silicate glass spheres. They found few craters larger than 1 μm in diameter and no craters larger than 10 μm in

diameter. They interpreted the less than 1 μm in diameter craters on the Type-I glass spheres to have occurred in an impact-produced debris cloud as a response to target viscosity.

4) The interpretation of the glass spheres being impacted while in an impact-produced debris cloud is consistent also with the impact by fragments of plagioclase and other angular debris of glass spheres whose surfaces were solidified whereas their interiors were capable of plastic deformation (Figs. 9 to 11 and 13; Carter and MacGregor, 1970; Tolansky, 1971).

ACKNOWLEDGEMENTS

Supported by NASA Grants NGL-44-004-001 and NGR-44-004-116, Suppl. #1. I thank J. B. Toney and E. Padovani for technical assistance. I thank the Material Characterization Laboratory of the Central Research Laboratories of Texas Instruments for use of their scanning electron microscope in determining the presence of oxygen. A. Albee, B. P. Glass, A. L. Hales, F. E. Senftle and E. Padovani have contributed to the improvement of the manuscript.

REFERENCES

Asunmaa, S. K., S. S. Liang, and G. Arrhenius (1970) Primordial accretion; inferences from the lunar surface. Proc. Apollo 11 Lunar Sci. Conf., Geochimica et Cosmochimica Acta, (Suppl. 1), Vol. 3, 1975-1985. Pergamon.

Carter, J. L. (1971) Chemistry and surface morphology of fragments from Apollo 12 soil. Proc. Sec. Lunar Sci. Conf., Geochimica et Cosmochimica Acta, (Suppl. 2), Vol. 1, 873-892. The M.I.T. Press.

Carter, J. L. (1972a) Morphology and chemistry of glass surface of breccia 15015,36. The Apollo 15 Lunar Samples, ed. by J. W. Chamberlin and C. Watkins, The Lunar Sci. Inst., Houston, Texas, 51-53.

Carter, J. L. (1972b) Surface morphology and chemistry of rock 15015,36. (abs.), Am. Geophys. Union, Fall Ann. Meeting.

Carter, J. L. and I. D. MacGregor (1970) Mineralogy, petrology and surface features of some Apollo 11 samples. Proc. Apollo 11 Lunar Sci. Conf., Geochimica et Cosmochimica Acta, (Suppl. 1), Vol. 1, 247-265. Pergamon.

Carter, J. L. and D. S. McKay (1971) Influence of target temperature on crater morphology and implications on the origin of craters on lunar glass spheres. Proc. Sec. Lunar Sci. Conf., Geochimica et Cosmochimica Acta, (Suppl. 2), Vol. 3, 2653-2670. The M.I.T. Press.

Carter, J. L. and D. S. McKay (1972) Metallic mounds produced by reduction of material of simulated lunar composition and implications on the origin of metallic mounds on lunar glasses. Proc. Third Lunar Sci. Conf., Geochimica et Cosmochimica Acta, (Suppl. 3), Vol. 1, 953-970. The M.I.T. Press.

Carusi, A., G. Cavarretta, F. Cinotti, G. Civitelli, A. Coradini, M. Fulchignoni, R. Funiciello, A. Taddeucci, and R. Trigila (1972) The source area of Apollo 15 "Green Glasses", The Apollo 15 Lunar Samples, ed. J. W. Chamberlain and C. Watkins, The Lunar Sci. Inst., Houston, Texas, 5-9.

Clanton, U. S., D. S. McKay, R. M. Taylor, and G. H. Heiken (1972) Relationships of exposure age to size distribution and particle types in the Apollo 15 drill core. The Apollo 15 Samples, ed. J. W. Chamberlain and C. Watkins, The Lunar Sci. Inst., Houston, Texas, 54-56.

Frondel, C., C. Klein, Jr., J. Ito, and J. C. Drake (1970) Mineralogical and chemical studies of Apollo 11 lunar fines and selected rocks. Proc. Apollo 11 Lunar Sci. Conf., Geochimica et Cosmochimica Acta, (Suppl. 1), Vol. 1, 445-474. Pergamon.

Glass, B. P. (1973) Major element analysis of Luna 20 glass particles (ed. see this issue).

Goldstein, J. I., H. J. Axon, and C. Y. Yen (1972) Metallic particles in the Apollo 14 lunar soil. Proc. Third Lunar Sci. Conf., Geochimica et Cosmochimica Acta, (Suppl. 3), Vol. 1, 1037-1064. The M.I.T. Press.

Hörz, F., J. B. Hartung, and D. E. Gault (1971) Microcraters on lunar rock surfaces. Jour. Geop. Res., Vol. 76, No. 23, 5770-5798.

LSPET (Lunar Sample Preliminary Examination Team) (1969) Preliminary examination of lunar samples from Apollo 11. Science 165, 1211-1227.

LSPET (Lunar Sample Preliminary Examination Team) (1970) Preliminary examination of lunar samples from Apollo 12. Science 167, 1325-1339.

McKay, D. S., W. R. Greenwood, and D. A. Morrison (1970) Origin of small lunar particles and breccia from the Apollo 11 site. Proc. Apollo 11 Lunar Sci. Conf., Geochimica et Cosmochimica Acta, (Suppl. 1), Vol. 1, 673-694. Pergamon.

McKay, D. S., U. S. Clanton, D. A. Morrison, and G. H. Ladle (1972) Vapor phase crystallization in Apollo 14 breccia. Proc. Third Lunar Sci. Conf., Geochimica et Cosmochimica Acta, (Suppl. 3), Vol. 1, 739-752. The M.I.T. Press.

Reid, A. M., J. L. Warner, W. I. Ridley, and R. W. Brown (1973) Luna 20 soil: Abundance and composition of phases in the 45-125 micron fraction (ed. see this issue).

Tolansky, S. (1971) Interferometric examination of Apollo 12 lunar glass spherules. Sec. Lunar Sci. Conf. (unpub. proc.).

Vinogradov, A. P. (1973) Preliminary data on lunar soil obtained by the automatic station 'Luna 20'. Geochim. Cosmochim. Acta 37, this issue.

FIGURE CAPTIONS

Fig. 1. Glass sphere 22003,C-3 showing impact craters and impacts of siliceous material.

Fig. 2. Enlarged view of feature on upper right side of Fig. 1 that contains K, Ca, Cl and minor Mg.

Fig. 3. Enlarged view of central feature in Fig. 1 that contains Ca, C and O_2, possibly $CaCO_3$.

Fig. 4. Glass sphere 22003,C-2 showing surface of metallic iron spherules.

Fig. 5. Enlarged view of center of Fig. 4 showing surface debris with protrusions that were possibly formed by vapor deposition of siliceous material.

Fig. 6. Enlarged view of bottom center of Fig. 4 showing thin surface film that is surrounded by an etched-like surface.

Fig. 7. Glass sphere 22003,C-1.

Fig. 8. Enlarged view of center of Fig. 7 showing surface of fused siliceous particles, siliceous spherules from 0.1 μm to 1 μm in diameter and partially buried metallic iron spherules (arrows).

Fig. 9. Glass sphere 22003,C-5 showing numerous impacts of siliceous debris.

Fig. 10. Enlarged view of left side of Fig. 9 showing impacts of angular plagioclase debris surrounded by radiating fractures revealing that the interior of the glass sphere was capable of plastic deformation, whereas the exterior was solid when impacted.

Fig. 11. Enlarged view of the top of Fig. 9 revealing a surface with metallic iron spherules from 0.15 μm to 1.5 μm in diameter and impact craters showing plastic deformation produced by angular fragments of plagioclase.

Fig. 12. Glass sphere 22003,C-7 showing numerous siliceous splashes and outgassing pores.

Fig. 13. Enlarged view of right side of Fig. 12 (rotated 90° counter clockwise) showing numerous impact-produced craters from 0.3 μm to 1.5 μm in diameter. The center of the larger craters contains an apparent projectile.

Fig. 14. Glass sphere 22003,C-6 showing numerous splashes and impacts of siliceous materials.

Fig. 15. Enlarged view of left center of Fig. 14 showing contact of debris with surface of glass sphere. Note splashed rays extending from debris.

Fig. 16. Enlarged view of debris in left center of Fig. 14. Large particle in right center of photograph , which is similar morphologically to the one shown in Fig. 3, contains only calcium by energy-dispersive techniques, probably it is also $CaCO_3$.

Fig. 17. Enlarged view of upper right part of Fig. 14 showing peculiar splash feature that contains Ca, Al, K, Fe and Cl as shown by energy-dispersive techniques.

Fig. 18. Glass-bonded agglutinate 22003,C-10.

Fig. 19. Enlarged view of upper center of Fig. 18 showing mound of FeS and stringers of metallic iron. Note the well developed cooling crack around the base of the FeS mound.

Fig. 20. Glass-bonded agglutinate 22003,C-11.

Fig. 21. Enlarged view of center of Fig. 20 showing a filament of siliceous glass bridging two silicate particles.

Fig. 22. Breccia sample 22003,C-12 showing porous surface.

Fig. 23. Enlarged view of center right of Fig. 22 showing vesicular or porous surface.

Fig. 24. Enlarged view of the far central right portion of Fig. 22 showing rounded edges, which suggests that the surface was at elevated temperatures.

Table 1. Number of craters versus crater diameter in μm, and surface area of glass measured in mm^2.

Sample number	≤.4	>.4 ≤.6	>.6 ≤1	>1 ≤1.6	>1.6 ≤3	>3 ≤5	>5 ≤7	Surface Area*
22003,C-1					2	2	1	0.07
22003,C-2	7	2	4		2			0.03
22003,C-3				14	9	1	1	0.07
22003,C-5			4	1		2		0.04
22003,C-6	13	4	12	5				0.04
22003,C-7	27	14	4	5	2			0.03
22003,C-10								0.07
22003,C-11								0.02
22003,C-12								0.09

*Assuming hemispherical shape for surface area of glass sphere measured.

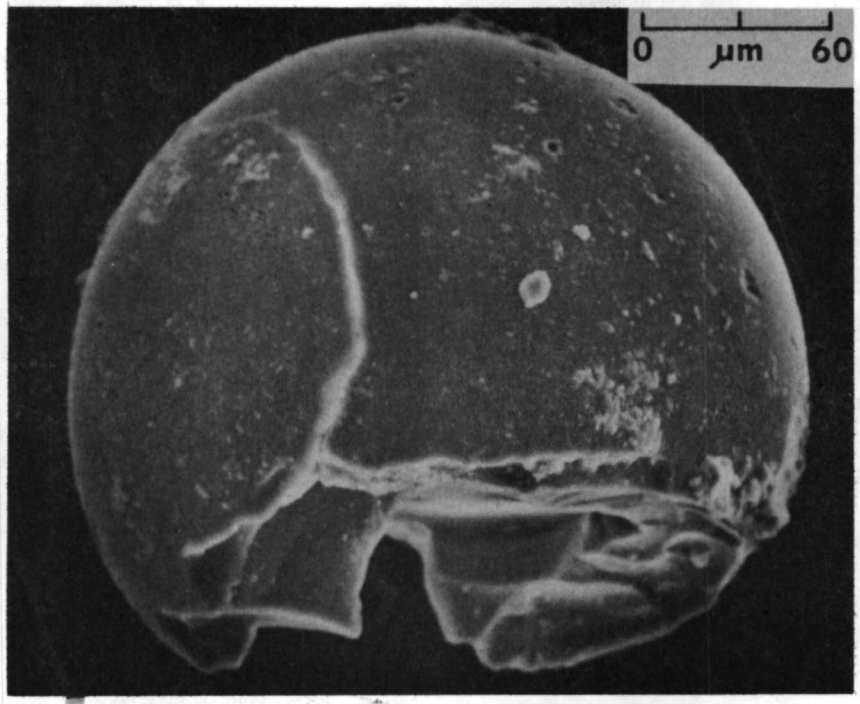

1

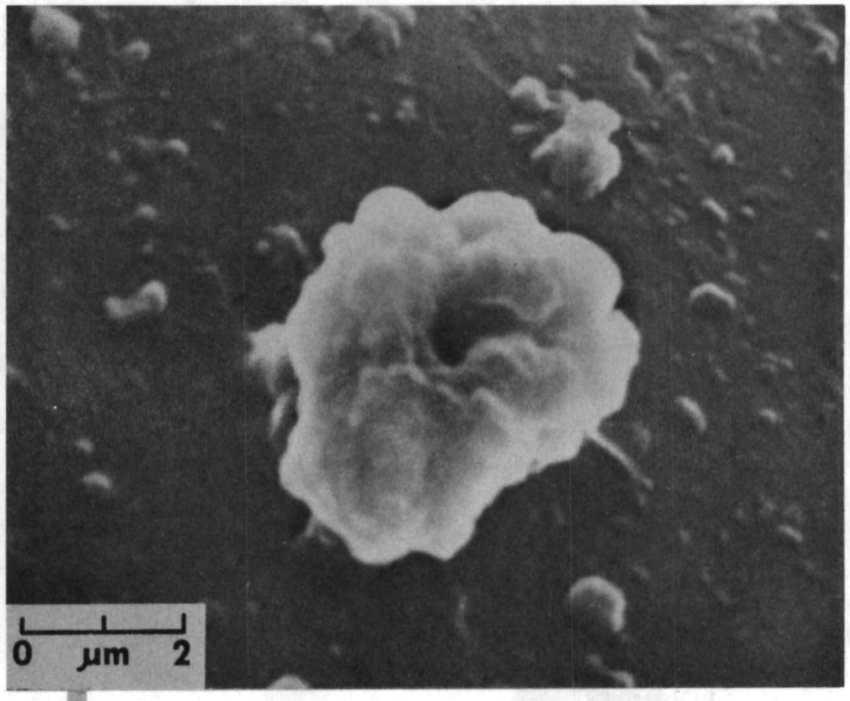

2

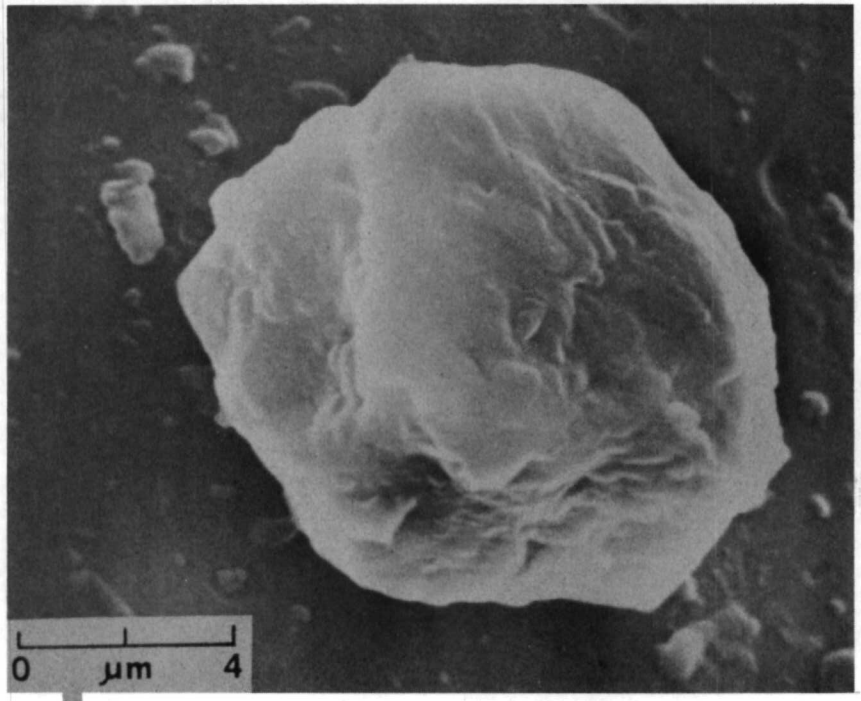

3

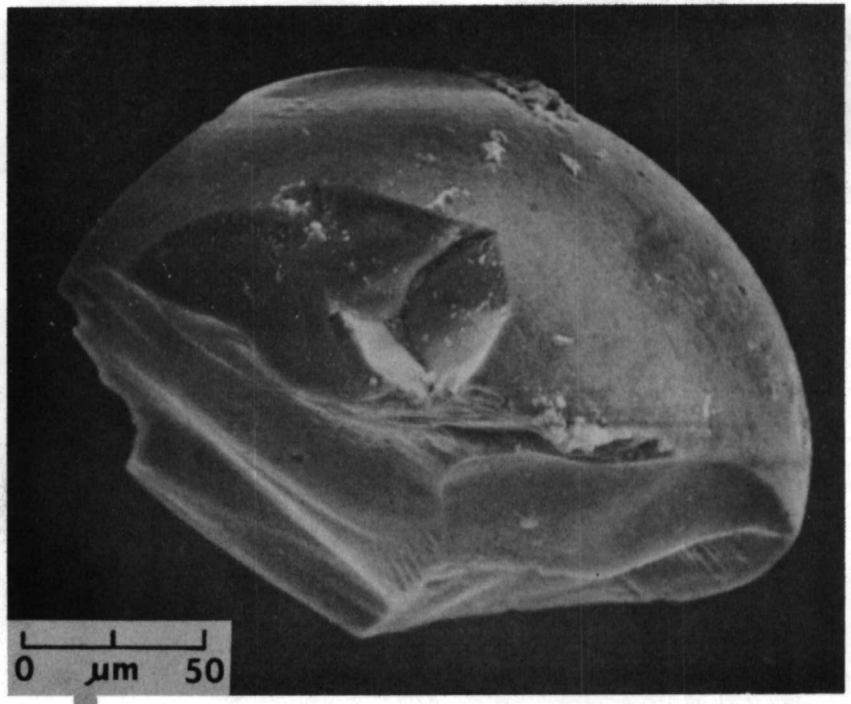

4

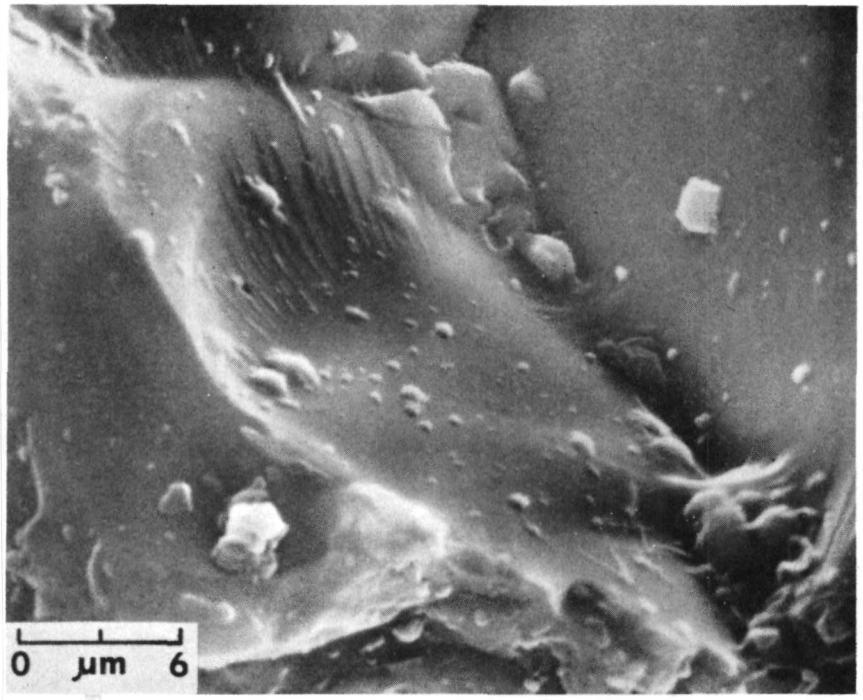

5

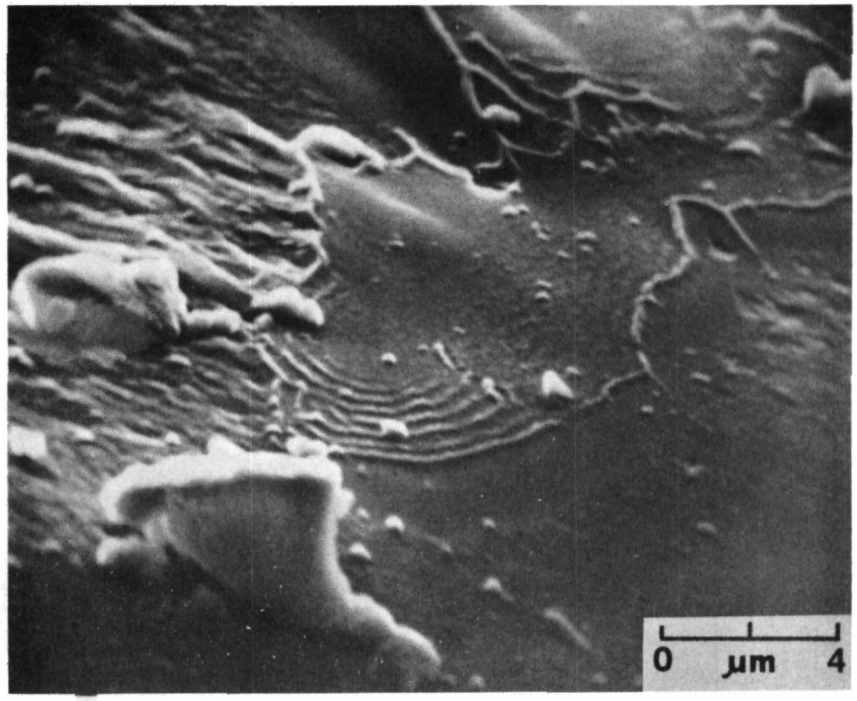

6

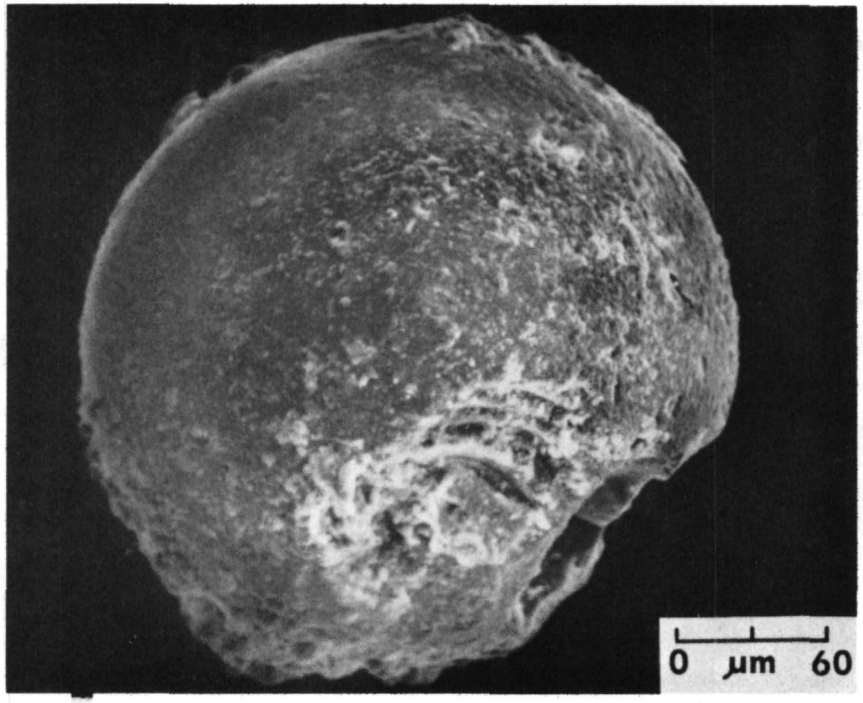

7

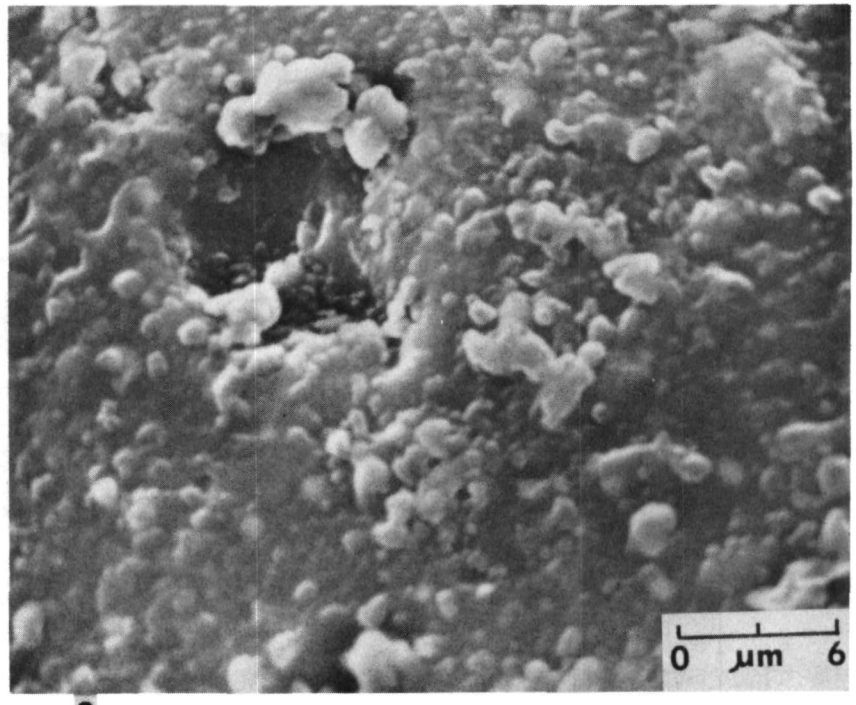

8

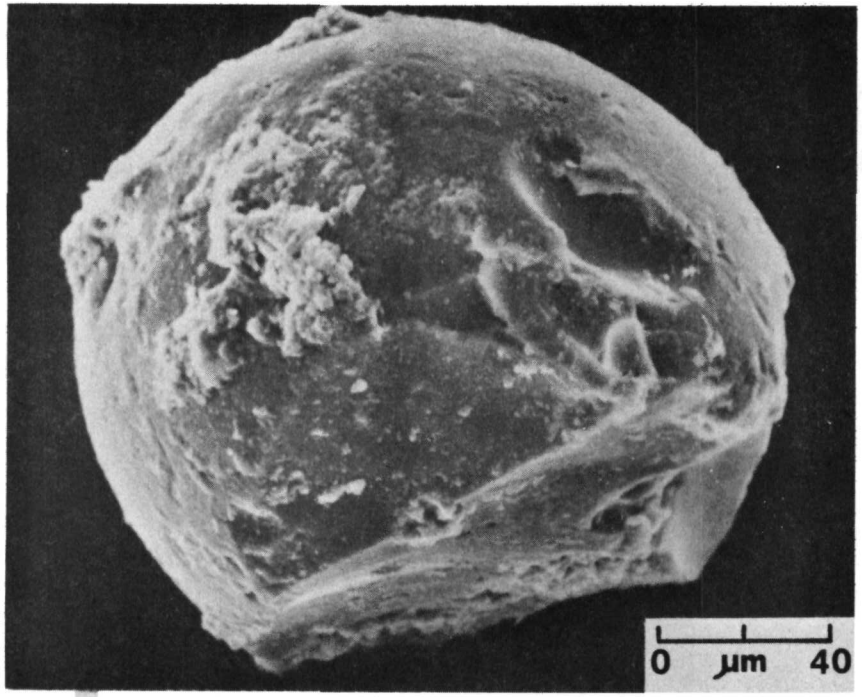

9

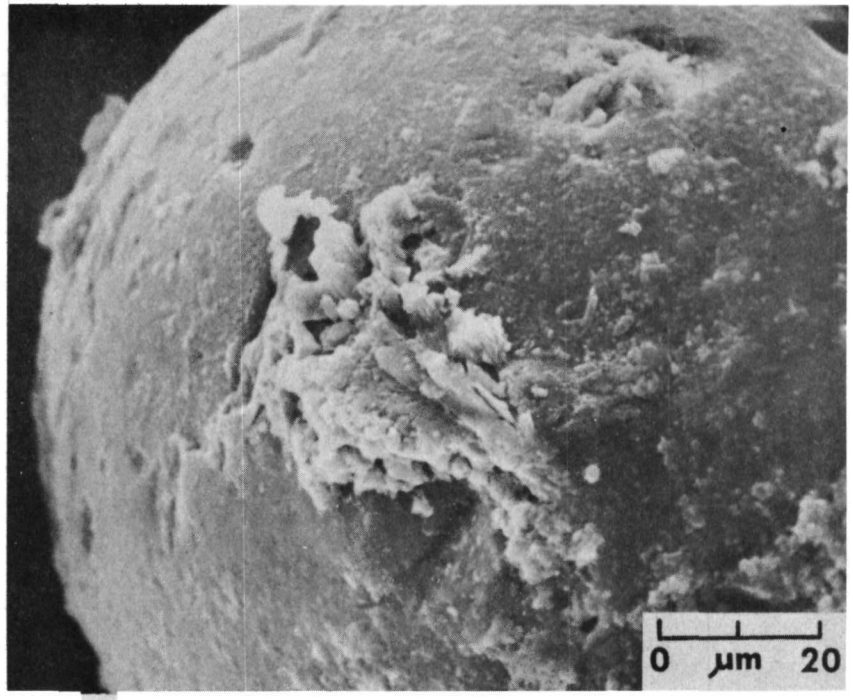

10

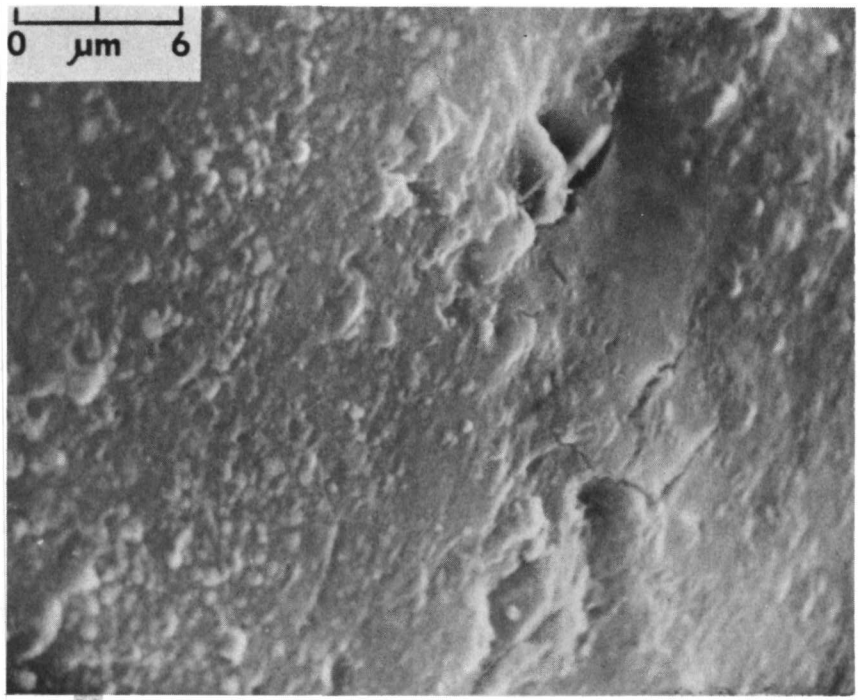

11

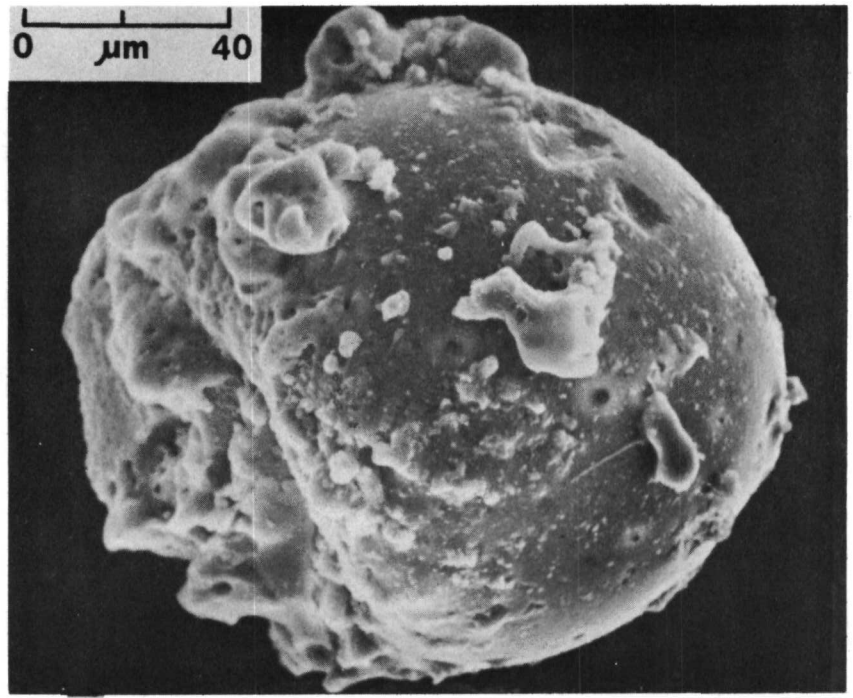

12

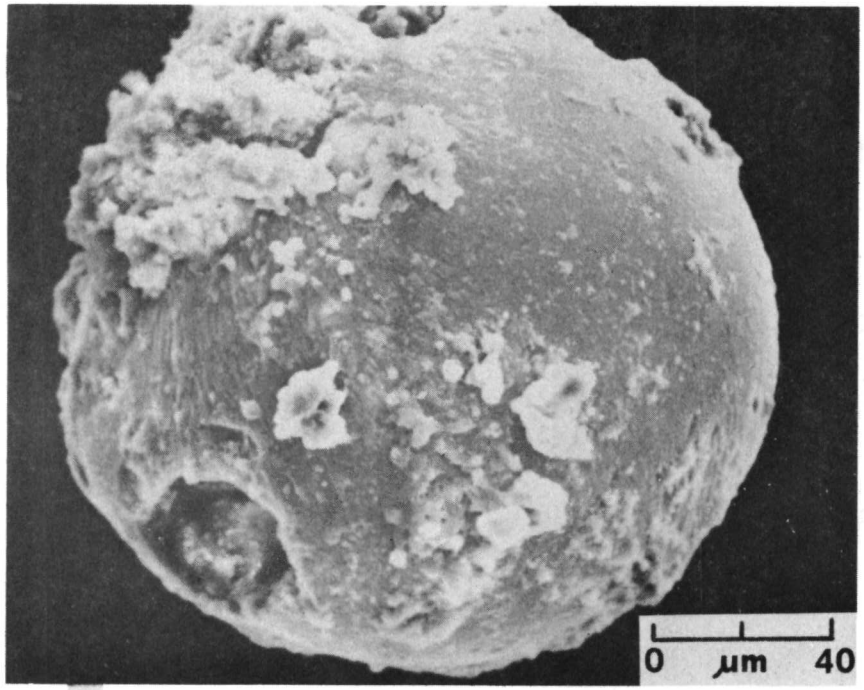

13

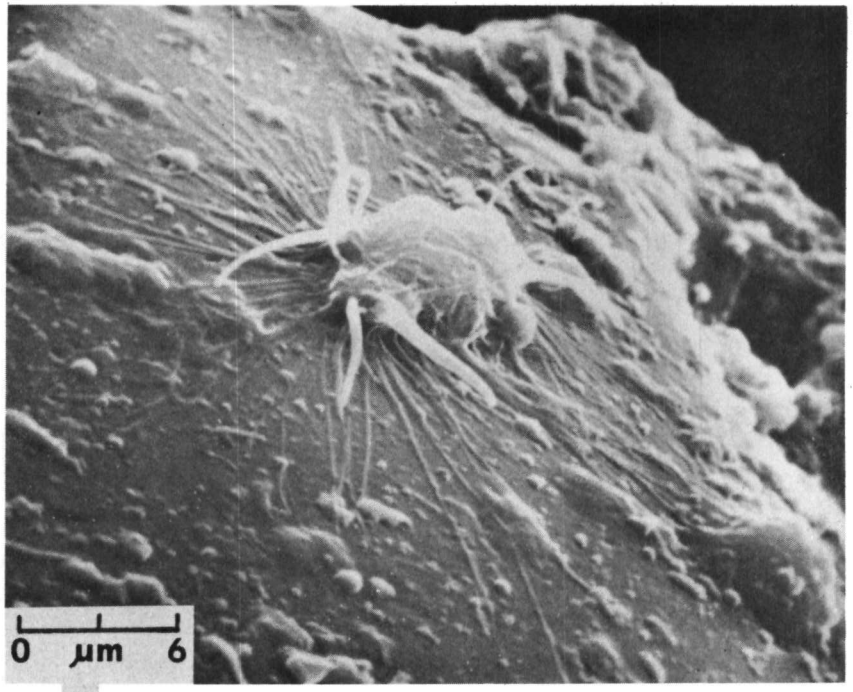

14

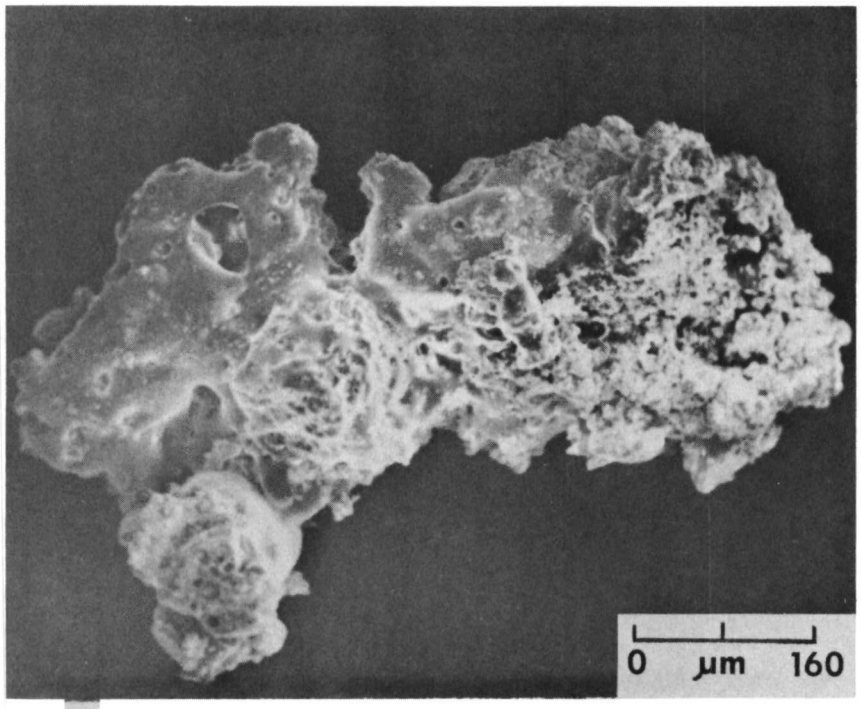

15

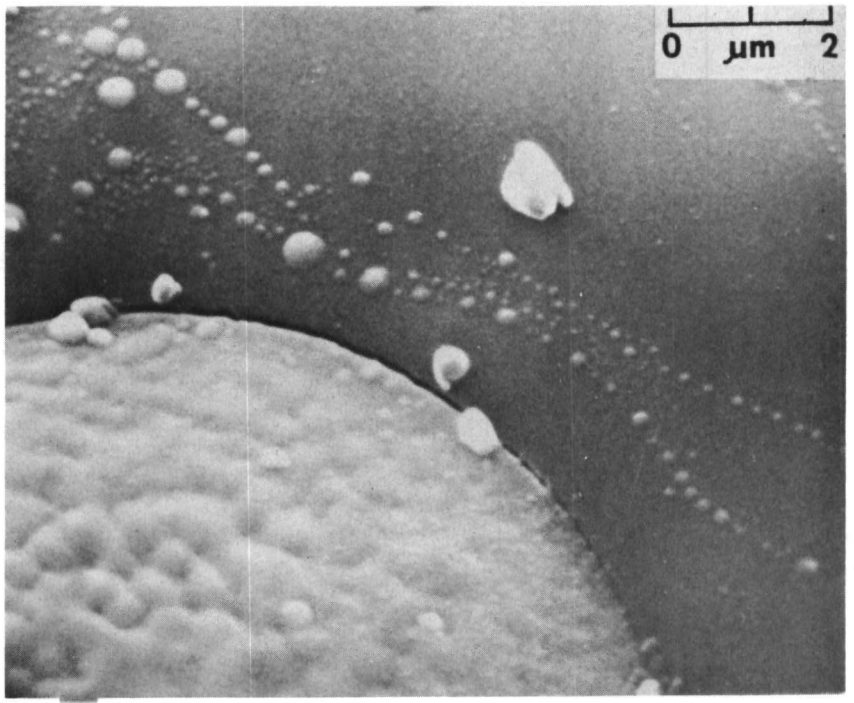

16

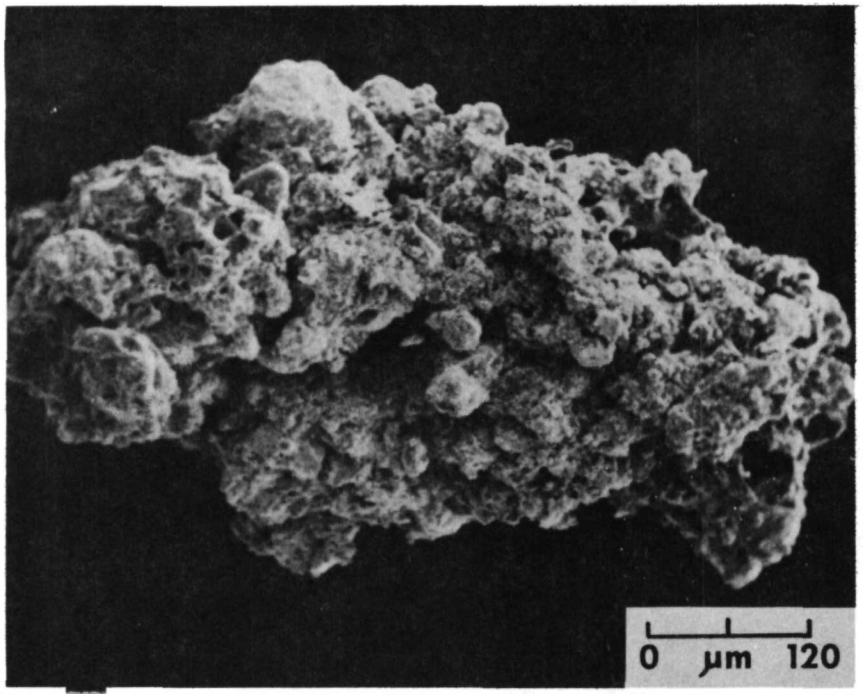

17

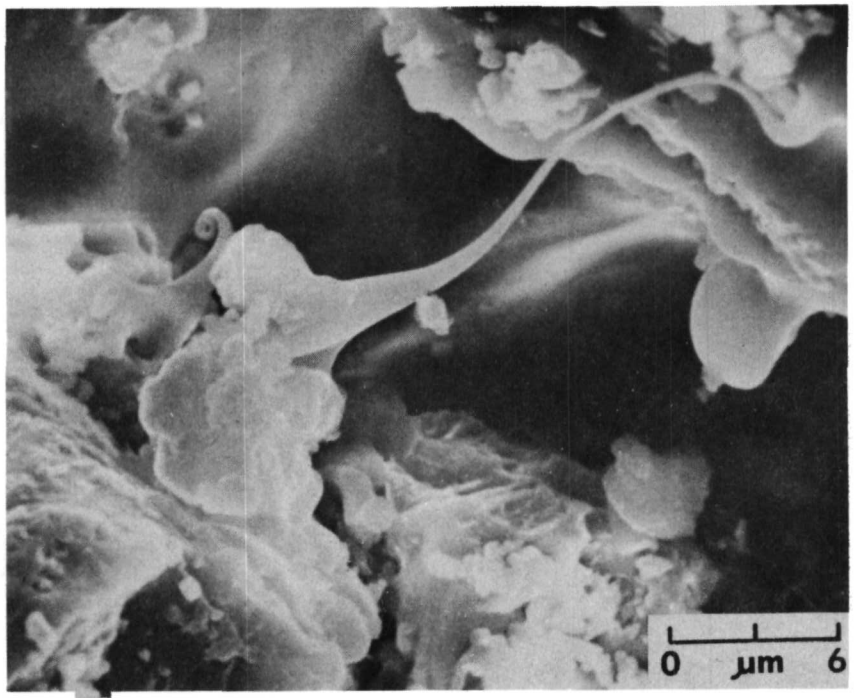

18

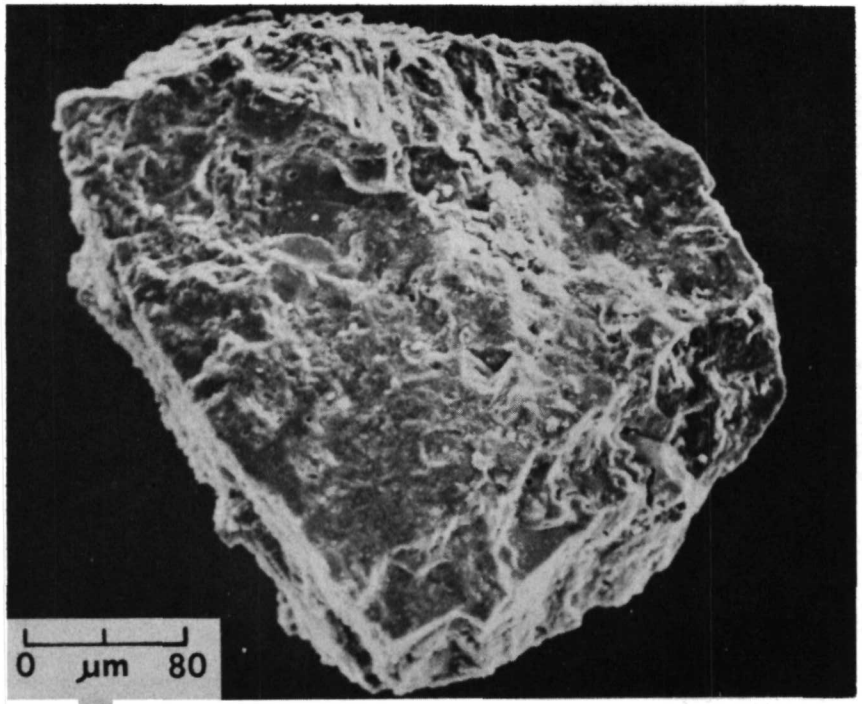

19

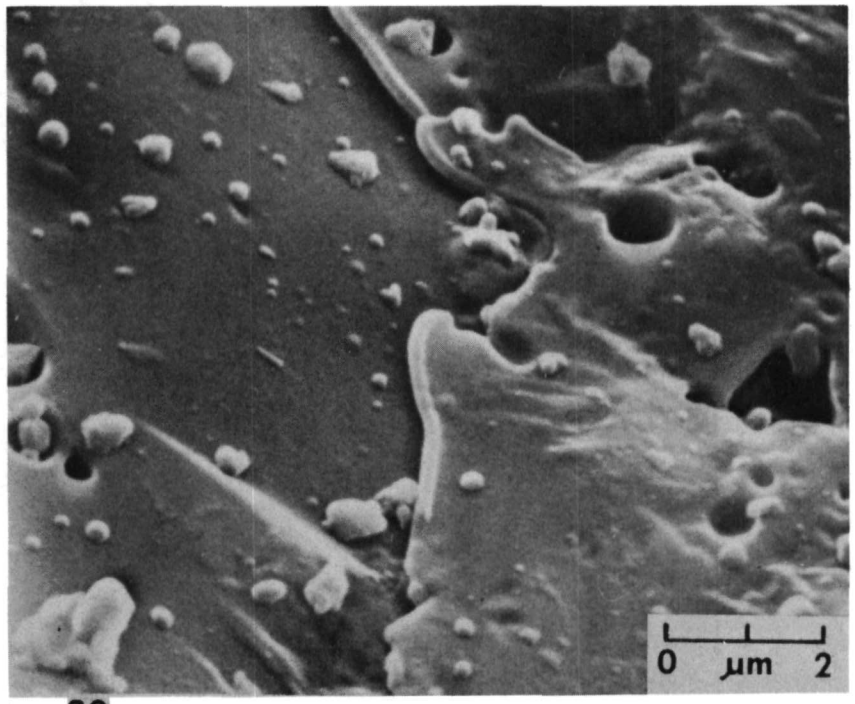

20

GENETIC IMPLICATIONS OF APOLLO 16 SOIL PARTICLES. James L. Carter and Elaine Padovani, The University of Texas at Dallas, The Institute for Geological Sciences, P. O. Box 30365, Dallas, Texas 75230. Contribution no. 230.

Forty-eight particles from four soil localities (twelve from each (62241, 14, 66081,5, 68841,11, and 69941,13) were examined using optical microscope, scanning electron microscope, scanning electron microprobe, and energy-dispersive techniques to compare and contrast their surface morphology and chemical characteristics. The samples are composed of transparent and opaque silicate spheres, rods, and fragments, broken and impacted feldspar and pyroxene crystals, variably colored silicate glass splashes, breccias, and several unusual types of reddish metallic spheres and porous crystalline silicate spheres not previously noted from our studies of other Apollo soil samples. Hypervelocity-type impact pits occur mainly on glass splashed surfaces, transparent to translucent spheres, and fragments. They were observed occasionally on metallic and opaque silicate spheres. The detailed morphology and chemistry of each particle will be given in the expanded version of this paper.

The soil from South Ray crater, especially sample 69941,13, contained two types of particles different than those from the other soil samples. One type is rounded metallic objects, mainly spheres, that have a surface of interlocking metallic iron crystals, patches of iron sulfide, and patches of intergrown silicate minerals, mainly feldspar. Five metallic objects larger than 150 microns in diameter were found in the 0.5 gram sample of 69941,13. The nickel content of the metallic iron crystals in wt. % varies from about 2 to 4. All of the metallic spheres have reddish patches on their surfaces, many of which are in the contact zone with feldspar. An enlarged view of a portion of one such patch is shown in Fig. 1, which shows that the reddish material is morphologically characterized by cracks and areas of crystals. In transmitted light they are reddish in color and in reflected light give the appearance of goethite. Goethite-like material has been described by Agrell et al. (1) and the PET (2). Examination with the microprobe showed iron to be the most abundant element with minor sulfur and chlorine and lesser amounts of nickel, calcium, and silicon. The material under the electron beam acted as if water or other volatile species were present. The color, reflective properties, morphological features, and chemistry suggests that the material is goethite. The abundance of this material and the lack of similar material on lunar material exposed to the Earth's atmosphere suggest that it formed on the lunar surface, possibly during an impact event or in a hot ejecta blanket (3).

The second type of particle is silicate spheres whose surfaces are porous and composed of a network of feldspar crystals (Figs. 2-5). The surfaces of most of the spheres are free of debris but contain hemispheres (Fig. 2) or spherules (Fig. 3) of silicate material attached to their surfaces. More rarely some of the spheres have debris firmly attached to their surfaces (Fig. 4). The textured surface of this sphere is composed of a network of small feldspar crystals as shown by Fig. 5. A thin-section of the sphere in Fig. 2 shows that there is no break in structure between the larger sphere and the silicate hemisphere and that both the hemispheres and spheres have textures that are reminiscent of quench textures (Fig. 6). A similar but not identical texture can be formed by crystallization of glass just above its solidus

GENETIC IMPLICATIONS

James L. Carter

temperature (Presnall, 1973, personal communication). The penetrating surface material, the attached silicate spherules, and the larger iron mounds that are partially buried in the spheres show that the spheres were once molten.

The determination of the nature of this texture is germane to the origin of these particles. There are two principal possibilities; either it resulted from devitrification of glass, or it resulted from quenching of a melt. If it resulted from devitrification of glass, these particles may be chondrules, probably of lunar origin because of their high feldspar content (Kuwat et al., 4; King et al., 5). A chondrule with a similar but not identical surface texture is shown by Cavarretta et al. (6). If it is a quench texture, the melt could be either impact-produced or volcanic in origin. As a working hypothesis, the quench hypothesis is favored, the texture probably resulted from the rapid cooling of melts of volcanic origin. This hypothesis is favored because of the apparent homogeneity of the original silicate melt, the similar composition of the spheres and the attached silicate spherules, and the general lack of surface debris.

REFERENCES

(1) Agrell S.O., J.H. Scoon, J.V.P. Long, and J.N. Coles (1972), In Lunar Science-III (ed. C. Watkins), 7-9, Lunar Sci. Inst. Contr. No. 88.
(2) Apollo 16 Preliminary Examination Team, Science 179, 23-34, 1973.
(3) Carter J.L. and D.S. McKay (1972), Proc. 3rd. Lunar Sci.Conf., Geochimica et Cosmochimica Acta, Suppl. 1, Vol. 1, 953-970, The M.I.T. Press.
(4) Kurat G., K. Keil, M. Prinz, and C.E. Nehru (1972), Proc. 3rd. Lunar Sci. Conf., Geochimica et Cosmochimica Acta, Suppl. 3, Vol. 1, 707-721.
(5) King E.A.,Jr., J.C. Butler, and M.F. Carman (1972), Proc. 3rd. Lunar Sci. Conf., Geochimica et Cosmochimica Acta, Suppl. 3, Vol. 1, 673-686.
(6) Cavarretta G., A. Coradini, R. Funiciello, M. Fulchignoni, A. Taddeucci, and R. Trigila (1972). Proc. 3rd. Lunar Sci. Conf., Geochimica et Cosmochimica Acta, Suppl. 3, Vol. 1, 1085-1094, The M.I.T. Press.

We acknowledge NASA Grant NGL-44-004-001 and NGR-44-004-116, Suppl. # 1.

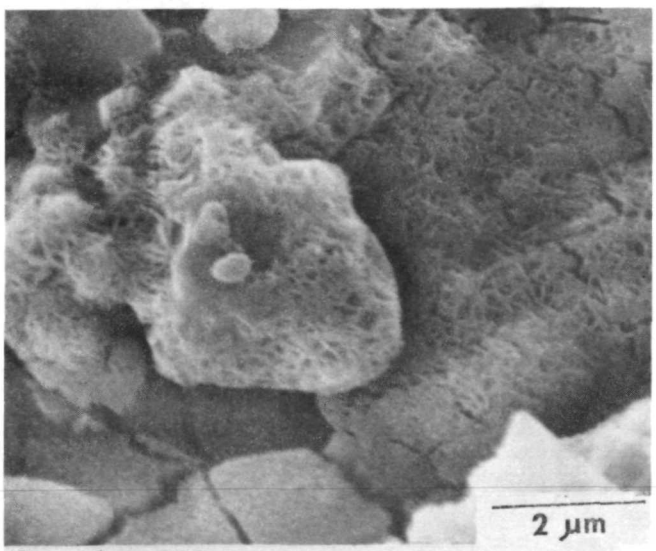

Fig. 1. Enlarged view of part of a reddish patch on a metallic particle.

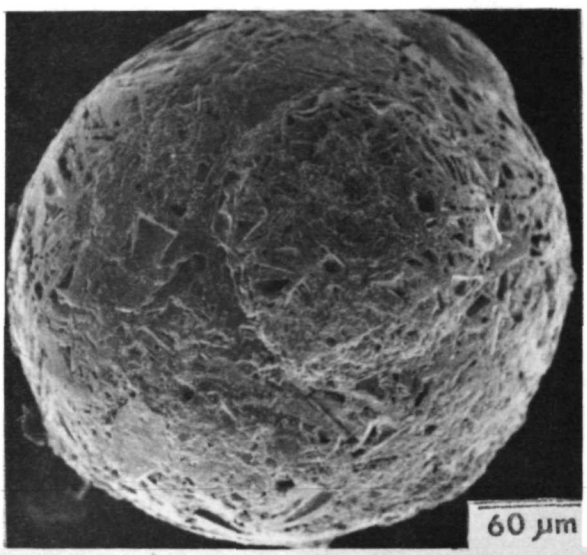

Fig. 2. Porous, crystallized, silicate sphere with attached hemispheres.

GENETIC IMPLICATIONS

James L. Carter

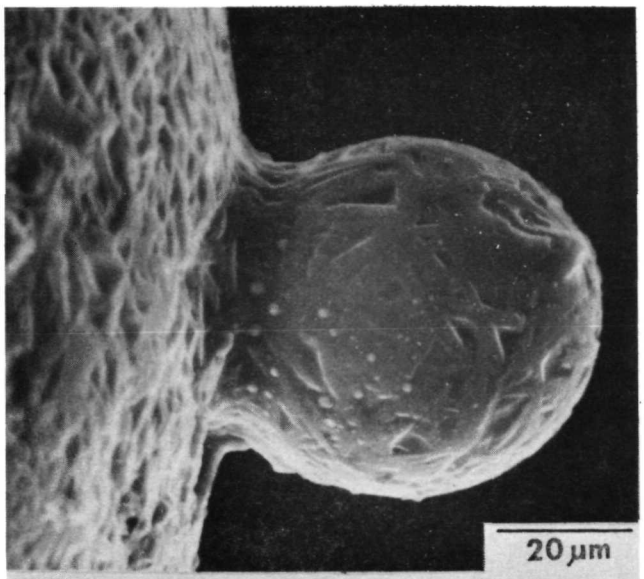

Fig. 3. Spherule of silicate material attached to surface of silicate sphere from 66941,13 (B-1). Note continuity of crystals between the spherule and the sphere.

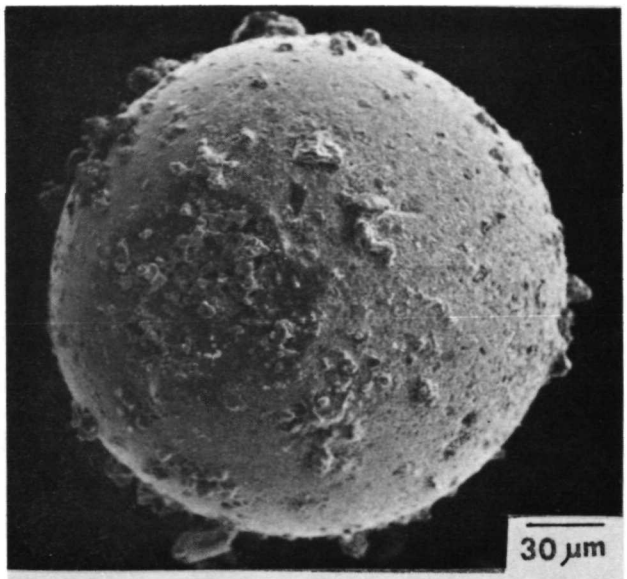

Fig. 4. Debris-coated crystallized silicate sphere from 69941,13 (B-4) whose surface is a network of feldspar crystals.

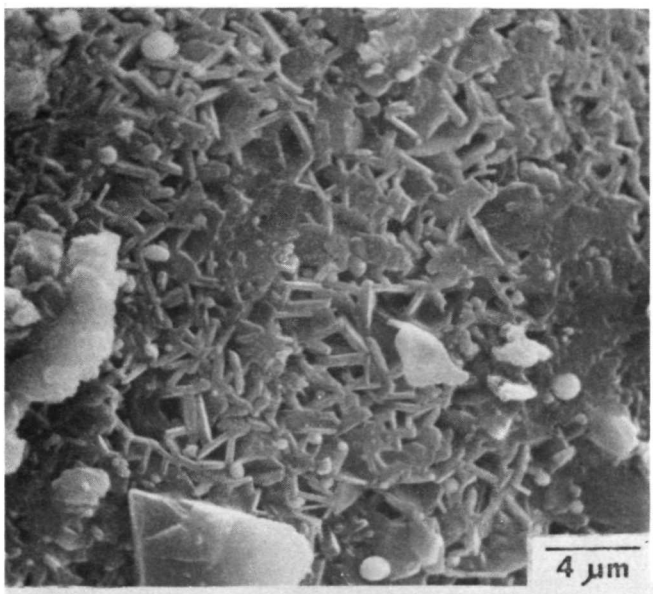

Fig. 5. Enlargement of surface of Fig. 4. Feldspar crystals average 2.5 microns by 0.5 microns in length.

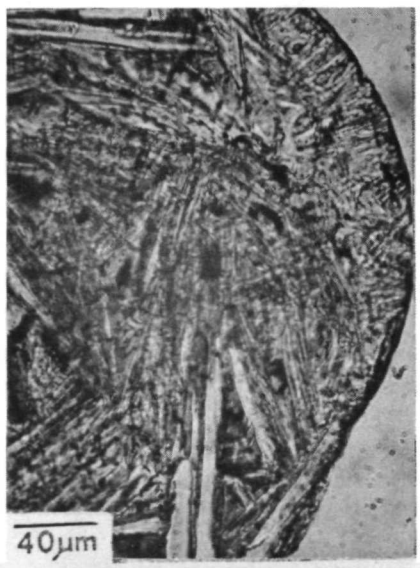

Fig. 6. Optical photograph of thin-section of sphere in Fig. 2 taken through the largest hemisphere showing continuity of structure between host sphere and attached hemisphere.

SILICATE MINERAL CHEMISTRY OF APOLLO SOIL 66081,5. H.C. Jim Taylor and James L. Carter, The University of Texas at Dallas, The Institute for Geological Sciences, Box 30365, Dallas, Texas 75230. Contribution no. 229.

Feldspars, pyroxenes, and olivines from Apollo 16 comprehensive sample 66081,5, collected at STA. 6 near the base of Stone Mountain (1), were analyzed in order to characterize these constituent phases chemically, with the ultimate aim of determining which local rock types may have contributed to the makeup of this soil. Major element concentrations in these principal soil minerals were determined by electron microprobe analysis of fragments in the 35 to 75 micron fraction of this sample.

Plagioclase fragments are the most abundant mineral phase in soil 66081, constituting about 9% of the particles in the 62.5 to 125 micron fraction, with agglutinates and glass particles making up about 70% (1). Microprobe analyses show these plagioclase fragments to be characterized by a high An content and a low total iron content expressed as FeO. Most plagioclase fragments range in composition from An_{93} to An_{97} and are distinctly low in iron, with FeO less than 0.3 wt. %. Such low iron contents are distinctive, relative to normally greater iron contents of feldspar from typical mare basalts (2). Whereas feldspars from KREEP commonly are low in iron, similar to those of 66081,5 feldspars, the KREEP feldspars contain a wide range of An values with many values lower than An_{90}. Thus, the feldspars from 66081,5 are unlike most mare and KREEP feldspars.

Pyroxenes constitute only about 3% of the particles present in the 62.5 to 125 micron fraction (1). Orthopyroxene fragments are approximately four times as abundant as clinopyroxene. The chemically defined orthopyroxenes range in composition from $En_{81}Wo_3Fs_{16}$ to $En_{70}Wo_4Fs_{26}$, whereas the clinopyroxenes range in composition from $En_{45}Wo_{41}Fs_{14}$ to $En_{36}Wo_{44}Fs_{20}$. The chemical analyses allow them to be termed bronzites and diopsidic augites, respectively. Plots of Ti vs. Al (atoms per formula unit) show two distinct groupings with the more Mg-rich orthopyroxenes plotting near Ti/Al = 1/4 and the more Fe-rich orthopyroxenes and the clinopyroxenes plotting near Ti/Al = 1/2. The lack of pyroxenes with intermediate Ti vs. Al ratios seems to infer a break in genetic relations between these two mineral groups and offers evidence for the origin of this soil as a mixture of two distinct rock types. A sparcity of intermediate metastable pyroxenes, the lack of progressive iron enrichment of pyroxenes toward pyroxferroite compositions, and the high percentage of Mg-rich pyroxenes are all prominent features of soil 66081,5 and enable one to distinguish these pyroxenes from mare-type pyroxenes. These criteria establish the lack of mare basalt component in this Apollo 16 soil sample.

Olivine fragments in the 35 to 75 micron fraction of soil 66081,5 constitute about 3% of the particles present in this soil and therefore exist in approximately equal quantities to pyroxene fragments, in comparison to the apparent lack of olivine reported in the 62.5 to 125 micron fraction of soil 66081 by the PET (1). Olivine fragments range in composition from Fo_{91} to Fo_{62}. The more Mg-rich members are thus distinct from Fe-rich olivines of mare basalts. The 66081,5 olivines contain less than 0.1 wt. % TiO_2 and less

SILICATE MINERAL CHEMISTRY

H. C. Jim Taylor

than 0.2 wt. % CaO, whereas Reid et al. (2) shows that CaO exceeds 0.2 wt. % in many mare, KREEP, and highland basalt olivines. The 66081,5 olivines, like the pyroxenes, are thus consistent with a non-mare origin and also offer evidence against a KREEP origin.

The chemical characteristics of this suite of minerals thus allow the 66081 soil to be distinguished from both mare and KREEP basalt soil components and present some evidence that two distinct, although possibly related, rock types have contributed to the soil mineralogy. These data also support the hypothesis that at least one of the parent rocks was olivine normative and therefore relatively undersaturated in silica. The lack of iron enrichment in the pyroxenes, the lack of pyroxenes demonstrating intermediate calcium values, the relative abundance of orthopyroxenes compared to clinopyroxenes, the Mg-rich character of the pyroxenes and some olivines, and the high An content of the plagioclase fragments are all features characteristic of crystallization in a plutonic environment of high-alumina, low-iron bulk chemistry.

The bulk chemistry of soil 66081,5 (1, Table 2), falls within the compositional range of the ANT (anorthositic-noritic-troctolitic) group of lithic fragments, glasses, and chondrules (3, Table 1). In keeping with the evidence that this soil may consist of at least two distinct rock types, a mixture of mineral fragments from two rocks of the ANT group, such as an anorthositic component plus a mafic or ultramafic component could be combined in the form of a breccia which might then have the bulk chemistry of an anorthositic gabbro.

Soil sample 66081 is described as an indurated clod of white impact ejecta; possibly from South Ray crater, but in a location generally shadowed from South Ray ejecta (4). The origin of this white impact ejecta is thus unknown. The possibility exists that downslope mass wasting of material from Stone Mountain could have transported the material to its sampling site where comminution occurred. The relationship of 66081 to other samples collected in the Descartes area is yet to be determined.

REFERENCES

(1) Apollo 16 Preliminary Examination Team, Science 179, 23, 1973.
(2) Reid, A. M., Warner, J. L., Ridley, W. I., and Brown, R. W., Luna 20 Soil: Abundance and Composition of Phases in the 45-125-Micron Fraction, Lunar Science Institute (preprint), 45p.
(3) Kurat, G., Keil, K., Prinz, M., and Nehru, C. E., Chondrules of Lunar Origin, Proc. 3rd. Lunar Sci. Conf., Geochim. Cosmochim. Acta 1, (Suppl. 3), 707, 1972.
(4) Apollo Lunar Geology Investigation Team, Interagency Rept.: Astrogeology 51, p. 121, 1972.

We acknowledge NASA Grant NGL-44-004-001 and NGR-44-004-116, Suppl. #1.

MORPHOLOGY AND CHEMISTRY OF PARTICLES FROM APOLLO 17 SOILS 74220, 74241 AND 75081

James L. Carter: University of Texas at Dallas, P.O. Box 30365, Dallas, Texas 75230
H.C. Jim Taylor and Elaine Padovani

Particles from these soils formed in a cloud of siliceous vapors. The melt was produced by large energetic impacts or by volcanism. The volcanic origin is favored because of the lack of shocked material and complex flow structures, the low content of metallic iron and the complex chemical zoning on a μm scale in the minerals. The lack of hypervelocity-type impact-produced craters and the old age of the orange soil (74220) suggests that it was laid down, rapidly covered and more recently exposed. The dark mantle material (75081) on the other hand has numerous impact-produced craters primarily less than 1 μm in diameter which suggests that it has been exposed for a longer period to micrometeoritic bombardment or that it has been in the high velocity portion of an impact-produced debris cloud [1, 2].

Selected fragments from soils 74220,87, 74241,46 and 75081,52 were examined by scanning electron microscope and scanning electron microprobe techniques. Orange soil 74220 consists primarily of dark orange brown non-vesicular glass, which occurs as transparent homogeneous (variation between and within particles is similar) rounded forms such as beads, wafers and tear drops, and two types of opaque particles, one having dust-welded surfaces (Fig. 1) and the other being layered with alternating layers of glass and quench-like olivine (Fo_{84-67}). This later type of particle has an average composition similar to the transparent homogeneous orange brown glass forms (Table 1). A feathery quench-like Ti-rich oxide phase (possibly ilmenite) and a Cr-ulvospinel approximately 1 μm in diameter occur between the olivine and glass. Cr-ulvospinel occurs more rarely as individual hollow crystals up to 5 μm in diameter (Table 1) in the glass. As shown by Table 1 the interstitial glass in these layered particles is preferentially depleted in these phases particularly in the olivine component. Other opaque particles in the soil are ilmenite, Cr-ulvospinel and metallic iron (5 wt. % Ni) with ilmenite the most abundant. These particle types along with basaltic and breccia rock fragments and other mineral fragments occur in soils 74241 and 75081. Agglutinated glass particles are rare in soils 74220 and 74241 but are common in soil 75081.

The opaque, dust-welded, particles consist of a transparent colorless glass core of highland basalt composition (Table 1) surrounded by welded particles of ilmenite, Cr-ulvospinel, orange glass, plagioclase and olivine. The particles of welded dust and the quench-like feathery Ti-rich oxide phase and other opaque phases contribute to the opaque nature of these particles. This type of particle is especially abundant in soil 74241 and contributes to its grey color.

	Orange	"Barred" Particle			
Wt.%	Glass	Glass	Olivine	Ulvospinel	Dust Coated
SiO_2	38.0	39.6	35.8	0.7	45.2
TiO_2	8.87	11.8	1.4	29.4	0.49
Al_2O_3	5.51	7.58	0.3	3.3	23.4
Cr_2O_3	0.70	0.55	0.6	10.6	0.17
FeO	22.4	21.4	27.1	47.8	6.77
MgO	14.5	6.73	34.6	3.8	9.25
CaO	6.99	11.1	0.5	0.5	14.0
Na_2O	0.39	0.48	0.0	0.1	0.30
K_2O	0.06	0.06	0.0	0.0	0.06
Total	97.42	99.27	100.3	96.2	99.71

Table 1. Chemical analysis of particles from 74220. Orange glass average of sixteen analyses.

All glass surfaces have a siliceous coating up to 0.2 μm in thickness that is composed of spherules up to 0.1 μm in diameter in a film-like matrix which is enriched in silicon and depleted in iron relative to the substrate. Very few metallic iron mounds were found but numerous large mounds and knobs of silicate material similar in composition to the host are present primarily on the opaque layered forms (Fig. 2). The contact between mounds and host substrates may be continuous or discontinuous (Fig. 2) suggesting a range in temperatures between host substrates and impacting silicate material. Quench-like olivine and ilmenite appear as surface expressions. One unusual surface particle consists of a core of CaS surrounded by material containing only K and S as shown by energy dispersive techniques. This type of material has not been recorded in lunar material.

No hypervelocity type impact-produced features occur on the surfaces of the particles from soil 74220 and craters less than 0.5 μm in diameter are rare. The transparent glass forms commonly have one smooth and shiny side, with or without micro-chips, while the opposite side has a frosted appearance optically due to the presence of scratches and low velocity impact-produced craters reminiscent of features produced in the heated target experiments just above the softening point of the glass [2]. The central pit contains a complex web-like flow structure of composition similar to the host (Fig. 3). In contrast to the particles from soil 74220 the surfaces of particles from the dark mantle soil 75081 have numerous impact-produced craters primarily less than 1 μm in diameter. The larger craters have a smooth surfaced central pit.

It is suggested from these data that the opaque orange particles formed in the upper portion of a cloud of siliceous vapors and liquid droplets. The mounds and knobs of material with a composition similar to the homogeneous host formed as the particles fell back through the cloud, possibly similar to a volcanic fire fountain on Earth. The transparent smooth surfaced rounded forms did not fall through the cloud and quenched in the cold environment of the moon. The particles were not tumbling in the cloud because low velocity impact-produced features occur mainly on one side. The cloud may have resulted from an energetic large impact event or volcanism. The lack of shocked material and complex flow structures in the glass, and the low content of surface metallic iron favors a volcanic origin. Since lunar soil contains hydrogen and carbon from solar wind bombardment, metallic iron would be produced by reduction processes during meterotic impact melting of iron rich silicates and oxides [3]. This type of melting results in porous glasses of variable composition [4]. It follows then that if the orange soil (74220) is impact produced, a large volume of material must have been melted, degassed and homogenized. This would not be obtained by bombardment of lunar soil with micrometeroids but may be in very large energetic impacts.

The chemistry of the minerals from soil 74220 add additional evidence with regard to the origin of this material and is consistent with a volcanic origin. The pyroxenes are dominantly clinopyroxenes with only one orthopyroxene and twenty nine clinopyroxenes. The clinopyroxenes are Mg-pigeonites, augites, salites, ferroaugites and subcalcic ferroaugites. These features are reminiscent of low pressure rapid crystallization environments on Earth. This observation is consistent also with the small grain size (on a μm scale) and sharp chemical zoning of these clinopyroxenes on a μm scale.

The olivines offer further evidence of a low pressure rapid crystallization environment. Most of the olivines are associated with orange glass, either as devtrification or quench products within orange glass or as particles with fragments of orange glass adhering to their surfaces. The unusually high Cr_2O_3 content of these olivines (0.35 wt. % to 0.80 wt. %) and the high CaO content (0.3 wt. % to 0.6 wt. %) of these olivines is consistent also with a low pressure rapid crystallization environment. However, these features may reflect the Cr_2O_3 and CaO contents of the probably genetically related orange glass.

The plagioclases range in composition from $An_{95.9}$ to $An_{73.8}$ with a mole percent Or component less than 1.1. They have a wide range of FeO contents ranging from 0.06 wt. % to 0.98 wt. %. The wide range in both An and FeO contents is consistent also with a low pressure rapid crystallization environment. Admixtures of plagioclase from mare basalts (FeO greater than 0.3 wt. %) as well as highland basalt and possibly KREEP (FeO usually less than 0.3 wt. %) may also contribute to this wide spread of values.

The presence of dark brown, highly vesicular, particles in soil 75081 (Fig. 4) is consistent also with a volcanic origin. This type of particle has angular unshocked fragments of plagiocalse and clinopyroxene with exsolution lamellae in a matrix of clinopyroxene crystals that range in diameter from 2 μm to 5 μm and plagioclase laths that are 0.5 μm wide and 2 μm long. No rock fragments were seen in these particles.

Acknowledgments: We thank J.B. Toney for technical assistance. Supported by NASA Grant NGR-44004-116. Cont. No. 238.

References:
[1] Carter,J.L. (1971). Proc.2nd.Lunar Sci.Conf.,Geochim. Cosmochim.Acta,Suppl.2, Vol.1, 873-892. M.I.T. Press.
[2] Carter,J.L. and D.S.McKay (1971). Proc.2nd Lunar Sci. Conf.,Geochim.Cosmochim. Acta,Suppl.2,Vol.3, 2653-2670. M.I.T. Press.
[3] Carter,J.L. and D.S.McKay (1972). Proc.3rd Lunar Sci. Conf.,Geochim.Cosmochim.Acta,Suppl.3,Vol.1,953-970. M.I.T. Press.
[4] McKay,D.S. and G.Ladle (1971).Proc.4th Ann.SEM Symp., 177-184, I.I.T. Res.Inst., Chicago.

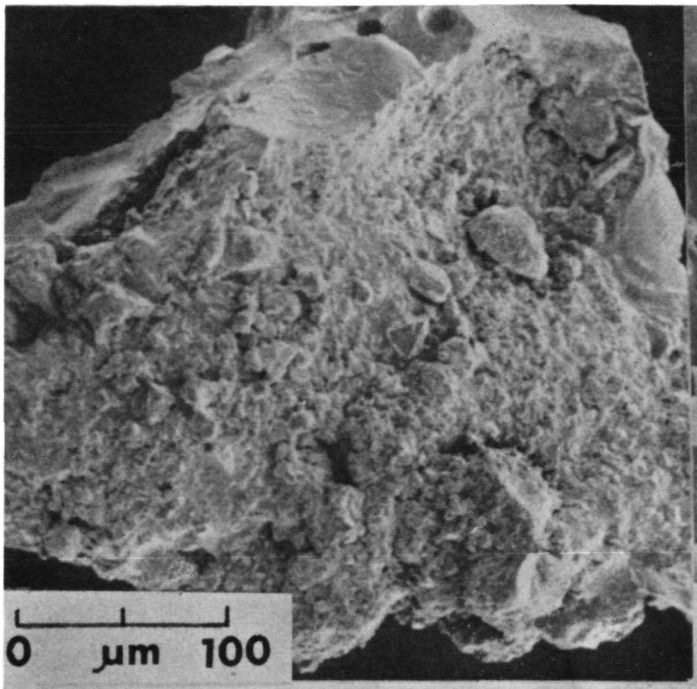

Fig.1. Particles welded to surface of highland basalt glass.

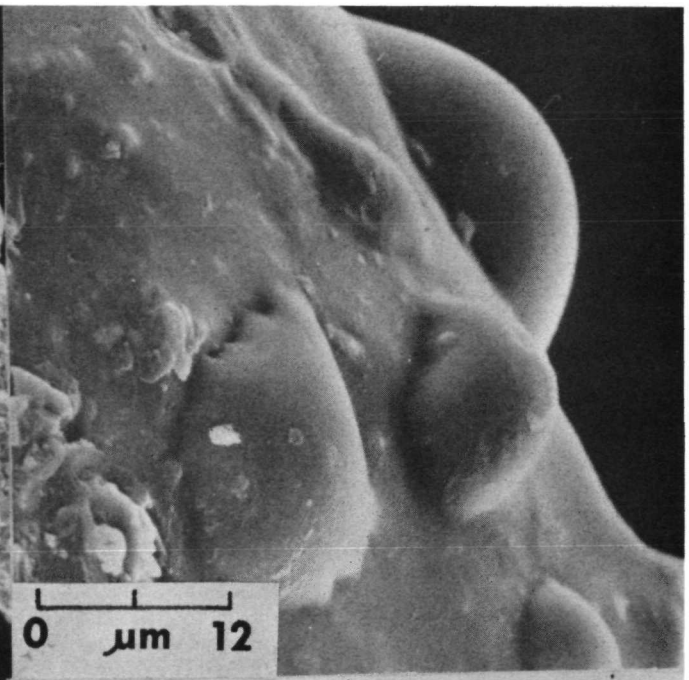

Fig.2. Mounds of composition similar to substrate.

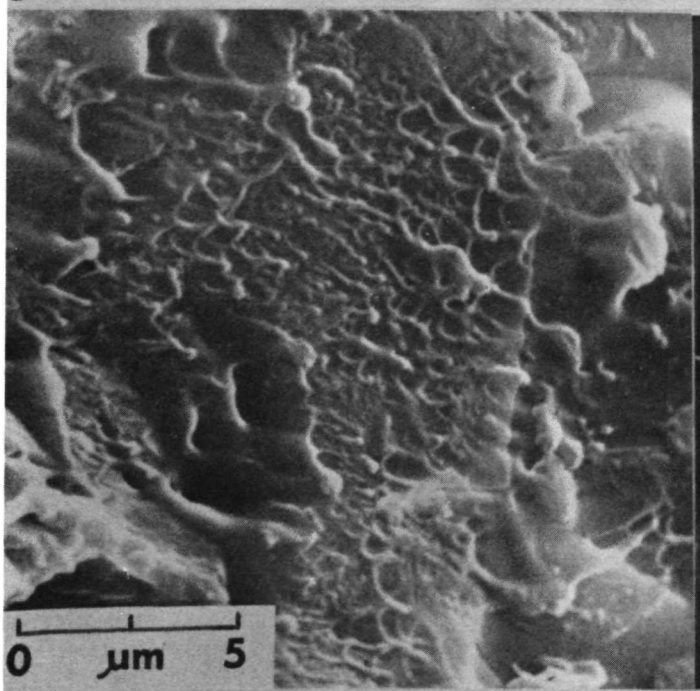

Fig.3. Web-like silicate material in center of impact pit.

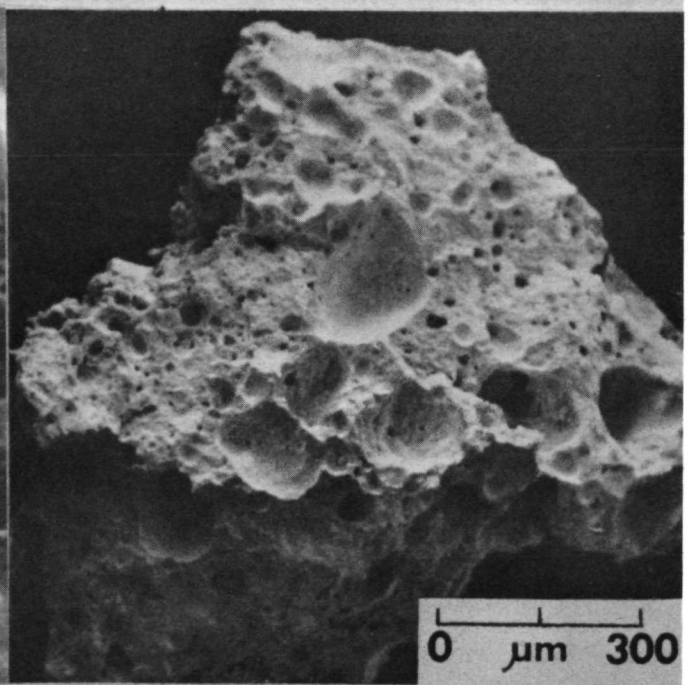

Fig.4. Very vesicular fine-grained volcanic-like particle.

Reprinted from:
"31st Ann. Proc. Electron Microscopy Soc. Amer."
New Orleans, La., 1973. C. J. Arceneaux (ed.).

VAPOR-LIQUID-SOLID WHISKER GROWTH ON LUNAR BRECCIA 15015

James L. Carter and D. L. Crosthwait, Jr. 1)

The University of Texas at Dallas, P.O. Box 30365, Dallas, Texas 75230.
1) Texas Instruments, Inc., P.O. Box 5012, Dallas, Texas 75222.

Possible VLS (Vapor-Liquid-Solid) whisker growth has been discovered for the first time in nature on the surface of lunar breccia 15015. Rock 15015 was collected on the Apollo 15 flight and is blocky, angular, largely glass-covered, almost 30 cm long and weighs 4.5 kg [1]. A 62 mm^2 glass-covered surface of a fragment of 15015 (15015,36) was coated with 150 Å of Au and selected areas studied in detail with a JEOLCO JSM-1 scanning electron microscope (SEM) [2], an ARL scanning electron microprobe (EMX SM) with a QANTA/METRIX energy dispersive spectrophotometer [2] and a Cambridge MK IIA SEM at Texas Instruments, Inc. of Dallas. The study of the surface of breccia 15015 [2] showed that 1) the siliceous coating was outgassing while solidifying, 2) it has numerous mounds of metallic iron and complex mixtures of metallic iron and sulfur, 3) there were at least four nucleation events resulting in mounds with average diameters in μm of 45, 19, 10 and 0.2, 4) the sulfur was supplied from an external source such as a meteoritic impact-generated cloud, 5) the iron was supplied both from an impact-generated cloud and by in situ reduction of the liquid siliceous surface and 6) it has patches that range from 0.4 μm to 400 μm in longest dimension consisting of rods and spherules that distort the EMX SM secondary electron image.

Investigation of the nature of these patches by means of montages and stereoscopic SEM photographs reveals that they occur 1) on "high" areas on the glass siliceous surface (Fig. 1), 2) on the surface of minerals that protrude through the glass surface (Fig. 2) and 3) on the surface of irregularly shaped metallic iron mounds that surround the silicate mineral "islands" (Fig. 3), but they do not occur on the surface of the intervening siliceous glass [2]. More detailed characterization of the surface morphology of a patch at Texas Instruments, Inc. revealed dendritic structures (rods) with bulbous heads similar in appearance to VLS growth [3] (Fig. 4). The bulbs are a maximum of 0.2 μm in diameter and the rods are a maximum of 0.15 μm in diameter. Rod length varies from 2 to 10 times bulb diameter. Elemental analysis from EMS SM and energy dispersive X-ray techniques indicates the presence of iron and sulfur in the bulbs but no sulfur in the rods which confirm the possibility of VLS. Wagner and Ellis [3] proposed a growth mechanism envolving vapor, liquid and solid phases to explain many laboratory observations of the effect of impurities in crystal growth. The proposed VLS growth on the surface of lunar rock 15015 is the first recognized in nature. Since this proposed VLS growth probably occurred in a meteoritic impact situation on the lunar surface, it may have been an important growth mechanism in the early accretionary history of the Earth and in other planetary situations where an appreciable oxidizing atmosphere is absent. Finally, since the metallic iron rods are either single domain or pseudo-single domain due to shape anisotropy, they may affect strongly the magnetic properties of rock 15015 and contribute to its hard magnetic component [4].

This work was supported by NASA Grant NGR-44004-116. Contribution No. 236.
[1] Apollo 15 Prelim. Sci. Rpt., NASA, Was. D.C., NASA SP-289, 5-49, 1972.
[2] James L. Carter, The Apollo 15 Lunar Samples (ed. by J.W. Chamberlain and C. Watkins), The Lunar Sci. Inst., Houston, Texas, 51, 1972.
[3] R. S. Wagner and W. C. Ellis, Appl. Phys. Letters, 89, 1964.
[4] D. J. Dunlop, Lunar Sci. IV (abs.), 4th. Lunar Sci. Conf. (ed. by J.W. Chamberlain and C. Watkins), The Lunar Sci. Inst., Houston, Texas, 193, 1973.

Reprinted from:
"31st Ann. Proc. Electron Microscopy Soc. Amer."
New Orleans, La., 1973. C. J. Arceneaux (ed.).

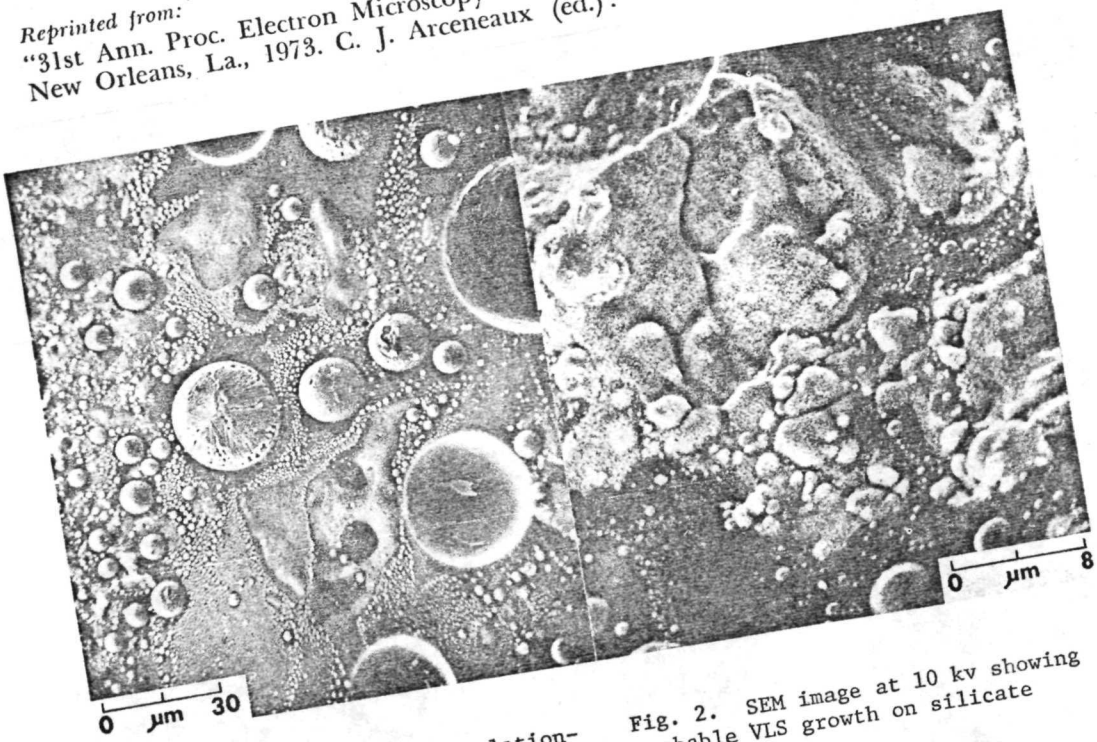

Fig. 1. SEM image showing relationship of mounds to probable VLS patches on "high" areas of glass surface.

Fig. 2. SEM image at 10 kv showing probable VLS growth on silicate mineral.

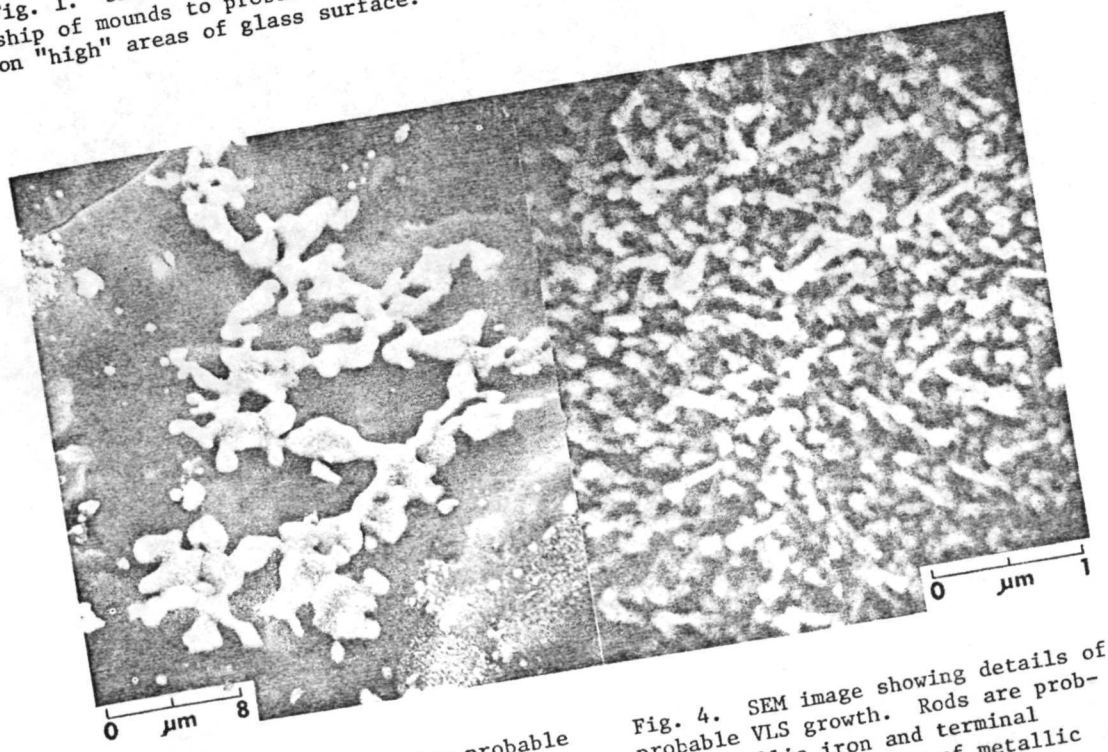

Fig. 3. SEM image showing probable VLS growth on surface of irregularly shaped metallic iron mounds.

Fig. 4. SEM image showing details of probable VLS growth. Rods are probably metallic iron and terminal spherules are mixtures of metallic iron and sulfur.

VLS (Vapor-Liquid-Solid): A Newly Discovered Growth Mechanism on the Lunar Surface?

by

James L. Carter

Contribution No. 235. Institute for Geological Sciences, The University of Texas at Dallas, Dallas, Texas, P. O. Box 30365, 75230.

ABSTRACT

Probable VLS (Vapor-Liquid-Solid)-type growth has been discovered for the first time in nature on the surface of lunar rock 15015. It occurs as probable metallic iron stalks from <0.015-0.15 μm in diameter with bulbous tips from <0.03-0.2 μm in diameter consisting of a mixture of iron and sulfur. Stalk length varies from 2 to 10 times bulb diameter.

INTRODUCTION

Astronauts David Scott and James Irwin on the Apollo 15 mission collected a blocky, angular, largely glass-covered breccia (15015) almost 30 cm long and weighing 4.5 kg [1]. The sample is the third largest one returned and no other rock of comparable size was in the collection area [1]. It was collected approximately 20 m west of the LM + Z footpad [1].

A 62 mm^2 glass-covered surface of a fragment of breccia 15015 (15015,36) was coated with approximately 150 Å of gold and selected areas studied by scanning electron microscope (SEM), scanning electron microprobe (SEMP) and energy dispersive X-ray (EDX) techniques [2]. The chemical and morphological nature of the surface features in the selected areas including numerous mounds of both metallic iron and complex mixtures of metallic iron and iron sulfide have been described in detail by Carter [2]. He also noted peculiar patches that ranged from 0.4 μm to 400 μm in longest dimension consisting of stalks with bulbous tips that distorted the scanning electron microprobe secondary electron image. This paper examines the nature of these patches and suggests that they are the result of VLS (Vapor-Liquid-Solid)-type growth [2,3,5].

VLS-TYPE GROWTH

Investigation of the siliceous glass surface of rock 15015 by means of montages and stereoscopic SEM photographs reveals that the patches occur on 1) "high" areas on the glass siliceous surface [2] (Figs. 1 and 2), 2) surface of minerals that protrude through the glass surface [2] (Fig. 1) and 3) surface of irregularly-shaped metallic iron mounds that surround the silicate mineral "islands" [2]. Patches do not occur on the surface of the intervening siliceous glass. The "high" areas are surface expressions of high points on the rock

substrate that were covered by a thin layer of siliceous melt which quenched faster than the thicker areas of melt. Examination of a patch at high magnification reveals that they are composed of a series of stalks with bulbs on their tips [2,5] (Figs. 3 and 4). The bulbs vary from less than 0.03 μm to 0.2 μm in diameter (Figs. 3 and 4), and the stalks vary from less than 0.015 μm to 0.15 μm in diameter (Figs. 3 and 4). Stalk length varies from 2 to 10 times bulb diameter.

DISCUSSION AND CONCLUSIONS

From SEMP and EDX data, the bulbs are probably a mixture of iron and sulfur, whereas the stalks are metallic iron [2]. However, because of the extremely small size of these structures it is not possible to ascertain precisely their chemistry. However, the chemical data and the morphological relationships are consistent with the stalks and bulbs being the result of a VLS-type growth mechanism operating in the lunar environment during a meteoritic impact event. This type of growth mechanism involving vapor, liquid and solid phases was proposed by Wagner and Ellis [3] to explain many observations of the effect of impurities in crystal growth from a vapor in laboratory experiments. Crystals formed in this way are usually of very pure composition and structure.

This proposed VLS-type growth on the surface of lunar rock fragment 15015,36 is the first recognized in nature. Since the metallic iron stalks are either single domain or pseudo-single domain due to shape anisotropy, they may affect strongly the magnetic properties of this rock and contribute to its hard magnetic component [4]. Low-grade metamorphic breccia produced from soil containing these VLS-type metallic iron needles would then contain metallic iron needles of single or pseudo-single domain type [4].

Since VLS-type growth has probably occurred in many impact situations on the lunar surface, it may have been an important growth mechanism in the early accretionary history of the Earth especially before it acquired an appreciable oxidizing atmosphere, and in other planetary situations.

REFERENCES AND NOTES

1] Apollo 15 Preliminary Science Report. National Aeronautics and Space Administration, Washington D. C., NASA SP-289, 5-49, 1972.

2] J. L. Carter, In "The Apollo 15 Lunar Samples" (edited by J. W. Chamberlain and C. Watkins), The Lunar Sci. Inst., Houston, Texas, 51, 1972. J. L. Carter, Proc. 5th Lunar Sci. Conf., Geochim. Cosmochim. Acta (in press).

3] R. S. Wagner and W. C. Ellis, Appl. Phys. Letters, 89, 1964. R. S. Wagner and W. C. Ellis, Trans. AIME 233, 1053, 1965.

4] D. J. Dunlop, In "Lunar Sci. IV" (edited by J. W. Chamberlain and C. Watkins), The Lunar Sci. Inst., Houston, Texas, 193, 1973.

5] I thank D. L. Crosthwait, Jr. of Texas Instruments, Inc., Dallas, Texas for introducing the author to the concept of VLS-type growth. I thank D. S. McKay of the Lyndon Baines Johnson Space Center, Houston, Texas for taking the high magnification SEM photographs shown on the cover and in Fig. 4. I thank J. B. Toney for technical assistance. Supported by NASA Grant NGR-44-004-116. Contribution No. 235, The Institute for Geological Sciences, The University of Texas at Dallas.

FIGURE CAPTIONS

Fig. 1. SEM photogrpah showing nature of probable VLS-type growth on "high" area and on silicate mineral "island".

Fig. 2. SEM photograph showing relationship of probable VLS-type growth on "high" area to metallic iron mounds.

Fig. 3. Enlarged view of center of Fig. 2 showing probable VLS-type growth of stalks with bulbous tips.

Fig. 4. Enlarged view of center of photograph on cover showong details of probable VLS-type growth. Stalks are probably metallic iron and bulbous tips are probably mixtures of iron and sulfur.

COVER CAPTION

Scanning electron microscope photographs of selected area of surface of lunar rock fragment 15015,36 showing the first discovery of probable VLS (Vapor-Liquid-Solid)-type growth in nature. 22,000X. Photograph courtesy of D. S. McKay, Lyndon Baines Johnson Space Center, Houston, Texas.

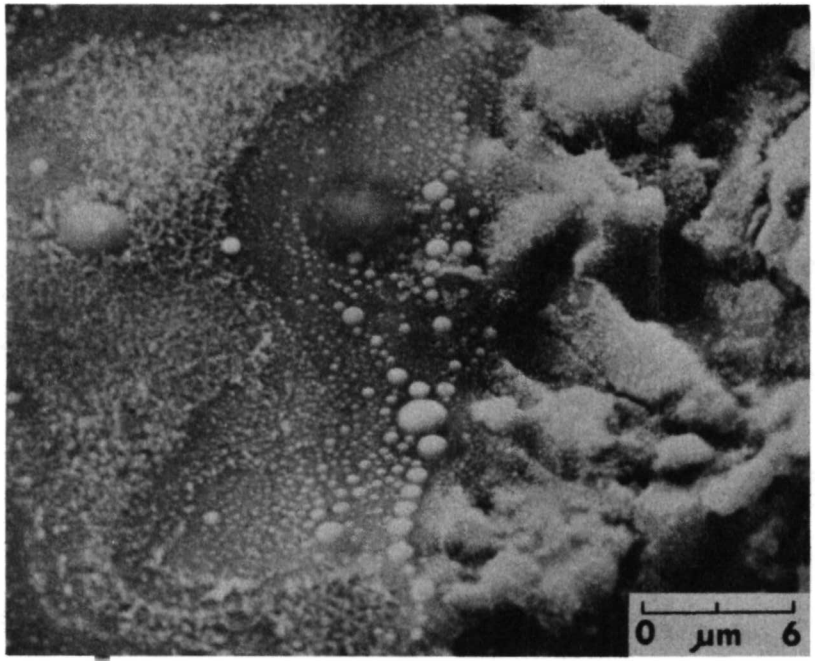

1

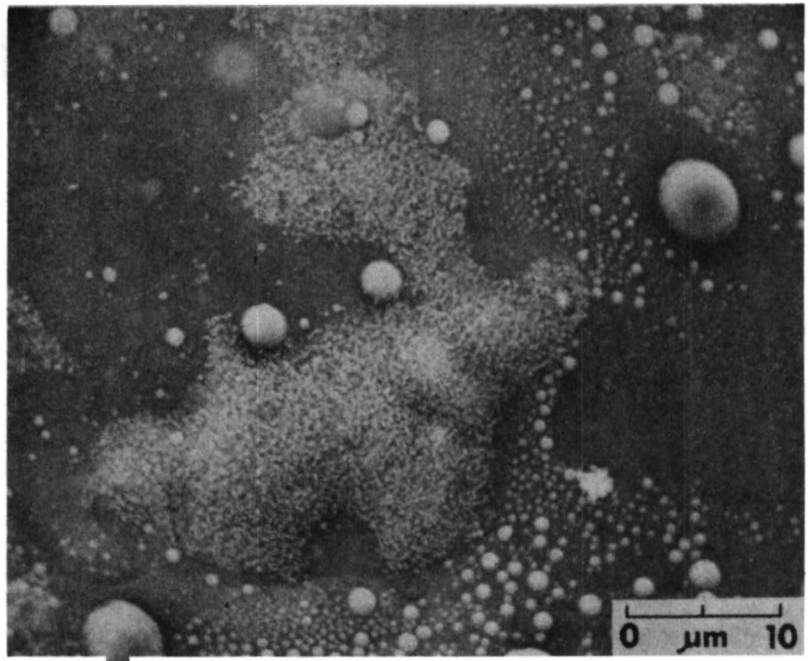

2

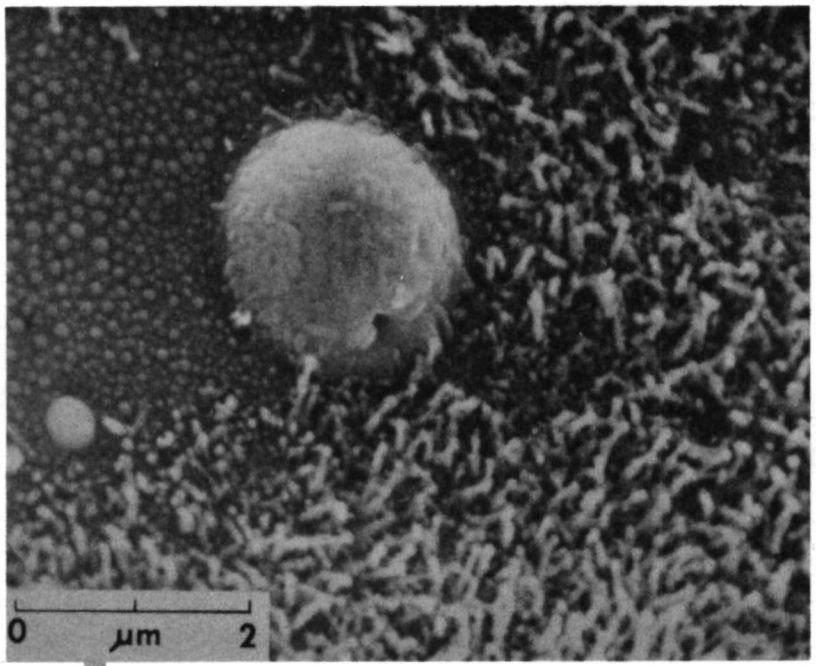

3

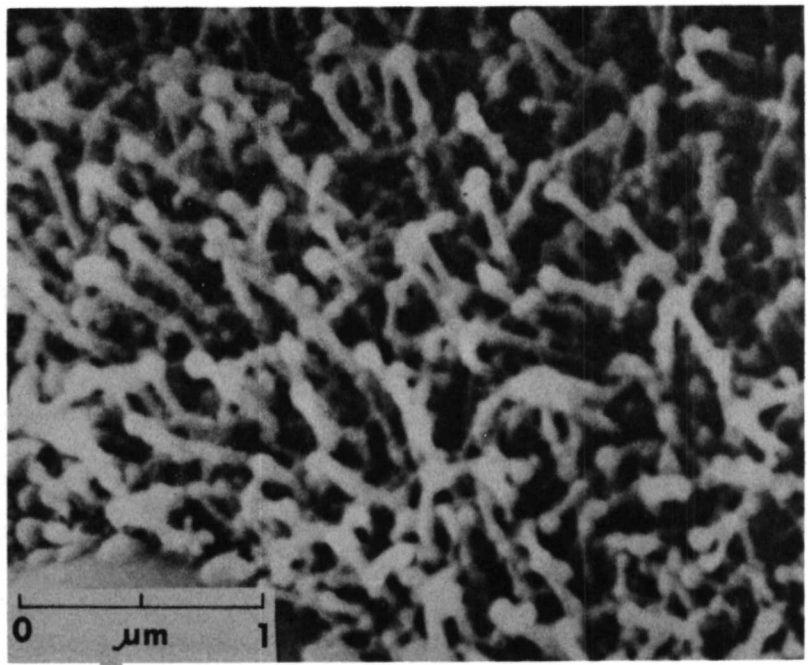

4

Genetic Implications of Some Unusual Particles in Apollo 16 less than 1 mm fines 68841,11 and 69941,13

by

James L. Carter

and

Elaine Padovani

University of Texas at Dallas

The Institute for Geological Sciences

P. O. Box 30365

Dallas, Texas 75230

Contribution No. 241, The Institute for Geological Sciences, University of Texas at Dallas, Dallas, Texas 75230.

ABSTRACT

The less than 1 mm fines 68841,11 (light-colored ray ejecta) and 69941,13 (dark-colored ray ejecta) from South Ray Crater contain unusual types of metallic particles and silicate spheres with textured surfaces. The metallic particles consist of two types: rounded forms and irregularly-shaped forms. The rounded forms have euhedral crystals of schreibersite (18.6 wt. % Ni) intergrown with metallic iron (4.1 wt. % Ni, 0.8 wt. % Co), FeS and chemically defined bornite (Cu_5FeS_4). The irregularly-shaped forms have low contents of schreibersite, are intergrown with plagioclase laths and olivine and have well-developed crystals of hydrated iron oxide probably lepidocrocite on their surfaces. It is suggested that this material formed in a hot impact ejecta blanket or in an igneous environment and later was exposed by meteoritic impact.

The silicate spheres have a porous surface consisting of a network of plagioclase laths that formed during quenching of melts of essentially highland basalt composition. Most sphere surfaces are free of angular debris but have attached spherules and hemispheres of the same composition and texture as the host sphere. The original melt could be either impact-produced or volcanic in origin. The volcanic hypothesis is favored because of 1) the apparent relative homogeneity of the original silicate melt, 2) the similar composition of the spheres and the attached spherules and hemispheres, 3) the general lack of surface debris, 4) the apparent lack of shocked debris and 5) the apparent lack of metallic iron of meteoritic composition within the spheres.

INTRODUCTION

A principal objective of the Apollo 16 mission was to study the lateral variation and petrology of the Cayley Formation between North and South Ray Craters (Apollo 16 Preliminary Science Report, 1972). Evidence for layering in the Cayley Formation is seen in the stratigraphic sections exposed at North and South Ray Craters suggesting a light colored and a dark colored layer, which may be two major sources of debris on the Cayley Plains. The light and dark material from the rays at South Ray Craters may represent material from these two layers in the Cayley Formation. This ray material provides the only igneous rocks collected by the Apollo 16 crew and may represent large clasts from the deepest breccias sampled at this locality (Apollo 16 Preliminary Science Report, 1972).

Selected particles from the less than 1 mm fines 68841,11 (light-colored ray ejecta) and 69941,13 (dark-colored ray ejecta) from South Ray Crater were examined by optical, scanning electron microscope (SEM), scanning electron microprobe and energy dispersive X-ray techniques to characterize them. These samples contain particles comparable to those reported by the Apollo 16 Preliminary Science Report (1972). In addition, they contain fragments and beads of green glass and several types of unusual particles (Carter and Padovani, 1973). The unusual particles consist of complex, metallic objects of various shapes with or without hydrated iron oxides, and surface textured alumina-rich silicate spheres with attached spherules of similar composition having quench-like textures.

METALLIC PARTICLES

The metallic particles consist of two types: rounded forms (Fig. 1) and irregularly-shaped forms (Fig. 5). The particles from fines 68841 shown by

Fig. 1 is composed of well-developed interlocking euhedral crystals of schreibersite (Fig. 2) intergrown with large crystals of metallic iron with patches of plagioclase on their surfaces (Fig. 1; Table 1). FeS (Fig. 3; Table 1) and chemically defined bornite (Cu_5FeS_4) (Fig. 4; Table 1) occur in minor amounts. Bornite has not been reported previously from lunar materials. In this particle, it is found in contact with metallic iron and possibly iron sulfide, an occurrence that implies a moderate temperature environment during its formation (Yund and Kullerud, 1966). From Table 1 it appears that the chemically defined bornite has excess Fe and S. This could result from 1) admixed FeS, 2) X-ray signal from substrate FeS or 3) solid solution of S with an X-ray signal from substrate Fe. The latter implies a moderately low temperature of formation (Kullerud, 1963). FeS occurs as irregularly-shaped, plate-like patches (Fig. 3), but not as distinct crystals. However, it occurs with euhedral outlines in the interior of the sphere where it is enclosed in schreibersite. Metallic iron and schreibersite (Figs. 1 and 2) show well-developed crystal habit with the latter superimposed on the growth steps of the former (Fig. 2) in some occurrences. The schreibersite contains approximately 18.6 wt. % nickel and the metallic iron 4.1 wt. % nickel (Table 1), which suggests also a relatively low temperature of formation (Doan and Goldstein, 1970).

The second type of metallic particle occurs in fines 69941 and is irregular in shape with metallic iron as its chief constituent with minor FeS (Fig. 5). Intergrown plagioclase laths occur on the surface (Fig. 6) along with patches of deep ruby-red to orange red material that have a crackled appearance similar to that of a dessicated gel (Figs. 7 and 8). This material occurs also as well-developed hollow box-like twinned crystals (Fig. 8). It

occurs commonly in the contact between the silicate minerals, especially olivine, and metallic iron (see also El Goresy et al., 1973). Microprobe and energy dispersive data show it to be composed of approximately 81 wt. % iron expressed as Fe_2O_3, 2-6 wt. % NiO, 1-2 wt. % Cl, less than 1 wt. % SO_3 and minor amounts of Ca, K and Si. The hydrated material deteriorates under the electron beam bombardment. Taylor (1973, personal communication) observed a rate of 5% increase in iron per minute with 0.2 μamps of beam current for similar material. This suggests the presence of volatiles, probably H_2O.

We suggest that this crystallized material is lepidocrocite formed through the hydration of lawrencite. This hydrated material appears to have formed later than the debris-coated surfaces of the iron particles because impact pits are present in small numbers on the surfaces of some of the metallic grains but are not observed on the hydrated material. The apparent absence of impact pits on the hydrated material does not rule out the possibility that the hydration products were initiated on the lunar surface and formed over a long time span, or that it formed after the metallic iron was exposed to bombardment. A possible source of water on the moon is the reduction of iron-bearing materials to metallic iron by remobilized meteoritic carbon and trapped solar wind components in the lunar soil (Carter and McKay, 1972).

SURFACED TEXTURED SILICATE SPHERES

A second type of unusual particle which is characteristic of the less than 1 mm fines 69941 consists of silicate spheres of essentially highland basalt composition with textured surfaces (Figs. 9 to 18). The surfaces of these spheres are porous and are made up of a network of plagioclase crystals (An_{95-96}) in devitrified (?) glass. Most sphere surfaces are free of angular debris but have attached spherules and hemispheres of the same composition

and texture as the host sphere (Figs. 9, 10 and 13 to 18; see also Carter and Padovani, 1973). Enlarged views of the plagioclase network are shown in Figs. 10 and 15. The porosity is a result of the reduction of volume as liquid pulled away from the plagioclase network during quenching. The large impact feature seen on the hemisphere in Fig. 9 appears to have formed after the crystals, because the surfaces of adjacent plagioclase laths have been wetted and partially covered by splashed glass flowage from the pit rim.

The origin of the attached hemispheres and spherules is somewhat of an enigma. If these features formed by extrusion of material during the volume reduction which accompanies crystallization, one would expect some kind of deformation of the host sphere which is not seen (Figs. 9, 11 and 13). Agrell et al. (1973) have shown several stages of hemispherically-shaped glass accumulations on green glass particles from Apollo 15 fines. Glassy particles from the Apollo 17 orange fines 74220, which have quench-like olivine crystals, also have rounded attachments of various shapes (Carter et al., 1973; McKay and Heiken, 1973). The host particles of the Apollo 17 materials have a wide range in shapes. The attached rounded siliceous materials show more extensive wetting of the host and are more variable in shape than those described on the Apollo 16 silicate spheres (Carter and Padovani, 1973) and generally are more variable than those described on Apollo 15 green glass spheres (Agrell et al., 1973; McKay et al., 1973a,b).

Doubly-polished thin-sections of several characteristic sphere types were made for further detailed studies. A transmitted light optical microscope photograph of the thin-section of the particle shown in Fig. 9 is seen in Fig. 11. This section shows a texture of sub-parallel and interlocking laths of plagioclase (Figs. 11 and 12). These textures show remarkable

similarity to those formed by quenching mixtures of olivine and plagioclase from high pressure experimental studies (Presnall, 1973, personal communication). The spherical opaque phases which occur interstitially between the plagioclase laths as shown by the reflected light photograph in Fig. 12 consist of round grains of iron sulfide (FeS) with minor amounts of euhedral iron crystals containing 0.5 wt. % Ni.

In contrast to the particle seen in Figs. 9 to 12, the silicate sphere seen in Fig. 13 has complex iron mounds on its surface. The mounds are characterized by a waist of FeS and a center composed of a mixture of metallic iron (with 5 wt. % Ni) and schreibersite (up to 30%) (Figs. 15 to 18). The mounds occur in meandering trains across the smoother portions of the silicate host (Fig. 16) and along the edges of the plagioclase crystals (Fig. 15). This suggests that the high temperature solidification of iron caused the siliceous melt in these areas to quench last and that the crystallization of plagioclase occurred subsequently. Also present on this surface are amoeboid-like mounds of metallic iron (Fig. 18). Similar types of mounds were produced in the hydrogen reduction experiments of Carter and McKay (1972). No shocked mineral fragments were observed in these silicate spheres.

DISCUSSION AND CONCLUSIONS

The presence of ZnS and PbS in metallic particles or in the hydrated iron oxides (El Gorsey et al., 1973, oral presentation, 4th. Lunar Sci. Conf.) and the presence of chemically defined bornite (Cu_5FeS_4) suggests that the oxidation may have been initiated on the lunar surface (Taylor et al., 1973). The presence of silicate minerals intergrown with metallic iron (see also Brett et al., 1973) suggest that the material may have formed in a hot impact ejecta blanket or in an igneous environment and later exposed by a meteoritic

impact. This would be consistent with the findings of Williams and Gibson (1972) on the stability of hydrated iron oxide under lunar conditions. The absence of microcraters on the hydrated iron oxide but their presence in very small numbers on iron crystals suggests that the hydrated iron oxide formed later than the metallic iron and after it was exposed to bombardment. The presence of microcraters on the surface of the hydrated iron oxide would be unequivocal evidence for the formation of that material on the moon.

The origin of the surface texture on the silicate spheres is germane to the origin of these spheres. There are two principal possibilites; either it resulted from devitrification of glass, or it resulted from quenching of a melt (Carter and Padovani, 1973). If it resulted from devitrification of glass, these particles may be chondrules, probably of lunar origin because of their high feldspar content (King et al., 1972; Kurat et al., 1972). An apparent lunar chondrule with a similar but not identical surface texture is shown by Cavarretta et al. (1972). The box-like network and the metallic mounds on their sides and in meandering trains demonstrates that the texture resulted from quenching of a melt and the hollow network resulted from pulling away of the melt into the interior as a result of volume reduction on crystallization. Therefore this texture is a quench texture.

The original melt could be either impact-produced or volcanic in origin. As a working hypothesis, the volcanic hypothesis is favored because of 1) the apparent relative homogeneity of the original silicate melt, 2) the similar composition of the spheres and the attached silicate spherules and hemispheres, 3) the general lack of surface debris, 4) the apparent lack of shocked debris (Stöhle, 1972) and 5) the apparent absence within the spheres of metallic iron with meteoritic nickel-cobalt ratios. The similarity of features

between the Apollo 15 green glass spheres, the Apollo 17 orange glass spheres and these Apollo 16 surface textured spheres suggests a similar mode of origin. The Apollo 17 orange glass spheres have been interpreted by Carter et al. (1973) and by McKay and Heiken (1973) as possibly resulting from a fire fountain type of eruption. This origin is also favored by McKay et al. (1973b) for the Apollo 15 composite green glass spheres. On the other hand Roedder and Weiblein (1973) suggests a meteoritic impact into a liquid lava lake for the formation of the orange glass spheres. This would require unique timing for the formation of lavas of different ages with their subsequent impact to form these similar types of composite spheres at different localities.

An impact into a lava lake with a hardened crust would eject fragments of the hardened crust and mix them with the molten ejecta. Such fragmental debris has not been observed admixed with the green glass spheres (Agrell et al., 1973; Carusi et al., 1972; McKay et al., 1973b) or reported from the Apollo 17 materials. Furthermore, later meteoritic impacts into a solidified lava lake would result in rock fragments of composition similar to the molten lava. Only two possible rock equivalents of the Apollo 15 green glass have been reported (Prinz et al., 1973), and no rock fragments equivalent to the Apollo 17 orange glass have been reported. However, Roedder and Weiblen (1973) believe that the relatively minor differences in composition between the orange glass and the various available high-titanium mare basalt samples are readily explicable and hence not of serious import. Because the volcanic working hypothesis is based on few data, it should not be considered as compelling without the confirmation of additional studies of large numbers of particles from different localities.

ACKNOWLEDGEMENTS

Supported by NASA Grant NGR-44-004-001. We thank J. B. Toney for technical assistance. We thank D. S. McKay for taking the SEM photograph shown in Fig. 8. We thank J. L. Linday, E. King, Jr. and H. C. J. Taylor for critically reviewing the manuscript.

REFERENCES

Apollo 16 Preliminar Science Report (1972) National Aeronautics and Space Administration, NASA-SP-315, pp. 6-1,81.

Agrell, S. O., Agrell, J. E. and Arnold, A. R. (1973) Observations on glass from 15425, 15426, 15427. In "Lunar Science IV" (editors J. W. Chamberlain and C. Watkins) pp. 12-14, Lunar Science Institute, Houston.

Carter, J. L. and McKay, D. S. (1972) Metallic mounds produced by reduction of material of simulated lunar composition and implications on the origin of metallic mounds on lunar glasses. "Proc. Third Lunar Sci. Conf., Geochim. Cosmochim. Acta" Suppl. 3, Vol. 1, pp. 953-970. MIT Press.

Carter, J. L. and Padovani, E. (1973) Genetic implications of Apollo 16 soil particles. In "Lunar Science IV" (editors J. W. Chamberlain and C. Watkins) pp. 121-123, Lunar Science Institute, Houston.

Carter, J. L., Taylor, H. C. J. and Padovani, E. (1973) Morphology and chemistry of particles from Apollo 17 soils 74220, 74241 and 75081. Trans. Am. Geop. Union, Vol. 54, No. 6, pp. 582-584.

Cavarretta, G., Coradini, A., Funiciello, R., Fulchignoni, M., Taddeucci, A. and Trigila, R. (1972) Glassy particles in Apollo 14 soil 14163,88: Peculiarities and genetic considerations. "Proc. Third Lunar Sci. Conf., Geochim. Cosmochim. Acta" Suppl. 3, Vol. 1, pp. 1085-1094. MIT Press.

Doan, A. S., Jr. and Goldstein, J. I. (1970) The ternary phase diagram, Fe-Ni-P. Met. Trans. Vol. 1, pp. 1759-1767.

El Goresy, A., Ramdohr, P. and Medenback, O. (1973) Lunar samples from the Descartes site: Mineralogy and geochemistry of the opaques. In "Lunar Science IV" (editors J. W. Chamberlain and C. Watkins) pp. 222-224, Lunar Science Institute, Houston.

King, E. A., Jr., Butler, J. C. and Carman, M. F. (1972) Chondrules in Apollo 14 samples and size analyses of Apollo 14 and 15 fines. "Proc. Third Lunar Sci. Conf., Geochim. Cosmochim. Acta" Suppl. 3, Vol. 1, pp. 673-686. MIT Press.

Kullerud, G. (1963) The Cu-Fe-S system. Ann. Rpt. Geop. Lab. Carnegie Inst. of Washington Year Book 63. pp. 200-202.

Kurat, G., Keil, K., Prinz, M. and Nehru, C. E. (1972) Chondrules of lunar origin. "Proc. Third Lunar Sci. Conf., Geochim. Cosmochim. Acta" Suppl. 3, Vol. 1, pp. 707-721. MIT Press.

McKay, D. S. and Heiken, G. H. (1973) Petrography and scanning electron microscope study of Apollo 17 orange and black glass. Trans. Am. Geop. Union, Vol. 54, No. 6, pp. 599-600.

McKay, D. S., Clanton, U. S. and Ladle, G. H. (1973a) Surface morphology of Apollo 15 green glass spheres. In "Lunar Science IV" (editors J. W. Chamberlain and C. Watkins) pp. 484-486, Lunar Science Institute, Houston.

McKay, D. S., Clanton, U. S. and Ladle, G. H. (1973b) Scanning electron microscope study of Apollo 15 green glass (ed. see this issue).

Prinz, M., Dowty, E. and Keil, K. (1973) A model for the origin of orange and green glasses and the filling of mare basins. Trans Am. Geop. Union, Vol. 54, No. 6, pp. 605-606.

Roedder, E. and Weiblen, P. W. (1973) Origin of orange glass spherules in Apollo 17 sample 74220. Trans. Am. Geop. Union, Vol. 54, No. 6, pp. 612-613.

Stähle, V. (1972) Impact glasses from the suevite of the Nordinger Ries. Earth and Planetary Sci. Lett., Vol. 17, No. 1, pp. 275-293.

Taylor, L. A., Mao, H. K. and Bell, P. M. (1973) Apollo 16 "rusty" rock 66095. In "Lunar Science IV" (editors J. W. Chamberlain and C. Watkins) pp. 715-716, Lunar Science Institute, Houston.

Williams, R. J. and Gibson, E. K. (1972) The origin and stability of lunar goethite, hematite and magnetite. Earth and Planetary Sci. Lett., Vol. 17, No. 1, pp. 84-88.

Yund, R. A. and Kullerd, G. (1966) Thermal stability of assemblages in the Cu-Fe-S system. Jour. of Petrology, Vol. 7, Pt. 3, pp. 454-488.

FIGURE CAPTIONS

Fig. 1. SEM view of metallic spherules from less than 1 mm fines 68841 consisting of inertlocking crystals of schreibersite and metallic iron with minor amounts of FeS and bornite (Cu_5FeS_4).

Fig. 2. Enlarged SEM view of bottom of Fig. 1 showing schreibersite crystal on metallic iron growth steps.

Fig. 3. Enlarged SEM view of upper right of Fig. 1 showing structure of FeS.

Fig. 4. Enlarged SEM view of lower right of Fig. 1 showing nature of bornite on metallic iron substrate.

Fig. 5. SEM view of irregularly-shaped metallic iron particle from less than 1 mm fines 69941.

Fig. 6. Enlarged SEM view of top-right of Fig. 5 showing nature of plagioclase laths intergrown with metallic iron.

Fig. 7. Enlarged SEM view of center left of Fig. 5 showing nature of hydrated iron oxide. Note dessicated appearance of surface and areas of crystallization.

Fig. 8. Enlarged SEM view of lower left of Fig. 5 showing details of hollow box-like twinned crystals of lepidocrocite (?).

Fig. 9. SEM view of surface textured silicate sphere from less than 1 mm fines 69941 showing attached hemispheres of silicate material of similar composition and texture as sphere.

Fig. 10. Enlarged SEM view of top of Fig. 9 showing details of the porous surface of plagioclase laths produced during quenching of melt of essentially highland basaltic composition.

Fig. 11. Transmitted light optical photograph of thin section of sphere shown in Fig. 9.

Fig. 12. Enlarged Reflected light optical view of center of Fig. 11. Dark gray laths are plagioclase. Light gray is devitrified (?) glass. Very light gray circular areas are FeS.

Fig. 13. SEM view of surface textrued silicate sphere from less than 1 mm fines 69941 with attached spherules of silicate material of similar composition and texture as the sphere. Note also large mounds of metallic iron (center and lower right).

Fig. 14. Enlarged SEM view of lower left of Fig. 13 showing nature of attached silicate hemisphere.

Fig. 15. Enlarged SEM view of center-left of Fig. 14 showing details of porous surface of plagioclase laths on attached silicate spherule. Metallic iron mounds with a waist of FeS occur on the edges of the plagioclase laths.

Fig. 16. Enlarged SEM view of bottom of Fig. 13 showing details of metallic iron mound development on surface of sphere. Mounds occur in trains on relatively smooth areas and not on the textured areas.

Fig. 17. Enlarged SEM view of metallic iron mound on bottom of sphere in Fig. 13 showing details of waist of iron sulfide. Textured surface of metallic iron mound results from intergrown schreibersite.

Fig. 18. Enlarged SEM view of unusual amoeboid-like metallic iron mound on surface of sphere in Fig. 13 (central area).

TABLE CAPTION

Table 1. Wt. % of elements in coexisting phases in metallic sphere from less than 1 mm fines 68841. Values in parenthesis are for stoichiometric bornite.

Table 1.

Wt. %	Fe(Ni,Co)	$(Fe,Ni)_3P$	FeS	Cu_5FeS_4
Fe	94.6	64.6	63.1	12.7 (11.1)
Ni	4.1	18.6	0.08	0.07
Co	0.8	0.35	0.09	0.2
Cu	0.0	0.0	0.0	60.7 (63.3)
S	0.01	0.08	35.8	26.2 (25.6)
P	0.12	15.6	0.04	0.1
Total	99.63	99.23	99.21	99.97

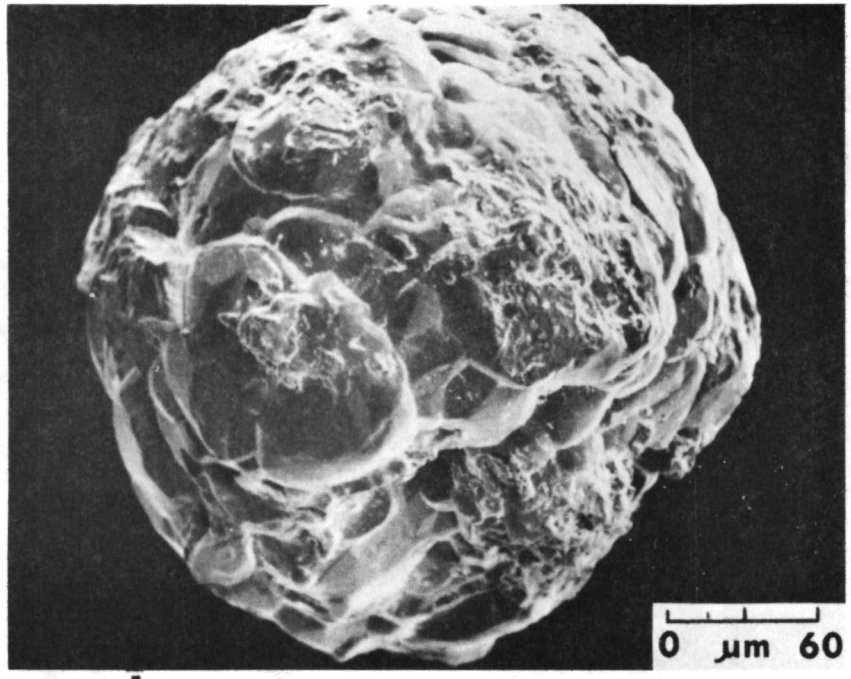

1

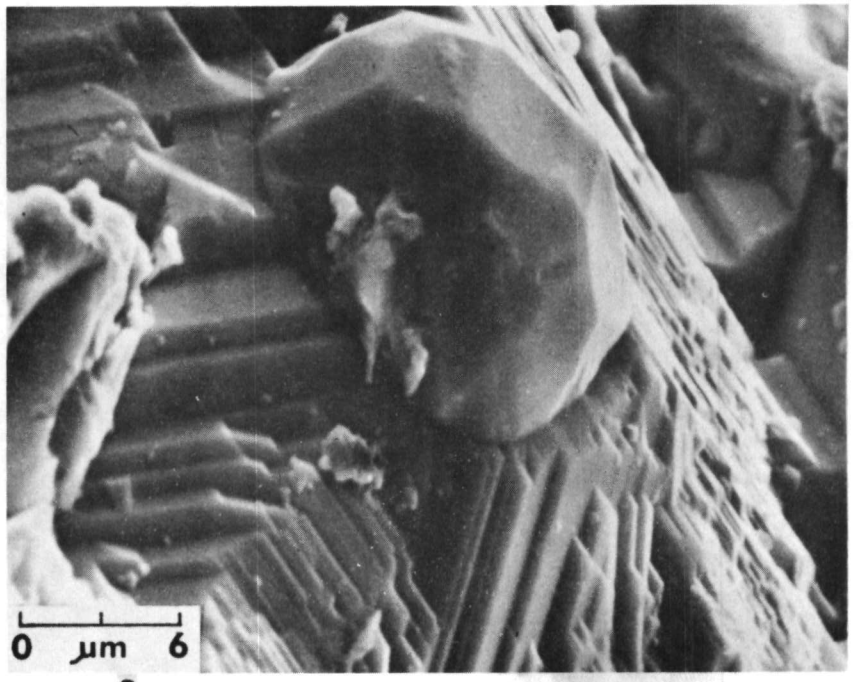

2

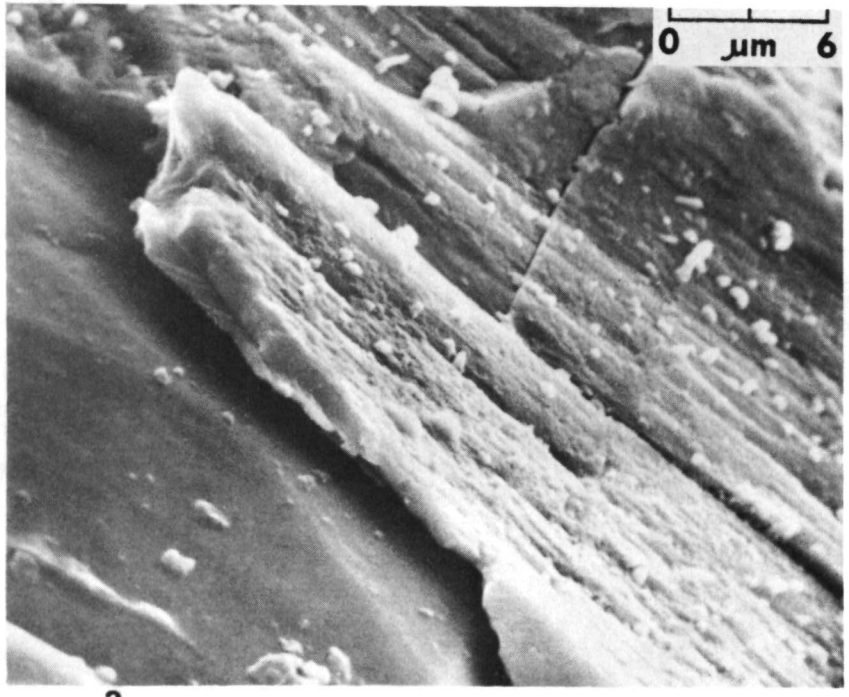

3

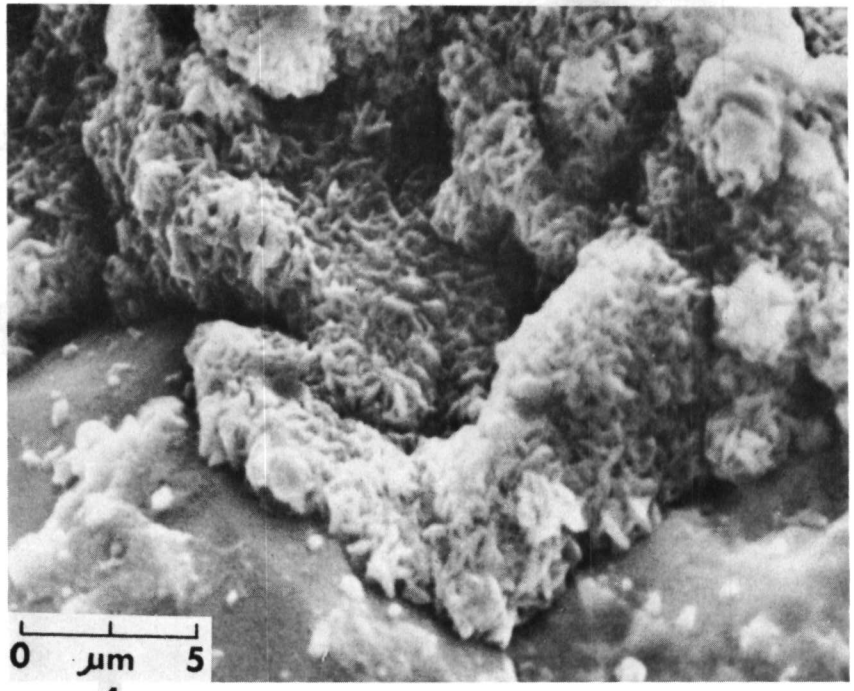

4

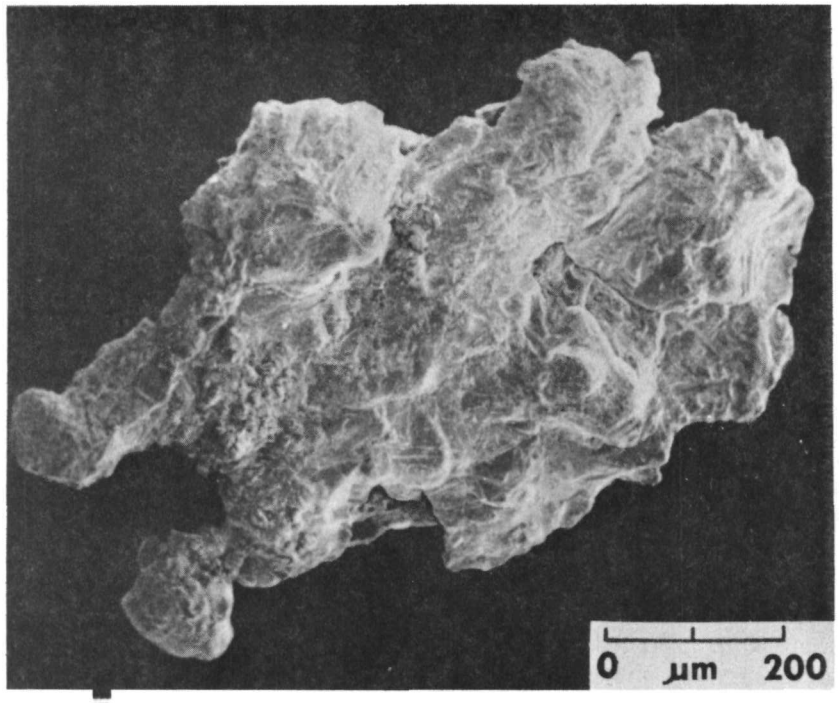

5

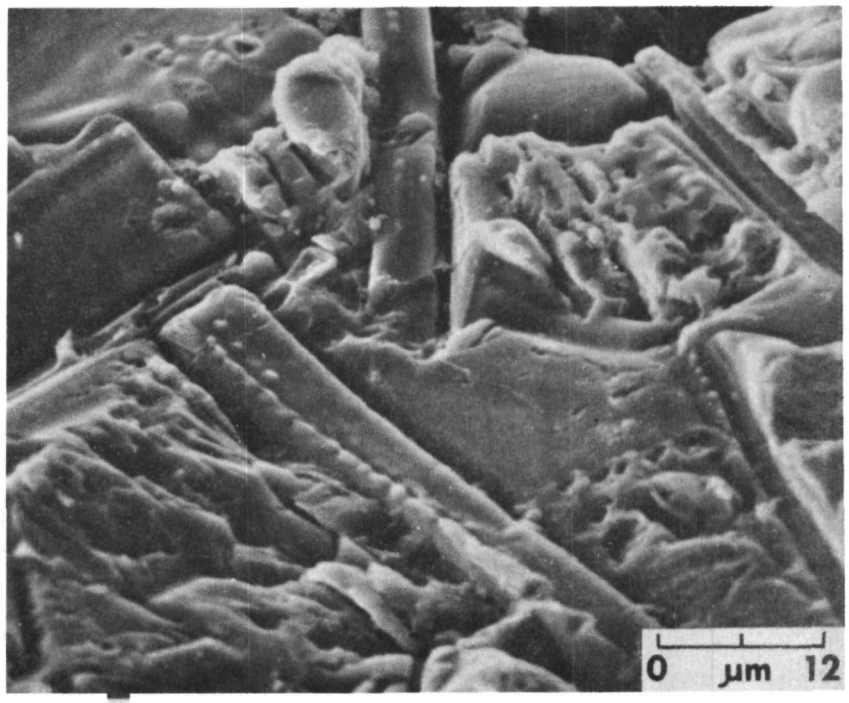

6

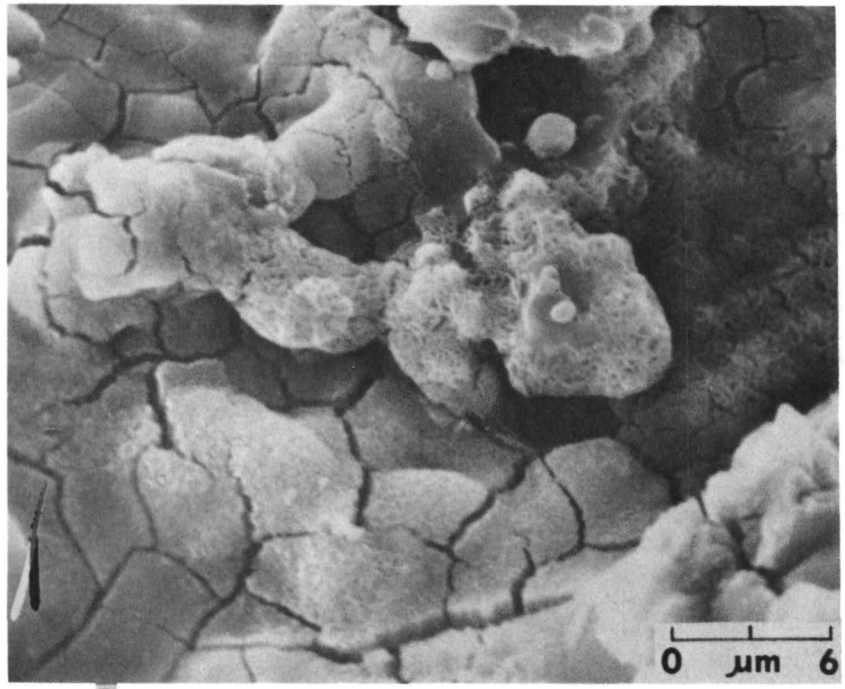

7

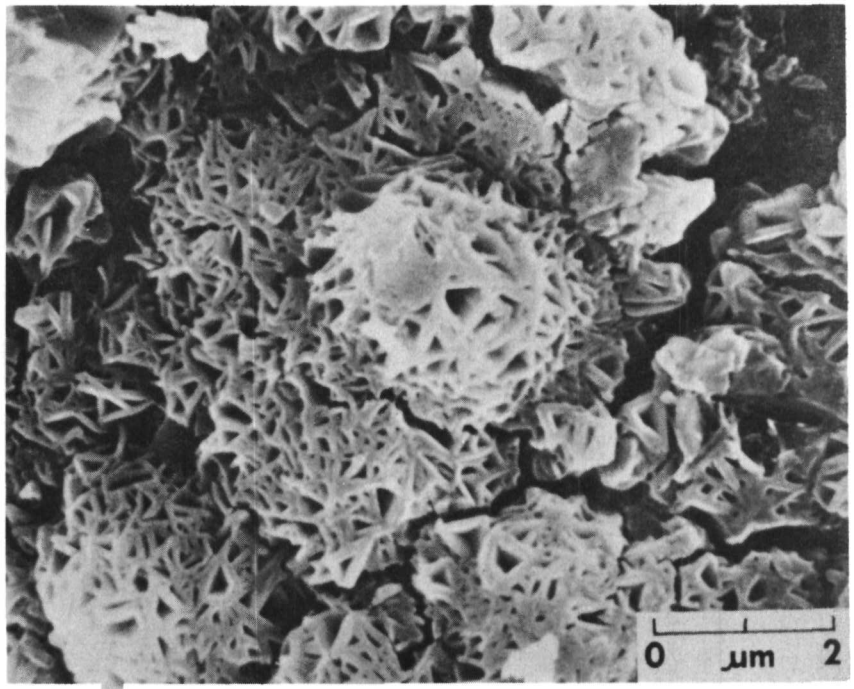

8

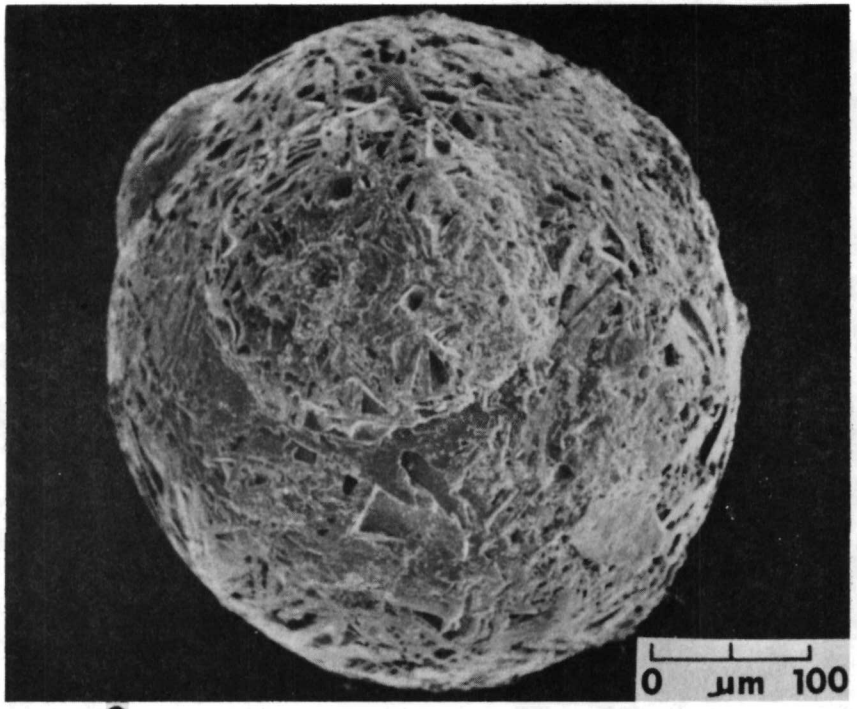

9

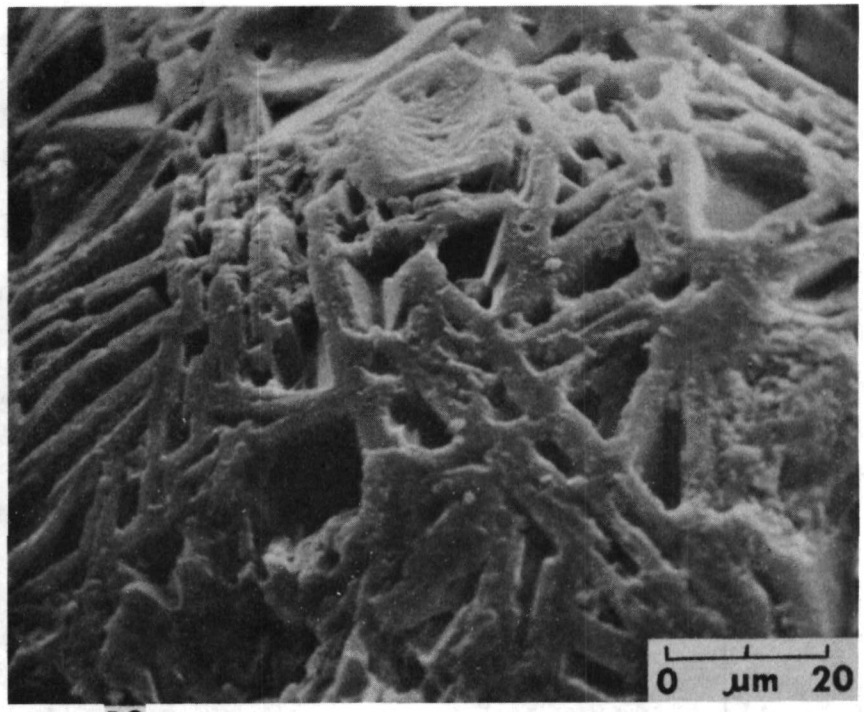

10

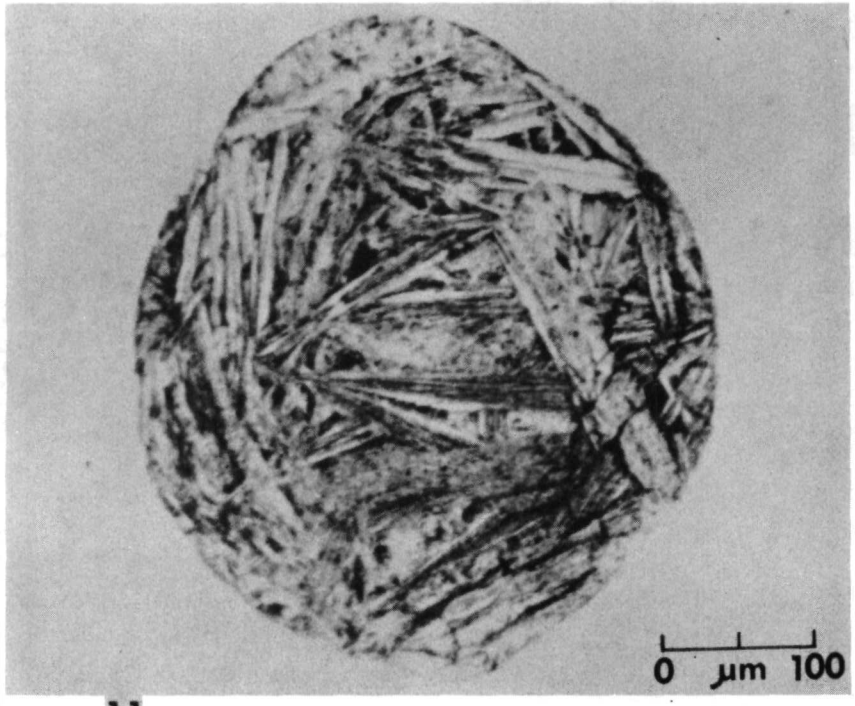

11

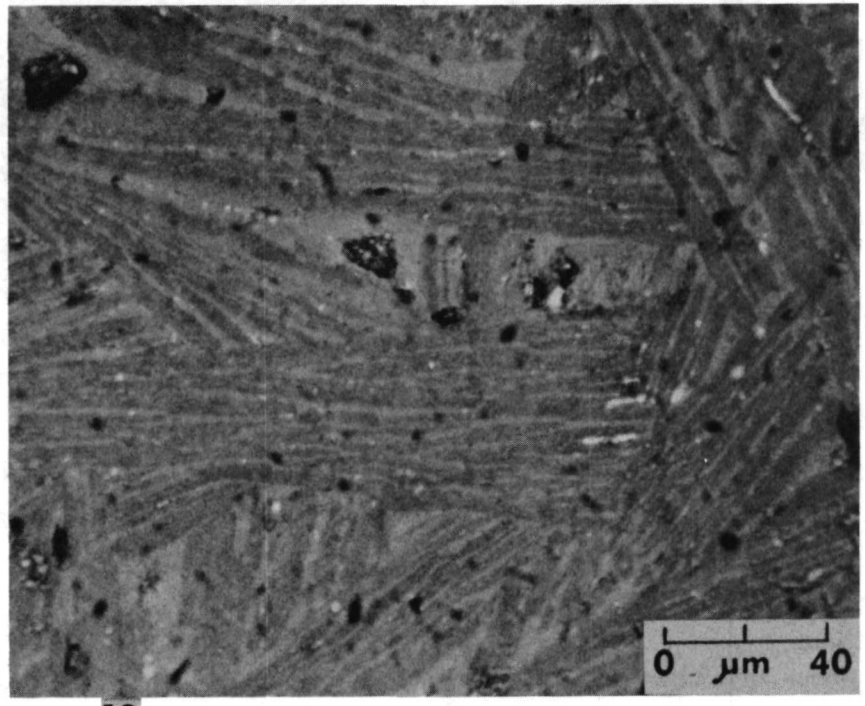

12

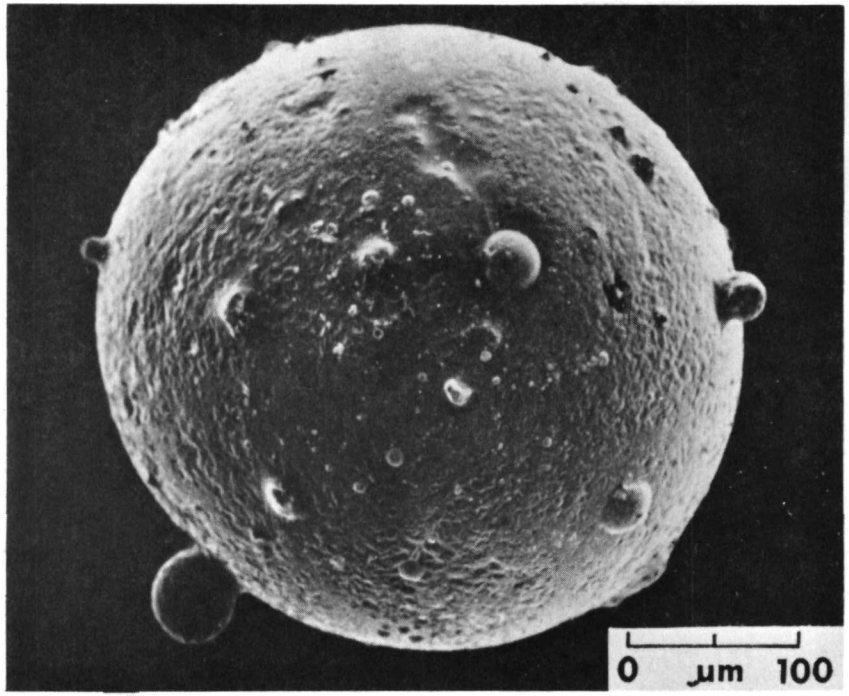

13

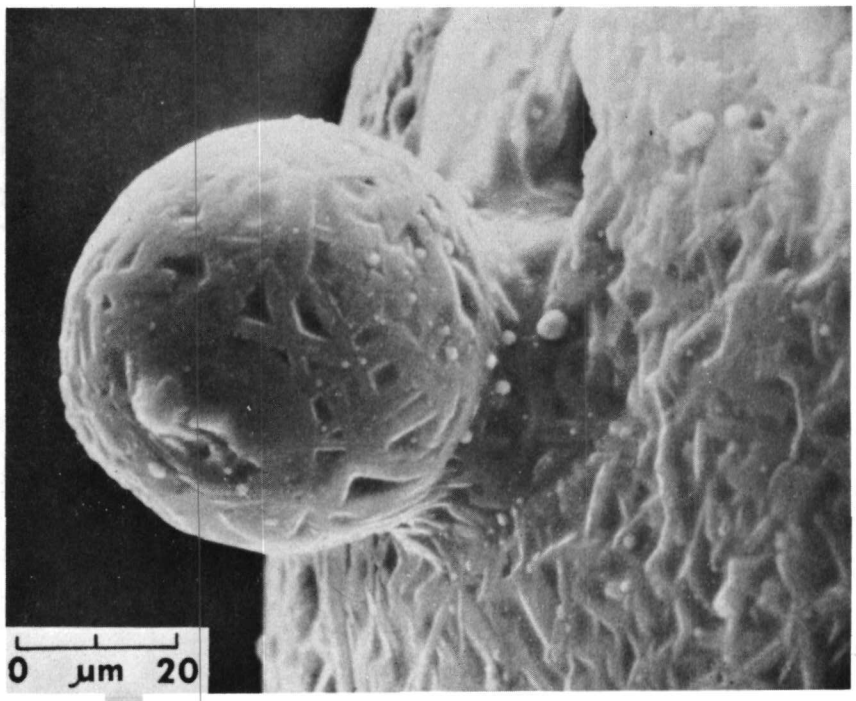

14

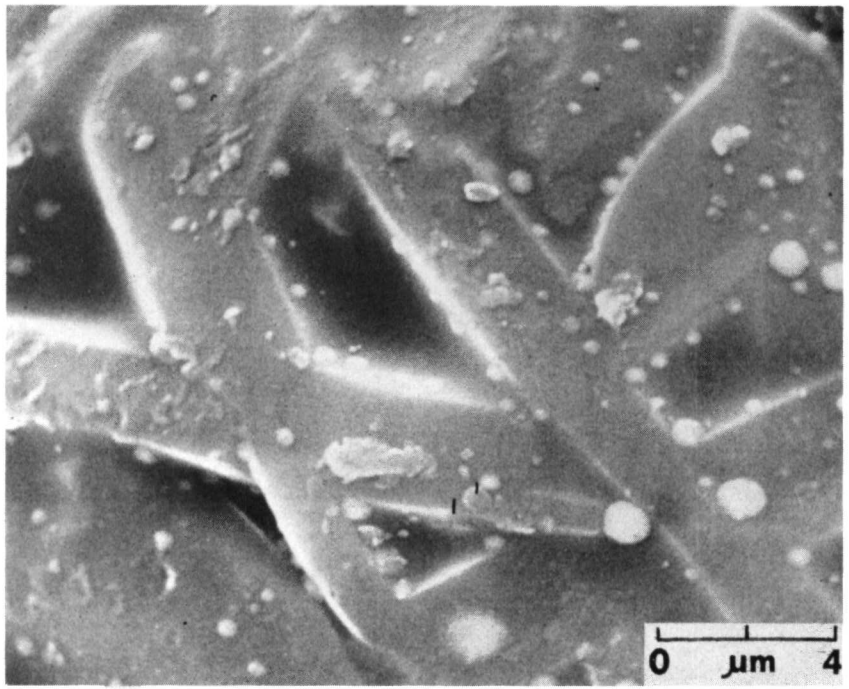

15

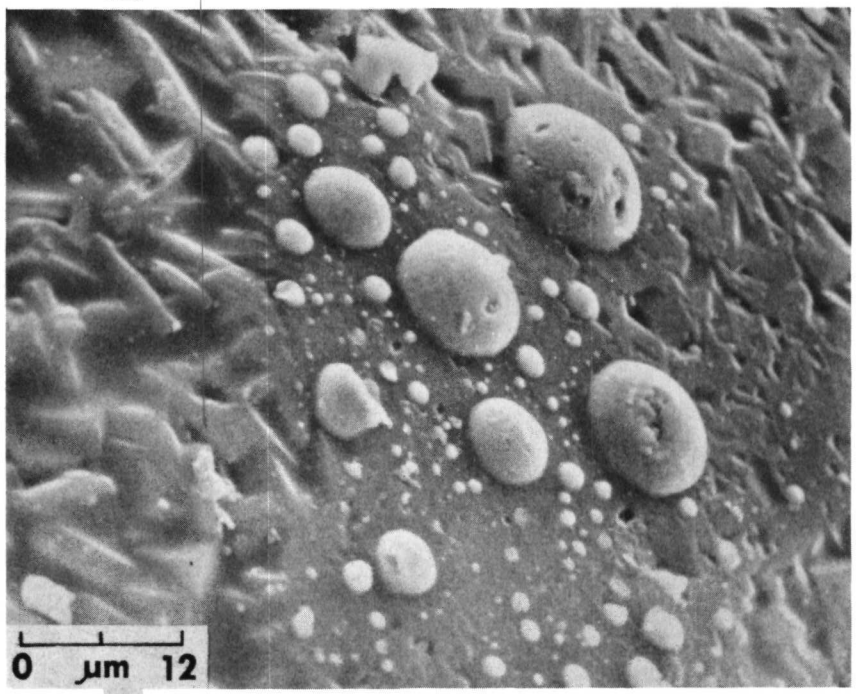

16

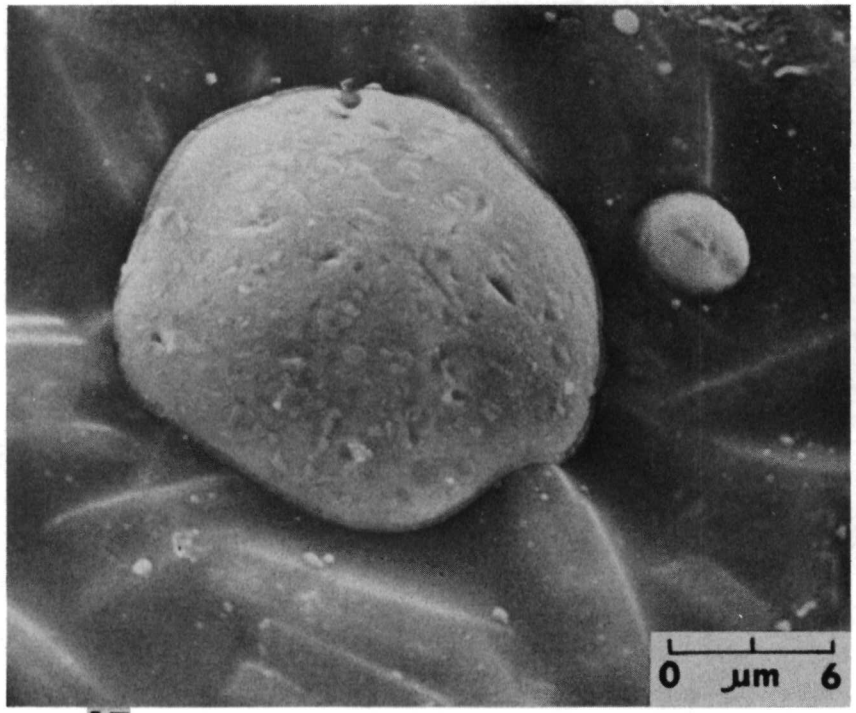

17

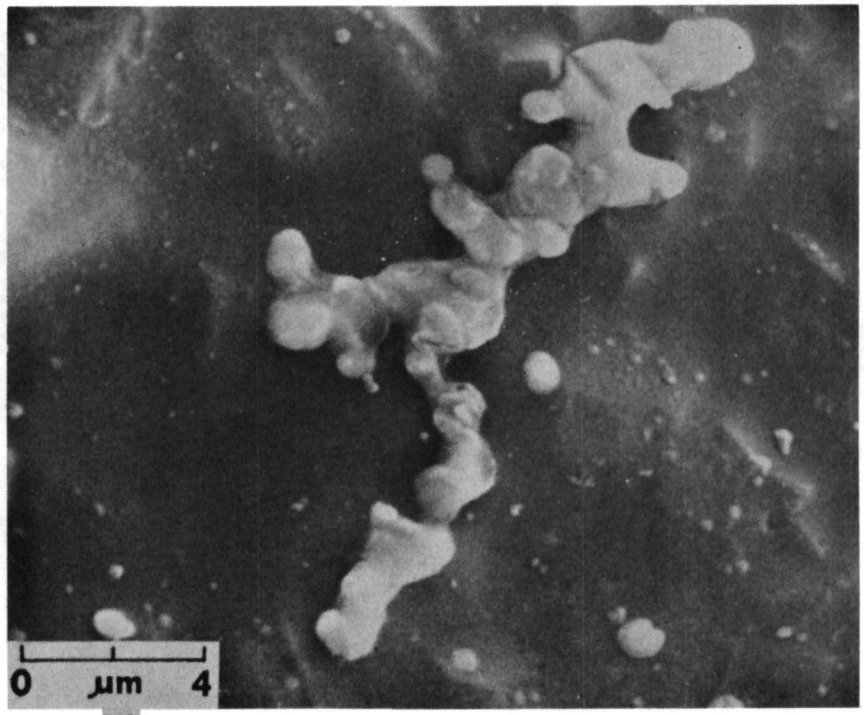

18

Silicate Mineral Chemistry of Apollo Soils 15501, 15411, 66081, and 69941

by

H. C. Jim Taylor

and

James L. Carter

The Institute for Geological Sciences

University of Texas at Dallas

Dallas, Texas 75230

Contribution No. 239, The Institute for Geological Sciences, University of Texas at Dallas, Dallas, Texas 75230.

ABSTRACT

The utilization of small amounts of material in the mineralogical and chemical characterization of lunar soil samples appears to be very successful in formulating major geolgical deductions. Such knowledge should be valuable in the planning of future extraterrestrial scientific missions. Mineral analyses of pyroxenes from the less than 1 mm size fraction of Apollo 15 soil samples 15411,46 and 15501,53 and plagioclase feldspars, pyroxenes and olivines from the less than 1 mm size fraction of Apollo 16 soil samples 66081,5 and 69941,13 can be used to distinguish mare, KREEP and ANT (anorthosite-norite-troctolite) or highland "basalt" components in these soils.

Comparison of mineral chemistry in soils 15411 and 15501 from the Apennine Front/Hadley Rille area allow characterization of the 15411 soil, collected at Spur Crater on the Hadley Delta front, as consisting primarily of gabbroic-anorthosite components, whereas the 15501 soil collected near Hadley Rille consists primarily of mare-type basaltic components. Contamination of the 15501 mare-type basalt soil with minor amounts of the gabbroic-anorthosite components may indicate the effect of downslope mass wasting of materials from the Apennine Front onto the mare surface.

Apollo 16 soil 66081 from the Descartes area shows only ANT components, whereas soil 69941 from South Ray Crater has a major ANT component together with a possible minor KREEP and ultramafic component. The possible ultramafic component consists of olivine as forsteritic as $Fo_{94.5}$ and by Mg-orthopyroxene with enstatite values as high as $En_{87.3}$.

INTRODUCTION

Future planetary missions may often be unmanned and relatively small quantities of samples may be returned for analysis. Therefore it is important to gain experience in the analysis and correlation of small amounts of soil particles from the lunar regolith with lunar rock types and observed geologic features of the lunar surface. Previous studies of this type include, along with others, the work of Duke et al., 1970; Frondel et al., 1970; Albee, 1971; King et al., 1971; Marvin et al., 1971; McKay et al., 1971, 1972; Quaide et al., 1971; Smith, 1971; Bence et al., 1972; Jakeš et al., 1972; Keil et al., 1972; Heiken et al., 1973; Reid et al., 1973 and Ridley et al., 1973.

If the local lunar regolith fine material (soil) represents a well-mixed impact-produced assemblage, it should be more variable, mineralogically and chemically, than the larger lithic fragments collected from the lunar surface in the immediate area as rake samples or individually chosen hand specimens. Although most of the crystalline fragments in the lunar soils may be derived from the breakdown of larger consolidated specimens within the immediate locality, some mineral fragments found in the soils may be distinctly different from mineral fragments in associated rock samples, and thus may permit identification of rock types not returned as hand specimens (e.g., Mason and Melson, 1970; Wood, 1970 and Steele and Smith, 1972).

Major and minor element concentrations in lunar crystalline rocks are commonly used as a key to their genetic relations. Similar techniques may be used to establish criteria defining the different sources of mineral fragments within lunar soil samples. Studies such as Jakeš et al. (1972) of the Mare Fecunditatis regolith stress the importance of the study of the crystalline components of the lunar soils, as well as the glasses in the soils,

in order to characterize the provenance of the various components in relation to other sampling localities. Such studies are important for the following reasons: 1) correlation of soil constituents between sampling sites within a lunar landing area, 2) correlation of soil constituents between different lunar landing sites and 3) information on the amount of mixing of different soil types.

Plagioclase feldspars, pyroxenes and olivines are the most abundant mineral phases occurring in the lunar soils. The widespread occurrence and chemical characteristics of these major mineral components in nearly all lunar rock types makes them extremely useful in the comparison and correlation of different rock and soil types occurring on the lunar surface. Major and minor element analysis of these soil components allows them to be characterized chemically, enabling the identification of rock types which have contributed to the makeup of the soil samples.

ANALYTICAL METHODS

Analyses were made of mineral fragments within the 35-75 μm fraction (unless otherwise specified) of the less than 1 mm size fraction soil samples after examination of the individual particles using transmitted and reflected light microscopy. The bulk sample was seperated by wet sieving in nanograde alcohol. The minerals occur as single fragments and as fragments within agglutinates, microbreccias and crystalline rocks. All fragments of each mineral studied within a randomly chosen area of the polished section were analyzed with an ARL EMX-SM electron microprobe. Mineral standards were used and corrections for background, dead time, drift, fluorescence, absorption and atomic number effects were applied using the computer program EMPADR VII of Rucklidge and Gasparrini (1969). Microprobe operating conditions of 15 KV and 0.02 microamperes sample current were used for all analyses. The electron beam was approximately

1 μm in diameter. Analytical precision varied from approximately ± 20% of the amount present for the smallest quantity of a minor element to ± 0.3% of the amount present for the largest quantity of a major element.

SOIL 15411,46

Sample 15411 from Station 7 is the soil collected with samples 15417 to 15419, which are breccia samples collected from the summit of the subdued rim crest of Spur Crater. Spur Crater is a 100 meter in diameter crater on the lower slope of Hadley Delta, approximately 60 meters above the level of the lunar module and approximately 4 kilometers south-southeast of it. The regional slope is approximately 10°N toward the mare surface. The flanks of Spur Crater are pocked by many small craters; the genesis of which has reworked the Spur Crater ejecta. Rock fragments from centimeter size to 1.5 meters in longest dimension are abundant on the upper flanks of Spur Crater, but the sample area is characterized by an abundance of fragments less than 1 centimeter in longest dimension. Of the samples collected on the rim of Spur Crater, 70 are breccias and 15 are crystalline rocks. These samples are reported to represent the major components of the Spur Crater ejecta from a maximum depth of approximately 20 meters below the surface of Hadley Delta (Apollo Lunar Geolgoy Investigation Team, 1971).

A total of 42 pyroxenes from sample 15411 were analyzed for Si, Fe, Mg, Ca, Ti, Al, Mn, Cr and Na. Selected analyses are presented in Table 1 and the observed range of element concentrations are presented in Table 2. Pyroxenes classified chemically as bronzites, Mg-pigeonites, subcalcic augites, augites, ferroaugites and subcalcic ferroaugites were present in an abundance ratio of approximately 3:3:1:1:1:1, respectively (Fig. 1). The pyroxenes from this soil show a distinctive abundance of Mg-rich pyroxenes and a lack of pyroxene compo-

sitions indicative of continuous and extreme iron enrichment (Taylor and Carter, 1972b). For the Spur Crater pyroxenes of Fig. 1, the central area of the pyroxene quadrilateral is notably devoid of pyroxenes, suggestive of a severe paucity of typical mare-type basalts.

SOIL 15501,53

Sample 15501, from Station 9, is a soil collected with breccia sample 15505. Station 9 is located on the mare surface approximately 1400 meters west of the lunar module and 300 meters east of Hadley Rille just outside the mapped limits of a diffuse ray or ridge that trends N30°W through the landing site. The area is flat and smooth, but hummocky in detail. The station is located at a 15 meter in diameter crater of very fresh appearance. The crater does not penetrate through the regolith, which appears locally to be greater than 3 meters thick. The sample was collected from the ejecta blanket approximately 15 meters from the crater rim. The ejecta blanket of this crater probably represents the freshest surface of any significant extent that has been sampled by the Apollo 11, 12, 14 or 15 missions (Apollo Lunar Geology Investigation Team, 1971).

In sample 15501, pyroxene fragments are more abundant than plagioclase feldspar fragments by a ratio of approximately 4 to 1. Analyses for Si, Fe, Mg, Ca, Ti, Al, Mn and Na were made on 57 pyroxene fragments within the 75-150 μm fraction. Selected analyses are presented in Table 1 and the observed range of element concentrations are presented in Table 2. No preferred compositions were observed in the single crystal occurrences versus the other pyroxene occurrences as components of larger fragments.

The pyroxene fragments analyzed cover a large area of the pyroxene quadrilateral (Fig. 1) ranging from augites, subcalcic augites, bronzites and Mg-pigeonites to ferroaugites, subcalcic ferroaugites, intermediate pigeonites and pyroxferroites, in an abundance ratio of approximately 2:3:1:3:1:4:2:1. These 15501 pyroxenes appear to represent a continuous basaltic fractionation trend demonstrating extreme iron enrichment as characterized by the pyroxferroites, and are more representative of typical mare-type basaltic pyroxenes than are those from 15411 (Taylor and Carter, 1972a,b). In contrast, sample 15411 shows an absence of a smooth continuous trend of pyroxene compositions demonstrating continuous and extreme iron enrichment. It is more diverse in the Fe-rich half of the pyroxene quadrilateral, with an overall pyroxene distribution similar to those from typical Apollo 15 breccias (Steele et al., 1972).

The high-Ca pyroxenes, in conjunction with the high-Mg and low-Ca pyroxenes shown in the 15411 plot, are more indicative of non-mare-type pyroxenes and correlate well with pyroxenes occurring as mineral grains in gabbroic-anorthosite clasts from Apollo 15 rake samples (Steele et al., 1972). The 15501 plot shows relatively small abundances of pyroxenes characteristic of Apollo 15 breccias, although a few Mg-rich orthopyroxenes of 15501 are more characteristic of Mg-orthopyroxenes of gabbroic-anorthosites than of typical mare basalts. Such a feature may represent a minor amount of Apollo 15 breccia fragments in the primarily mare-type basaltic soil. This is suggestive of downslope transport of soil of the type found at Station 7 (Spur Crater) to the vicinity of Station 9. However, an upslope transport of soil components from the vicinity of Hadley Rille to Spur Crater on the Apennine Front by a meteoritic impact mechanism is not readily apparent from the pyroxene data of this study.

Silver (1973), through the study of U-Th-Pb isotopes in Apollo 15 samples, found evidence that visited surfaces of the mare and the front at the Apollo 15 site are veneered by at least several meters with a recently acquired uranium- and thorium-rich glassy debris layer from an undefined source. He suggests from his data that a single radiogenic isotopic system, that is not contained in the local basalts, dominates all other contributions to the U-Th-Pb characteristics of the Apollo 15 regolith. He suggests further that the vitric breccias appear to be the largest fragment of debris containing the dominant isotopic system. Since the pyroxenes of the present study seem to characterize two distinctly different suites of source rocks one of which is breccias, the U-Th-Pb isotopic data of Silver (1973) appears not to contradict the the conclusions reached in the present study.

Although the transport of soil by meteoritic impact phenomena is certainly established on the lunar surface by the large number of mapable rays extending from multitudes of craters and by numerous petrographic and soil survey glass studies, the comparison of pyroxenes from these two Apollo 15 soil samples allows the suggestion that downslope transport of regolith material by mass wasting from the slopes of the Apennine Front was perhaps the more efficient transport mechanism at the Hadley Rille/Apennine Front landing site.

Downslope movement of loose regolith material, even in the comparatively weak lunar gravitational field, may thus be an important transport process for areas of even moderate relief on the lunar surface. Whether driven mainly by lunar gravitational energy, by electrostatic effects (Gold, 1971) or by other processes, geographical regions demonstrating extensive relief within the lunar highlands and bordering highland areas would become prime targets in which to expect large scale transport of loosely consolidated regolith.

SOIL 66081,5

Apollo 16 sample 66081 was collected at Station 6 near the base of Stone Mountain in the Descartes region of the lunar highlands. The sample is described as an indurated clod of white impact ejecta; possibly from South Ray Crater, but in a location generally shadowed from South Ray ejecta (Apollo Lunar Geology Investigation Team, 1972). The origin of this white impact ejecta is unknown. The possibility exists that downslope movement of material from Stone Mountain could have transported the material to its sampling location where comminution of the once coherent clod occurred.

Mineral fragments, primarily plagioclase feldspars, pyroxenes and olivines, of soil 66081 were analyzed for major and minor elements (Taylor and Carter, 1973). Selected analyses of these minerals from 66081 are presented in Table 1 and the observed range of element concentrations of the analyzed minerals are presented in Table 2.

Plagioclase feldspars are the most abundant mineral phase in this soil sample. Plagioclase fragments constitue about 9% of the particles in the 62.5-125 μm fraction of this sample, with agglutinates and glass particles making up about 70% of the sample (LSPET, 1973). A total of 43 plagioclase feldspars were analyzed for Si, K, Al, Ca, Fe and Na. No K-feldspar was found in this sample. The plagioclase feldspars are characterized by a high anorthite (An) content, with an observed range of $An_{88.7-97.8}$, and a mode occurring within the An_{96-98} group (Fig. 2). The most Na-rich plagioclase feldspar examined ($An_{88.7}$) contained the greatest amount of potassium of any plagioclase feldspar analyzed. The K_2O content of this fragment was only 0.16 wt. %, producing an Or component of 0.9 mole %. The minimum K_2O content observed in plagioclase feldspar was 0.01 wt. %.

The plagioclase feldspars also have a low iron content (Fig. 3). Total iron expressed as wt. % FeO never exceeds 0.22 and values range as low as 0.04, with a precision of ± 20% of the amount present for the lowest values. Iron concentrations in plagioclase feldspars are distinctive in distinguishing between major basalt types occurring on the lunar surface (Steele and Smith, 1973). Mare basalts characteristically have Fe-rich plagioclase feldspars that normally contain FeO contents greater than 0.4 wt. %. Plagioclase feldspars from mare basalts also display a wide range of An values, but usually they are much less calcic than those found in this sample. Plagioclase feldspars from KREEP basalts have low iron contents, similar to those in this sample, but KREEP-type basaltic plagioclase feldspars show a much wider range of An values, extending from high calcium values, similar to those in this sample, to less calcic values, well below the minimum An value found in this Apollo 16 sample. These plagioclase feldspars from 66081 are thus distinctive from both mare- and KREEP-type basaltic plagioclase feldspars.

Pyroxene fragments are only about 1/3 as abundant as plagioclase feldspar fragments in this sample. A total of 62 pyroxenes were analyzed for Si, Fe, Mg, Ca, Ti, Al, Mn, Cr and Na. Pyroxenes in soil 66081 are primarily bronzites and diopsidic augites with lesser abundances of Mg-pigeonites, subcalcic augites, hypersthenes and ferriferous pigeonites. A single fragment of ferriferous pigeonite suggests possible high iron enrichment, but the overall picture is one of an extreme lack of fractionation-related iron enrichment (Fig. 4). Approximately 40% of the analyzed pyroxenes are chemically defined orthopyroxenes (Fig. 4).

A plot of Ti versus Al (atoms per formula unit) of these pyroxenes show the more Mg-rich orthopyroxenes plotting near a Ti/Al ratio of 1/4,

whereas the more Fe-rich orthopyroxenes and the clinopyroxenes plot near a Ti/Al ratio of 1/2 (Fig. 5). These features are consistent with the findings of Bence et al. (1970, 1972) in which the early crystallization of pyroxenes, in the absence of plagioclase crystallization, become enriched in alumina. This process changes during later stages of the crystallization sequence with the onset of plagioclase crystallization, at which time plagioclase competes with pyroxene for the alumina component in the melt and allows only enough alumina to be admitted to the pyroxene structure to compensate the clinopyroxene titania component. The general lack of iron enrichment in the clinopyroxenes, the abundance of Mg-rich pyroxenes demonstrating an Mg/(Mg+Fe) atomic ratio greater than 0.7, the abundance of high-Ca and high-Mg clinopyroxenes and the relatively low population of intermediate clinopyroxenes (low-Ca augites) are all prominent features of soil 66081 which enable the distinction of these pyroxenes from mare-type basaltic pyroxenes. These criteria establish the almost total absence of a mare-type basaltic component in this Apollo 16 soil sample. The single analysis of an Fe-rich ferriferous pigeonite probably represents another rock type which is clearly not genetically related to the other pyroxenes in this sample. The sample is otherwise extremely "clean" for a soil sample since all the other pyroxenes appear to demonstrate a genetic relationship on the basis of the pyroxene quadrilaterial trends and the Ti/Al trends.

Olivine fragments are approximately 1/2 as abundant as pyroxene fragments in this sample. A total of 30 olivine fragments were analyzed for Si, Fe, Mg, Ca, Ti, Al, Mn, Cr and Na. A histogram of the olivine population observed relative to the forsteritic (Fo) component is plotted in Fig. 6. This plot shows a bimodal distribution occurring within the range of Fo_{70-78} with modes

at Fo_{70-72} and at Fo_{76-78}. The olivines have a total compositional range of $Fo_{58.6-91.2}$ and are typically more forsteritic than mare-type basaltic olivines, which seldom have olivines more forsteritic than Fo_{70}.

The CaO content of these olivines rarely exceeds 0.3 wt. % and averages about 0.2 wt. %. Reid et al. (1973) found that CaO content commonly exceeds 0.3 wt. % in both mare- and KREEP-type basaltic olivines. The Cr_2O_3 content of these olivines is low and exceeds 0.1 wt. % in only one case. The 66081 olivines therefore are characteristic of neither mare- or KREEP-type basaltic olivines, but are characteristic of the ANT (anorthosite-norite-troctolite) group of lunar rock types (Keil et al., 1972).

A few other mineral fragments were noted and analyzed in this sample. Included were 4 fragments of a crystalline SiO_2 phase, one fragment (possibly a carbonate) giving a CaO analysis of approximately 57 wt. % ($CaCO_3$ contains approximately 56 wt. % CaO) and one fragment of reddish iron oxide, which resembles a geothite-like phase (The material deteriorated under the electron beam, but gave an analysis of 57.7 wt. % Fe).

SOIL 69941,13

Apollo 16 sample 69941 was collected at Station 9 near South Ray Crater. This sample is believed to represent the dark-colored breccias which form a stratigraphic unit approximately 30 meters thick above a bench in South Ray Crater (Apollo Field Geology Investigation Team, 1973).

Plagioclase feldspars, pyroxenes and olivines of soil 69941 were analyzed for major and minor elements and selected analyses are presented in Table 1. The observed range of element concentrations of the analyzed minerals are presented in Table 2.

Like soil 66081, plagioclase feldspar is the most abundant mineral phase comprising approximately 7% of the particles in the 62.5-125 μm fraction of soil 69941 (LSPET, 1973). Analyses of 42 plagioclase feldspar fragments gave a range of $An_{79.3-98}$, with a mode occurring in the range of An_{94-96} (Fig. 2). The K_2O contents ranged from 0.01-0.23 wt. % giving an Or component range of 0.1-1.4 mole %. FeO contents ranged from 0.09-0.55 wt. %, with the majority of fragments averaging about 0.2 wt. % FeO (Fig. 3). Since the majority of plagioclase feldspar fragments have FeO contents less than 0.3 wt. % and high CaO contents, as shown by An values greater than 90, these fragments fall within the range of chemistry characteristics of plagioclase feldspars from the ANT group of highland rocks (Steele and Smith, 1973). Three plagioclase feldspar fragments, however, fall within the compositional range of KREEP-type basaltic plagioclase feldspars as defined by Steele and Smith (1972) as having low-Fe (FeO less than 0.6 wt. %), high-K (K_2O of 0.1-0.5 wt. %) and Ca values producing a range of An values from 75 to 90.

Pyroxene fragments are only about 1/3 as abundant as plagioclase feldspar fragments. Fifty-four pyroxenes of soil 69941 were analyzed for Si, Fe, Mg, Ca, Ti, Al, Mn, Cr and Na. Bronzites are the predominant pyroxene type, with lesser amounts of diopsidic augites and Mg-pigeonites (Fig. 4). Minor amounts of hypersthene, subcalcic augite and ferroaugite are also represented. A plot of the Ti/Al ratios (atoms per formula unit) shows the more Mg-rich orthopyroxenes to have a Ti/Al = 1/4 or less, while the more Fe-rich orthopyroxenes and clinopyroxenes have a Ti/Al = 1/2 (Fig. 5), similar to that observed in the 66081 pyroxenes. Greater variations of Ti content of 69941 pyroxenes compared to the Ti content of 66081 pyroxenes, as observed on the Ti/Al plot (Fig. 5), may be due to 1) a more complex crystallization history caused by

discontinuities in the crystallization sequence, 2) magma mixing or contamination of the magma during implacement or 3) a greater variety of rock types contributing to the makeup of soil 69941. These 69941 pyroxenes have compositions similar to those described previously from sample 66081 and the same criteria may be applied to this sample in permitting the suggestion that a mare-type basaltic component is virtually absent from 69941. The narrow compositional range of the pyroxenes represented on the pyroxene quadrilateral is again characteristic of the ANT group of lunar rock types.

Olivine fragments are approximately 1/3 as abundant as pyroxene fragments in this sample. Twenty-four olivine fragments were analyzed for Si, Fe, Mg, Ca, Ti, Al, Mn, Cr and Na and a histogram of the olivine abundances with respect to the forsteritic component is plotted in Fig. 6. Olivines show a compositional range of $Fo_{49.8-94.5}$, with a mode occurring in the range of Fo_{74-76}. The olivine chemistry, similar to that of sample 66081, again demonstrates a mode more Mg-rich than olivines from typical mare basalts. An ultramafic component in the soil may be represented by Mg-rich olivines as forsteritic as $Fo_{94.5}$ and by Mg-rich orthopyroxenes as high as $En_{87.3}$. Steele and Smith (1972) reported olivine as forsteritic as Fo_{89} and orthopyroxene as enstatite-rich as En_{88} in the Apollo 14 samples. They considered olivines and pyroxenes with an Mg/(Mg+Fe) atomic ratio greater than 0.8 as characteristic of rock types with ultrabasic affinities. The most Mg-rich olivines and pyroxenes analyzed in the 69941 soil (Figs. 4 and 6) certainly meet the requirements of Steele and Smith (1972) as ultrabasic components.

The CaO content of olivines from 69941 exceeds 0.3 wt. % in only one case, the typical olivine averaging about 0.2 wt. % CaO. These olivines thus do not demonstrate an apparent mare- or KREEP-type basaltic affinity.

In addition to the plagioclase feldspar, pyroxene and olivine analyses completed in soil 69941, one fragment of a crystalline SiO_2 phase was analyzed and a fragment of a goethite-like phase similar to the one described previously in sample 66081 was analyzed.

From the chemical data presented on the Apollo 16 mineral fragments (Tables 1 and 2), the chemical characteristics of the suite of minerals from soils 66081 and 69941 suggest a distinctive highland classification for these soils, which is distinguishable from both mare- and KREEP-type basaltic soils. In general the chemical variations within a mineral fragment is less for these Apollo 16 soil fragments than for mare-type soil fragments suggesting a slower cooling rate for the Apollo 16 rocks. The relatively large amount of olivine in these Apollo 16 soils suggests an olivine normative classification for one of the contributing rock types. The presence of the crystalline SiO_2 phase may be due to a second contributing rock type or to the crystallization of the minor components of an original two-liquid system (John C. Butler, 1973, personal communication). Two or more rock types thus may have contributed to the makeup of these soils. Ridley et al. (1973) found evidence for at least five rock types in the two Apollo 16 soils which they studied.

Rock types of the ANT group (Keil et al., 1972) are likely contributors. The high-Ca and low-Fe plagioclases, the high-Mg orthopyroxenes and clinopyroxenes, the lack of abundant clinopyroxenes with intermediate Ca values and the abundance of Mg-rich olivines in the soil are all features similar to those observed in the Luna 20 soil by Reid et al. (1973). This present study offers evidence of some similarities between soils 66081 and 69941 of the Apollo 16 highland site at Descartes and the Luna 20 highland region north of Mare Fecunditatis. Similarities in the chemical composition of

different areas of the central lunar highlands of the Moon's near side are indeed suggested from the ratio of Al to Si as determined by Adler et al. (1972) from orbiting X-ray fluorescence spectrometry. The Apollo 16 soil pyroxenes, however, do not approach the degree of iron enrichment of the Luna 20 soil pyroxenes, possibly indicating a deeper level of crystallization for the Apollo 16 pyroxenes.

CONCLUSIONS

1) The pyroxene chemistry of Apollo 15 soil fractions allows the suggestions that soil 15501 from the mare surface may be contaminated with material having a mineral constituency similar to soil 15411 from Spur Crater, but that soil 15411 does not seem to be contaminated by the mare surface rocks.

2) The downslope transport of soil from Hadley Delta on the Apennine Front to a lower elevation near Hadley Rille by mass wasting of highland material seems to be a more efficient soil transport mechanism than is the upslope transport of soil within the same area as ejecta of meteorite impacts on the mare surface.

3) The plagioclase, pyroxene and olivine chemistry of Apollo 16 soils 66081 and 69941 allows the suggestions that a) a mare-type basaltic component is virtually absent from both soils, b) a KREEP-type basaltic component is absent from soil 66081, but it possibly appears as a minor component of soil 69941, c) a possible ultramafic component appears in soil 69941 as olivine as forsteritic as $Fo_{94.5}$ and by Mg-orthopyroxene with enstatite values as high as $En_{87.3}$, d) the abundance of olivine in both soils necessitates an olivine normative classification for at least one of the major contributing rock types, e) the presence of crystalline SiO_2 in both soils may necessitate more than one contributing rock type; howver, it may be the result of crystal-

lization of the minor components of an original two-liquid system, f) a crystallization environment is favored for the minerals of both samples in which slow cooling took place with little opportunity for iron enrichment to occur and g) rock types such as gabbroic-anorthosite or other members of the ANT (anorthosite-norite-troctolite) suite of highland rocks are likely contributors to the mineralogical constituency of these Apollo 16 soils.

4) The many similarities observed between the mineral chemistry of soils 66081 and 69941 of the Apollo 16 highland site at Descartes and the soil of the Luna 20 highland region north of Mare Fecunditatis studied by Reid et al. (1973) support the orbital X-ray spectrometry evidence for widespread chemical similarities within the central lunar highlands of the Moon's near side (Adler et al., 1972).

ACKNOWLEDGEMENTS

Supported by NASA Grants NGR-44-004-116 and NGL-44-004-001. We thank J. B. Toney for technical assistance. Critical review by J. C. Butler, D. S. McKay and E. A. King, Jr. has contributed to the improvement of the manuscript.

REFERENCES

Adler, I., Trombka, J., Gerard, J., Schmadebeck, R., Lowman, P., Blodgett, H., Yin, L., Eller, E., Lamothe, R., Gorenstein, P., Bjorkholm, P., Harris, B., and Gursky, H. (1972). X-ray fluorescence experiment. Sec. 17 of Apollo 15 Preliminary Science Report. NASA SP-289.

Albee, A. L. (1971). Mineralogy, petrology and geochemistry of the lunar samples. Trans. Amer. Geophys. Union 52, pp. 57-118.

Apollo Field Geology Investigation Team (1973). Apollo 16 exploration of Descartes: a geologic summary. Science, 174, pp. 62-69.

Apollo Lunar Geology Investigation Team (1971). Preliminary report on the geology and field petrology at the Apollo 15 landing site. U. S. Geol. Survey Interagency Report 32.

Apollo Lunar Geology Investigation Team (1972). Interagency Report. Astrogeology 51, p. 121.

Bence, A. E., Papike, J. J., and Prewitt, C. T. (1970). Apollo 12 clinopyroxenes: chemical trends. Earth Planet. Sci. Lett. 8, pp. 393-399.

Bence, A. E., Holzwarth, W., and Papike, J. J. (1972). Petrology of basaltic and monomineralic soil fragments from the sea of fertility. Earth Planet. Sci. Lett., 13, pp. 299-311.

Duke, M. B., Woo, C. C., Sellers, G. A., Bird, M. L., and Finkelman, R. B. (1970). Genesis of lunar soil at Tranquility Base. "Proc. Apollo 11 Lunar Sci. Conf., Geochim. Cosmochim. Acta", Suppl. 1, Vol. 1, pp. 347-361. Pergamon.

Frondel, C., Klein, C., Jr., Ito, J., and Drake, J. C. (1970). Mineralogical and chemical studies of Apollo 11 lunar fines and selected rocks. "Proc. Apollo 11 Lunar Sci. Conf., Geochim. Cosmochim. Acta", Suppl. 1, Vol. 1, pp. 445-474. Pergman.

Gold, T. (1971). Evolution of mare surface. "Proc. Second Lunar Sci. Conf., Geochim. Cosmochim. Acta", Suppl. 2, Vol. 3, pp. 2675-2680. MIT Press.

Heiken, G. H., Clanton, U. S., McKay, D. S., Duke, M. B., Fryxell, R., Sellers, G. A., Scott, R., Nagle, J. S. (1973). Preliminary stratigraphy of the regolith at the Apollo 15 site. In "Lunar Science IV" (editors J. W. Chamberlain and C. Watkins), pp. 345-346, The Lunar Sci. Inst., Houston, Texas.

Jakeš, P., Warner, J., Ridley, W. I., Reid, A. M., Harmon, R. S., Brett, R., and Brown, R. W. (1972). Petrology of a portion of the Mare Fecunditatis regolith. Earth Planet. Sci. Lett. 13, pp. 257-271.

Keil, K., Kurat, G., Prinz, M., and Green, J. A. (1972). Lithic fragments, glasses and chondrules from Luna 16 fines. Earth Planet. Sci. Lett. 13, pp. 243-256.

King, E. A., Jr., Butler, J. C., and Carman, M. F. (1971). The lunar regolith as sampled by Apollo 11 and Apollo 12: Grain size analyses, modal analyses, and origns of particles. "Proc. Second Lunar Sci. Conf., Geochim. Cosmochim. Acta", Suppl. 2, Vol. 1, pp. 737-746, MIT Press.

LSPET (Lunar Sample Preliminary Examination Team) (1973). Preliminary examination of lunar sample from Apollo 16. Science, 179, pp. 23-34.

McKay, D. S., Morrison, D. A., Clanton, U. S., Ladle, G. H., and Lindsay, J. F. (1971). Apollo 12 soil and breccia. "Proc. Second Lunar Sci. Conf., Geochim. Cosmochim. Acta", Suppl. 2, Vol. 1, pp. 755-773, MIT Press.

McKay, D. S., Heiken, G. H., Taylor, R. M., Clanton, U. S., Morrison, D. A., and Ladle, G. H. (1972). Apollo 14 soils: size distribution and particle type. "Proc. Third Lunar Sci. Conf., Geochim. Cosmochim. Acta", Suppl. 3, Vol. 1, pp. 983-994, MIT Press.

Marvin, U. B., Wood, J. A., Taylor, G. J., Reid, J. B., Jr., Powell, B. N., Dickey, J. S., and Bower, J. F. (1971). Relative proportions and probable sources of rock fragments in the Apollo 12 soil samples. "Proc. Second Lunar Sci. Conf., Geochim. Cosmochim. Acta", Suppl. 2, Vol. 1, pp. 679-699, MIT Press.

Mason, B. and Melson, W. G. (1970). The Lunar Rocks, 179 p. Wiley-Interscience, New York.

Quaide, W., Oberbeck, V., Bunch, T., and Polkowski, G. (1971). Investigation of the natural history of the regolith at the Apollo 12 site. "Proc. Second Lunar Sci. Conf., Geochim. Cosmochim. Acta", Suppl. 2, Vol. 1, pp. 701-718, MIT Press.

Reid, A. M., Warner, J. L., Ridley, W. I., and Brown, R. W. (1973). Luna 20 soil: abundance and compositions of phases in the 45-125 micron fraction. Earth Planet. Sci. Lett. 37, pp. 1011-1030.

Ridley, W. I., Reid, A. M., Warner, J., Brown, R. W., Gooley, R., and Donaldson, C. (1973). Major element composition of glasses in two Apollo 16 soils and a comparison with Luna 20 glasses. In "Lunar Science IV" (editors J. W. Chamberlain and C. Watkins), pp. 625-627, The Lunar Sci. Inst., Houston, Texas.

Rucklidge, J. and Gasparrini, E. L. (1969). Specifications of a computer program for processing electron micro-probe analytical data: EMPADR VII. Dept. of Geology, Univ. of Toronto, Toronto, Canada.

Silver, L. T. (1973). Uranium-thorium-lead isotope relations in the remarkable debris blanket at Hadley-Apennine. In "Lunar Science IV" (editors J. W. Chamberlain and C. Watkins), pp. 669-671, Lunar Sci. Inst., Houston, Texas.

Smith, J. V. (1971). Minor elements in Apollo 11 and Apollo 12 olivine and plagioclase. "Proc. Second Lunar Sci. Conf., Geochim. Cosmochim. Acta", Suppl. 2, Vol. 1, pp. 143-150, MIT Press.

Steele, I. M. and Smith, J. V. (1972). Ultrabasic lunar samples. Nature Physical Science, 240, pp. 5-6.

Steele, I. M., Smith, J. V., and Grossman, L. (1972). Mineralogy and petrology of Apollo 15 rake samples: II. Breccias (abstract). In "The Apollo 15 Lunar Samples" (editors J. W. Chamberlain and C. Watkines), pp. 161-164, The Lunar Sci. Inst., Houston, Texas.

Steele, I. M. and Smith, J. V. (1973). Identification of lunar rock types from small clasts and single mineral grains. Trans. Amer. Geophys. Union, 54, p. 493.

Taylor, H. C. J. and Carter, J. L. (1972a). Chemistry of pryoxenes from Apollo soil 15501,53. In "The Apollo 15 Lunar Samples (editors J. W. Chamberlain and C. Watkins), pp. 260-261, The Lunar Sci. Inst., Houston, Texas.

Taylor, H. C. J. and Carter, J. L. (1972b). Acomparison of pyroxenes from lunar soil samples 15411,46 and 15501,53 (abstract). In "Trans. Amer. Geophys. Union", 53, p. 1131.

Taylor, H. C. J. and Carter, J. L. (1973). Silicate mineral chemistry of Apollo soil 66081,5. In "Lunar Science IV" (editors J. W. Chamberlain and C. Watkins), pp. 713-714, The Lunar Sci. Inst., Houston, Texas.

Wood, J. A. (1970). Petrology of the lunar soil and geophysical implications. Jour. Geophys. Research, 75, pp. 6497-6513.

Table 1. Electron microprobe analyses (in wt. %) of selected minerals from soils 15411,46; 15501,53; 66081,5 and 69941,13.

	15411,46		15501,53		66081,5						69941,13					
Wt. %	Pyx	Pyx	Pyx	Pyx	Plag	Pyx	Pyx	Pyx	Ol	Ol	Plag	Plag	Pyx	Pyx	Ol	Ol
SiO_2	49.0	54.8	49.8	45.7	44.6	54.3	50.7	49.9	40.6	36.5	43.6	49.4	55.2	50.4	41.3	34.4
TiO_2	2.03	0.29	0.85	0.51	----	0.74	2.74	1.62	0.02	0.09	----	----	0.55	1.37	0.03	0.1
Al_2O_3	2.66	0.61	1.24	0.42	34.3	1.96	3.02	2.52	0.05	0.04	36.0	31.4	1.50	1.72	0.14	0.0
Cr_2O_3	0.66	0.25	----	----	----	0.33	0.54	0.27	0.02	0.04	----	----	0.33	0.36	0.06	0.0
*FeO	11.5	14.8	25.3	44.9	0.22	12.4	6.38	19.2	8.58	32.5	0.18	0.33	11.5	11.2	5.20	41.0
MnO	0.24	0.23	0.42	0.69	----	0.25	0.15	0.45	0.10	0.30	----	----	0.18	0.22	0.03	0.4
MgO	14.0	27.9	15.0	1.14	----	28.1	15.8	17.8	50.1	29.9	----	----	28.3	13.9	50.6	22.9
CaO	18.2	0.29	6.32	5.64	20.4	1.79	19.5	7.79	0.11	0.22	19.3	15.8	1.98	20.3	0.26	0.3
Na_2O	0.02	0.09	0.02	0.01	0.24	0.00	0.26	0.05	0.00	0.00	0.21	2.12	0.01	0.04	0.00	0.0
K_2O	----	----	----	----	0.02	----	----	----	----	----	0.01	0.23	----	----	----	----
TOTAL	98.38	99.19	98.95	99.01	99.78	99.87	99.09	99.60	99.58	99.59	99.30	99.28	99.55	99.51	97.62	99.2
Plag Pyx Ol																
An En Fo	41.7	76.6	44.4	3.7	97.8	77.4	47.4	52.1	91.2	62.1	98.0	79.3	78.2	40.0	94.5	49.8
Ab Fs Fa	19.2	22.8	42.1	82.9	2.1	19.1	10.7	31.5	8.8	37.9	1.9	19.3	17.8	18.0	5.5	50.2
Or Wo	39.1	0.6	13.5	13.4	0.1	3.5	41.9	16.4	----	----	0.1	1.4	4.0	42.0	----	----

Note: *Total iron expressed as FeO.

Table 2. Minor element compositional ranges (in wt. %) of selected minerals from soils 15411,46; 155501,56; 66081,5; and 69941.13.

	Pyroxene			Plagioclase			Pyroxene			Olivine	
	15411,46	15501,56		66081,5	69941,13		66081,5	69941,13		66081,5	69941,13
	(42)	(57)		(43)	(42)		(62)	(54)		(30)	(24)
TiO_2	(0.21-2.03)	(0.26-1.39)	**FeO	(0.04-0.22)	(0.09-0.55)	TiO_2	(0.25-3.15)	(0.20-2.32)	TiO_2	(0.01-0.16)	(0.01-0.2
Al_2O_3	(0.43-3.41)	(0.28-3.78)	K_2O	(0.01-0.16)	(0.01-0.23)	Al_2O_3	(0.53-4.52)	(0.40-3.02)	Al_2O_3	(0.01-0.33)	(0.01-0.14
Cr_2O_3	(0.10-1.00)					Cr_2O_3	(0.11-0.59)	(0.05-0.48)	Cr_2O_3	(0.01-0.13)	(0.01-0.1
MnO	(0.12-0.49)	(0.17-0.69)				MnO	(0.13-0.54)	(0.09-0.53)	MnO	(0.10-0.42)	(0.03-0.41
Na_2O	(0.01-0.11)	(0.01-0.05)				Na_2O	(0.01-0.26)	(0.01-0.21)	CaO	(0.11-0.33)	(0.03-0.31

Note: *( ) = Number of fragments analyzed.

**Total iron expressed as FeO.

FIGURE CAPTIONS

Figure 1. Electron microprobe analyses of pyroxenes from soils 15411,46 (Station 7, Spur Crater) and 15501,53 (Station 9, mare surface) plotted in terms of mole % end members: En (enstatite, $Mg_2Si_2O_6$), Fs (Ferrosilite, $Fe_2Si_2O_6$), and Wo (Wollastonite, $Ca_2Si_2O_6$, not shown). Di = Diopside, $MgCaSi_2O_6$; and Hd = Hedenbergite, $FeCaSi_2O_6$.

Figure 2. Electron microprobe analyses of plagioclase fragments from soils 66081,5 and 69941,13 plotted in frequency distribution diamgrams in terms of mole % An (Anorthite, $CaAl_2Si_2O_8$).

Figure 3. Electron microprobe analyses of FeO (in wt. %) in plagioclase fragments from soils 66081,5 and 69941,13 plotted against mole % An (Anorthite, $CaAl_2Si_2O_8$).

Figure 4. Electron microprobe analyses of pyroxenes from soils 66081,5 and 69941,13 plotted in terms of mole % end members. Abbreciations are as in Fig. 1.

Figure 5. Ti/Al relationships in atomic proportions for pyroxenes from soils 66081,5 and 69941,13.

Figure 6. Electron microprobe analyses of olivines from soils 66081,5 and 69941,13 plotted in frequency distribution diagrams in terms of mole % Fo (Forsterite, Mg_2SiO_4).

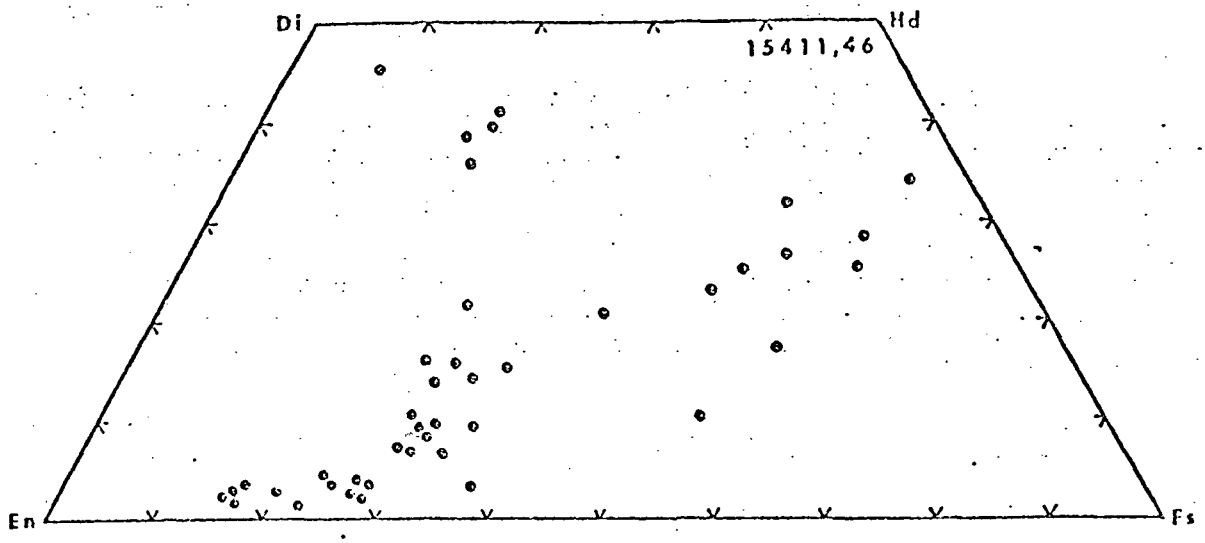

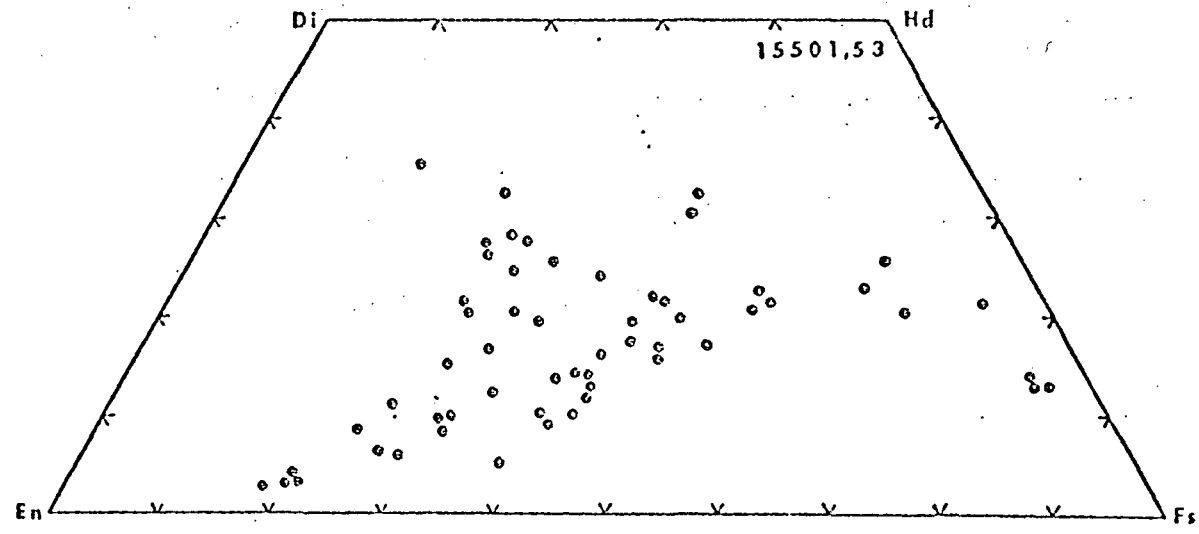

Fig. 1

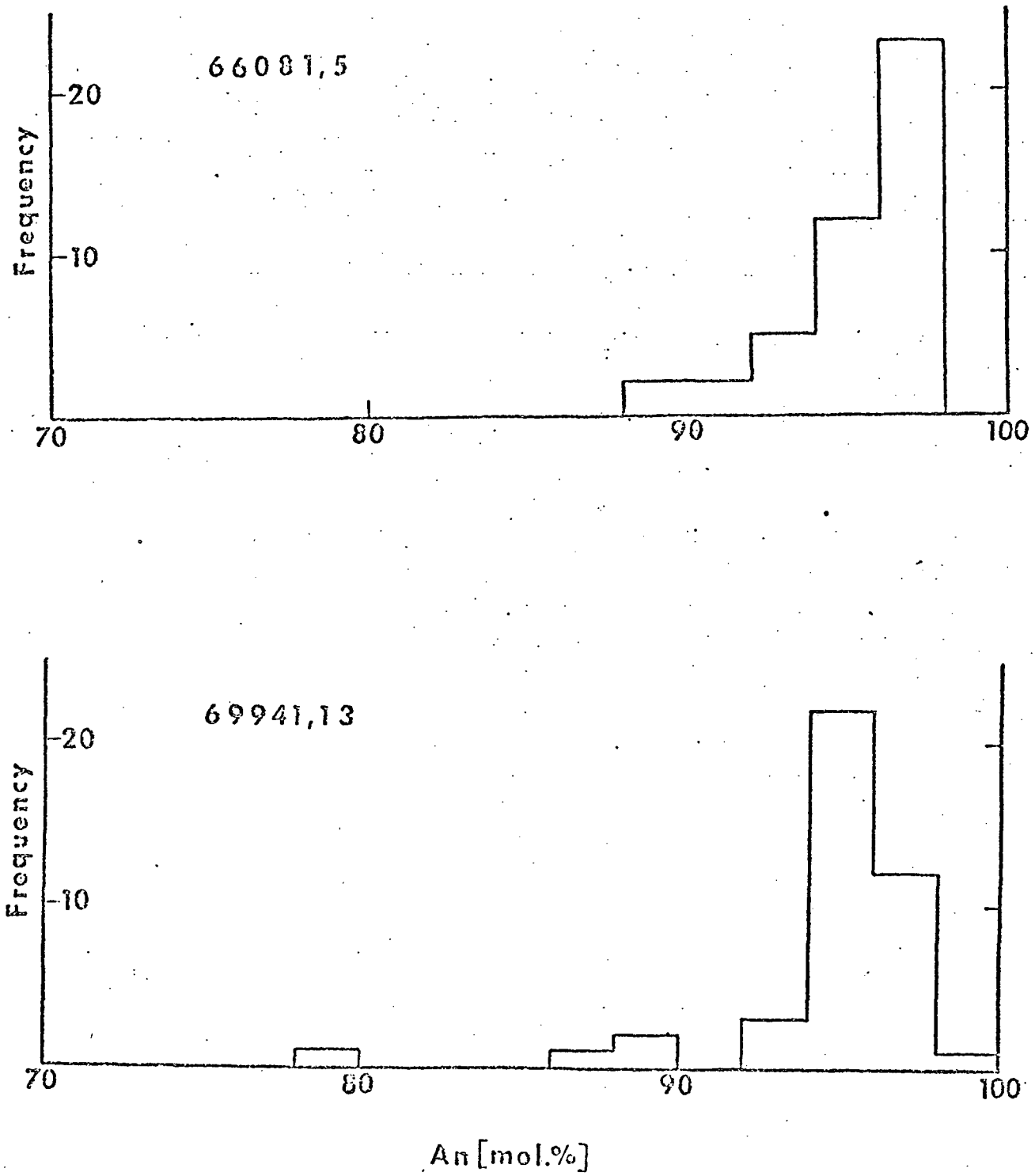
66081,5
Frequency
20
10
70
80
90
100
69941,13
Frequency
20
10
70
80
90
100
An [mol.%]

Fig. 2

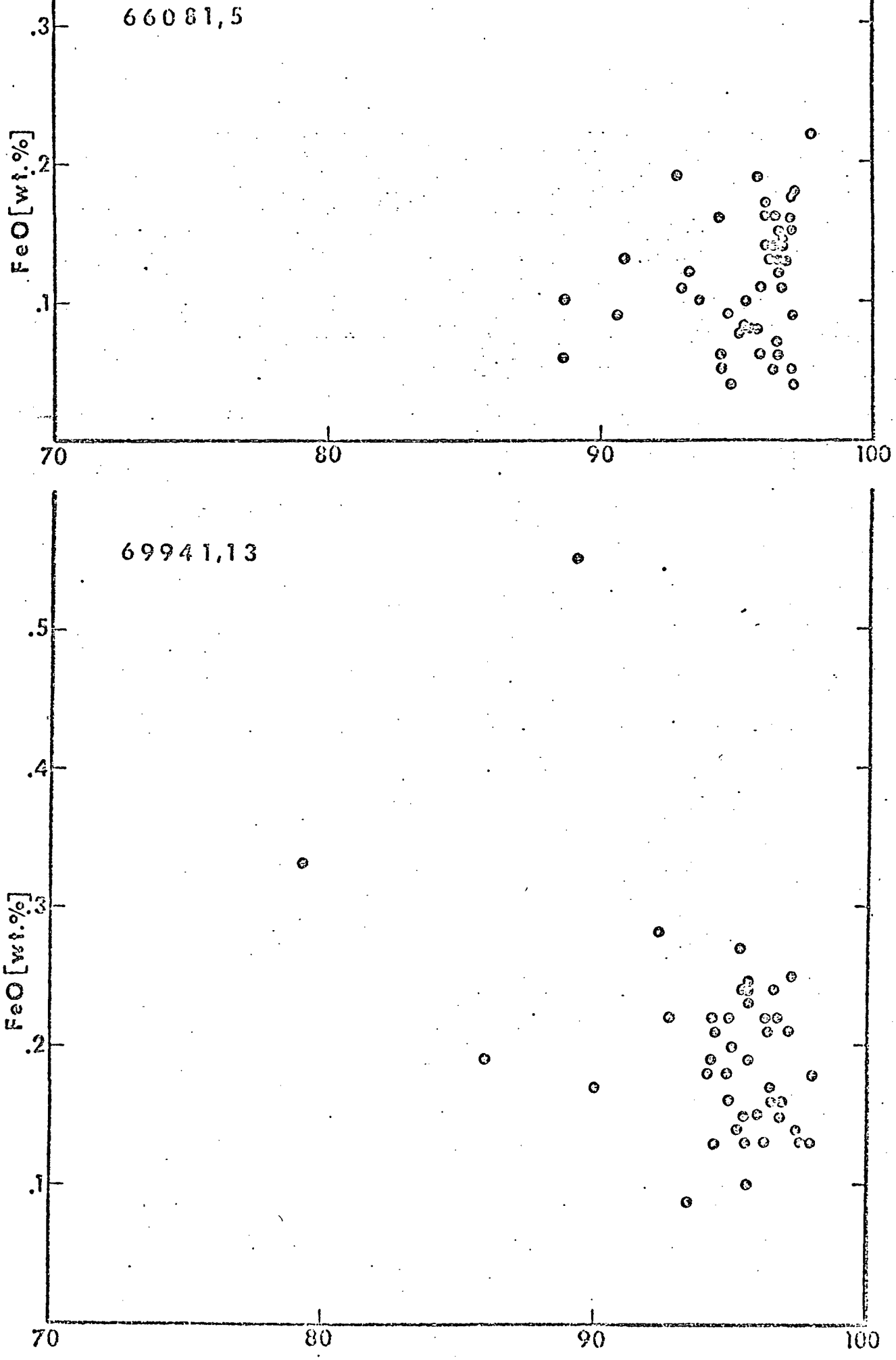

Fig. 3

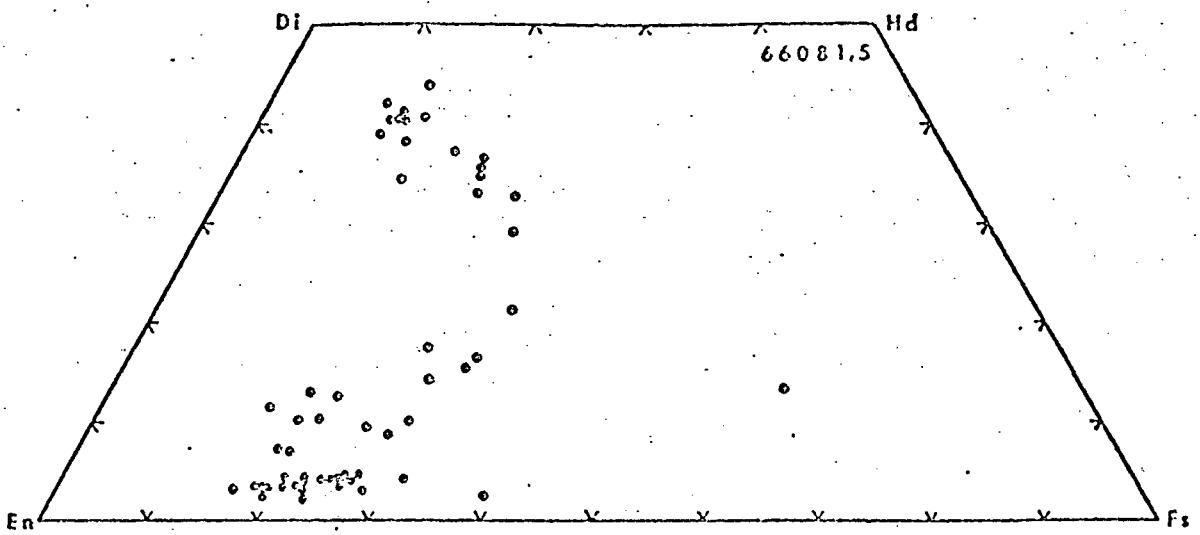

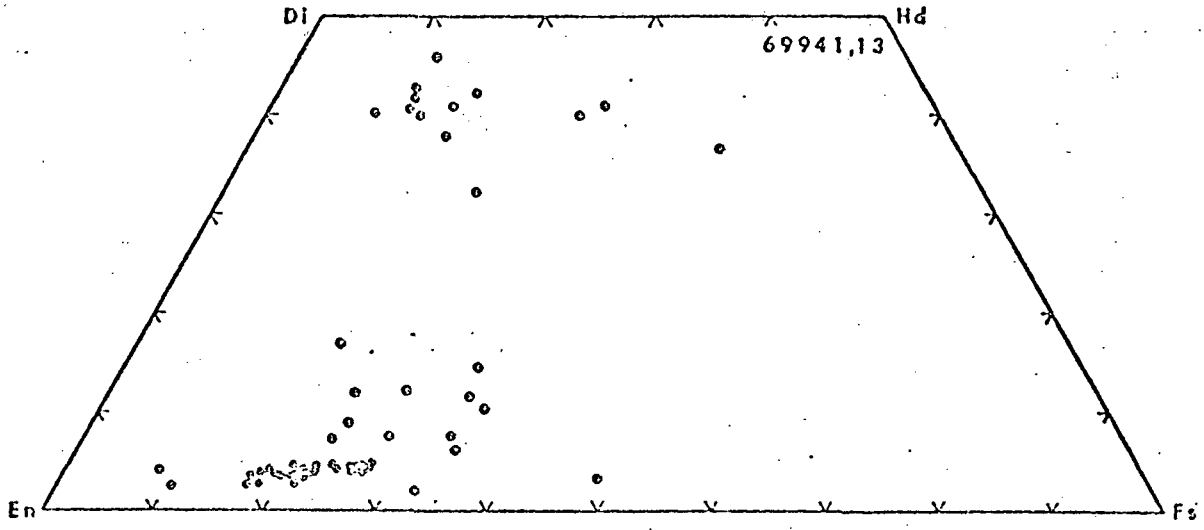

Fig. 4

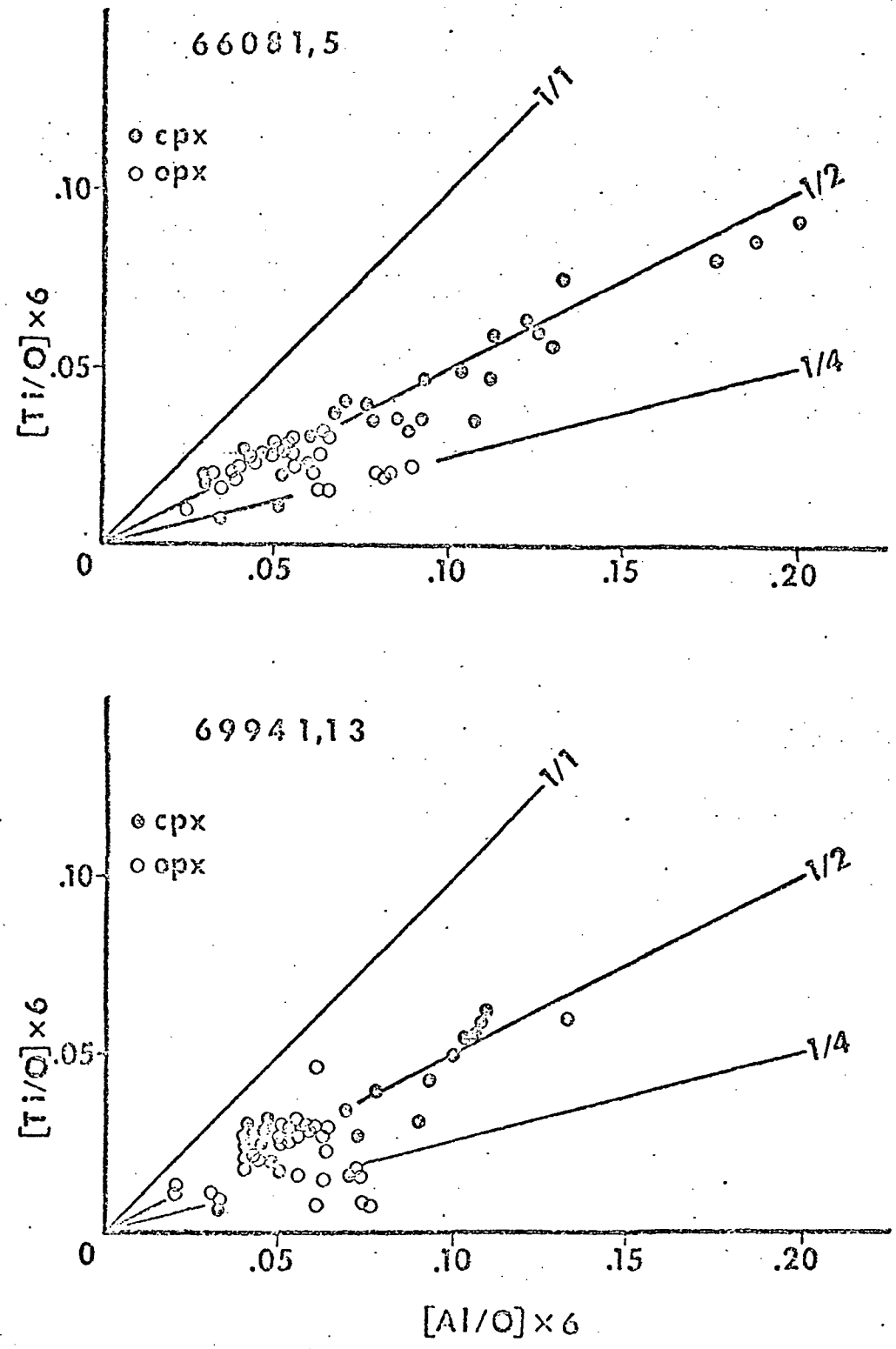
66081,5
cpx
opx
1/1
1/2
1/4
.10
.05
0
[Ti/O]×6
.05
.10
.15
.20
69941,13
cpx
opx
1/1
1/2
1/4
.10
.05
0
[Ti/O]×6
.05
.10
.15
.20
[Al/O]×6

Fig. 5

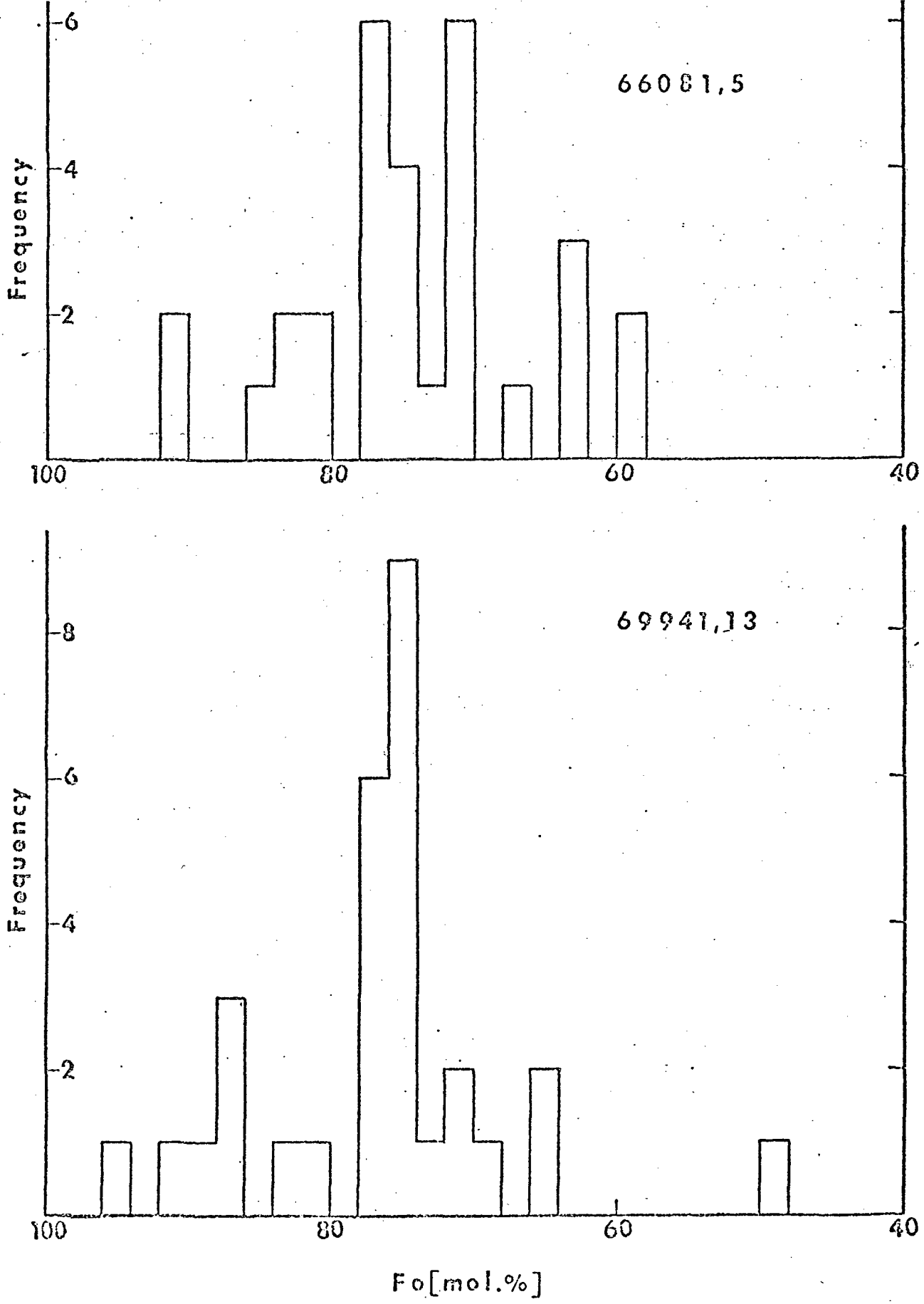

Fig. 6

Morphology and Chemistry of VLS (Vapor-Liquid-Solid)-type of Whisker Structures and other Features on the Surface of Breccia 15015,36

by

James L. Carter

University of Texas at Dallas

P. O. Box 30365

Dallas, Texas 75230

Contribution No. 240, The Institute for Geological Sciences, University of Texas at Dallas, Dallas, Texas 75230.

ABSTRACT

A 62 mm^2 siliceous glass-covered surface of a fragment of breccia 15015 (15015,36) was studied in detail by scanning electron microscope, scanning electron microprobe and energy dispersive techniques. Four types of features were observed: 1) low velocity, hot target-type impacts, 2) out-gassing structures, 3) several types of metallic iron mounds, primarily with a waist of iron sulfide and 4) whisker structures. It is concluded that 1) an irregularly-shaped breccia surface was partially coated with siliceous melt to various depths in an impact-generated hot debris cloud, 2) the siliceous melt coating the breccia was out-gassing while solidifying, 3) there were at least four nucleation events resulting in mounds with average diameters of approximately 45, 19, 10 and 0.2 μm, 4) the whisker structures are of probable VLS (Vapor-Liquid-Solid)-type growth, 5) the sulfur was supplied from an external source such as an impact-generated cloud, 6) the iron was supplied both from an impact-generated cloud and by in situ reduction of the liquid siliceous surface, 7) the lack of hypervelocity-type craters suggests that the siliceous glass coated surface was exposed when cold for only a very short time to either micrometeoritic bombardment or to high velocity projectiles in an impact-generated debris cloud and 8) sample 15015,36 is, thus, from the shielded (probably buried) portion of the rock.

The proposed VLS-type growth on the surface of breccia 15015,36 is the first recognized in nature. It occurs as probable metallic iron stalks with bulbous tips of a mixture of iron and sulfur. The stalks vary from less than 0.015 μm to 0.15 μm in diameter with a length 2 to 10 times bulb diameter. The bulbs vary from less than 0.03 μm to 0.2 μm in diameter. VLS produced metallic iron needles may be the source of some of the hard magnetic component in low-grade breccia. Since probable VLS-type of whisker growth has occurred in an impact situation on the lunar surface, it may have been an important growth mechanism in the early accretionary history of the Earth especially before it acquired an appreciable oxidizing atmosphere.

INTRODUCTION

The morphology and chemistry of surface features including various types of mounds consisting of both metallic iron and mixtures of metallic iron and iron sulfide, and whisker structures on the siliceous glass coating of breccia 15015,36 have been studied by scanning electron microscope (SEM), scanning electron microprobe and energy dispersive X-ray techniques (Carter, 1972) to determine their origin. Breccia 15015 is blocky, angular, largely glass-covered, weighs 4.5 kg and is almost 30 cm long (Apollo 15 Preliminary Science Report, 1972). It was collected approximately 20 m west of the LM + Z footpad and is the third largest rock returned with no other rock of comparable size in the collection area (Apollo 15 Preliminary Science Report, 1972).

SURFACE FEATURES

A 62 mm^2 siliceous glass-covered surface of a fragment of breccia 15015 (15015,36) was coated with approximately 150 Å of gold and selected areas studied in detail (Carter, 1972). A 60X SEM montage of the entire area was made and four types of features observed: 1) impact, 2) out-gassing structures, 3) various types of mounds and 4) patchy areas of relative high electron emission that distort the scanning electron microprobe secondary electron image.

Impact Features

Examination of the 60X SEM montage with a spatial resolution of 3 μm revealed no hypervelocity-type craters. 1.07 mm^2 was scanned at 1,150X with a spatial resolution of 0.2 μm and again no hypervelocity-type craters were observed, but an unusual type of depression (Figs. 1 and 2) reminiscent of craters produced in the heated target experiments (Carter and McKay, 1971)

was observed. The central area of the depression contains clusters of globules from 1 μm to 3 μm in diameter with spherules from 0.1 μm to 0.3 μm in diameter on their surfaces (Figs. 2 and 3). Energy dispersive X-ray analysis reveals major quantities of Si with minor amounts of K, Fe and S, which suggests K-rich siliceous globules with FeS spherules on their surfaces. This is similar to the laboratory produced situation in which spherules, probably of Na-rich silicate composition, occur on pure silica globules (Carter and McKay, 1971) as a result of vaporization and precipitation. Isolated mounds of metallic iron, some of which are rimmed with FeS, also occur. Two additional similar types of low velocity-type impacts were observed of 25 μm and 35 μm in diameter.

Out-gassing Structures

The siliceous glass surface is very frothy or hummocky and consists of a series of large depressions and bumps (blisters) (Carter, 1972). Many of the siliceous bumps are ruptured revealing cavities. Two major areas occur in which large depressions are absent. A view of one such area is shown in Fig. 4 and enlarged in Fig. 5 revealing a wrinkled and convoluted surface with numerous siliceous droplets of the same composition as the substrate. The droplets reveal a wide degree of wetting of the substrate. These droplets are not present on the siliceous glass surface outside of these areas. The diameter of the depressions in the wrinkled areas are less than for the overall surface (Fig. 6). The smaller depressions in the collapse areas result from the higher viscosity of the partially solidified siliceous melt and the rounding of the broken edges of the burst bubbles due to surface tension.

The breccia substrate next to the siliceous glass coating is very porous, with the volume of a pore decreasing away from the siliceous glass coating. This suggests that the siliceous melt heated the underlying breccia surface to the point of mobilization of trapped gases.

Mounds

The surface of the siliceous glass has numerous clusters of various types of iron-rich, nickel-poor mounds. The nickel contents measured by energy dispersive techniques generally ranged from approximately 0.2 wt. % to 1 wt. %, with a maximum of 2.5 wt. %. One such cluster is shown in Fig. 1. The larger mounds are primarily concentrated on the sides of low ridges with mound size decreasing towards a depression. This suggests that material from a vapor was deposited on the "high" areas and, due to diffusion and migration of it along the surface, mound growth took place there. The larger mounds consist of a central area of metallic iron or, less commonly, mixtures of metallic iron and iron sulfide surrounded by a waist of iron sulfide (Fig. 7). The iron sulfide incompletely wets the mound. Many of the smaller mounds are not circular in plan view but have subhedral outlines (Fig. 7). This is similar to small metallic iron mounds formed by reduction with hydrogen (Carter and McKay, 1972).

A 1,150X SEM montage of the 0.47 mm^2 area shown in Fig. 1 revealed that the siliceous glass surface is covered with mounds over approximately 25% to 30% of its surface with a distribution as shown in Fig. 1. The area immediately surrounding the larger mounds is devoid of smaller mounds. The area depleted in smaller mounds is elliptical, not circular in plan view, suggesting longitudional migration of material on a liquid siliceous surface. A histogram of the percentage of surface area covered by the various sizes of mounds is shown in Fig. 8. A histogram of the number of mounds versus mound diameter, Fig. 9, reveals that the number of mounds rapidly decreases

with an increase in mound diameter. All mounds larger than 0.5 μm in diameter were measured over the entire 1,150X montage. The number of mounds smaller than 0.5 μm in diameter was established from a measurement at 11,500X, with a spatial resolution of 0.02 μm, of 45 μm^2, which gave approximately 2×10^7 mounds greater than 0.4 μm in diameter and less than 0.5 μm in diameter per square millimeter of the siliceous glass surface. A plot of the volume of material in a mound, assuming a sphere for the shape of a mound, reveals that there are four main groupings (Fig. 10) suggesting at least four nucleation events resulting in mounds with average diameters of approximately 45, 19, 10 and 0.2 μm.

The mounds less than 4 μm in diameter are predominately metallic iron, whereas those larger than 12 μm in diameter are entirely a mixture of iron sulfide and metallic iron. In the case of dimples for which the mounds are absent the adherance of fragments of iron sulfide to the surface of the dimples (Carter, 1972) suggests that the original mounds were probably mixtures of iron sulfide and metallic iron (see also Carter and MacGregor, 1970; Carter, 1971; Carter and McKay, 1972). The close correspondence of the size of the dimples to the size of the metallic iron and iron sulfide mounds as shown in Fig. 10 also suggests that the dimples originally contained mounds of this composition. With the exception of the larger dimples and those near the left margin of the sample, which probably resulted from the stress of breaking the sample, the dimples are concentrated around a low velocity-type impact crater.

An interesting feature of the siliceous glass surface of breccia 15015 is the concentration of irregular or amoeboid-shaped mounds around "hills" of silicate minerals (Figs. 1 and 11; Carter, 1973; Carter and Crosthwait, 1973). It is speculated that the relatively cooler silicate mineral "hills"

effectively quenched the growth process of these mounds. Thus there was not sufficient heat to allow the material to coalesce into a sphere by surface tension. This may also explain the paucity of small mounds near the silicate mineral "hills".

Patches of High Electron Emission

Intermingled with the mounds are peculiar patches of high electron emission that range from 0.4 μm to 400 μm in longest dimension (Figs. 1 and 11 to 15) that distort the scanning electron microprobe secondary electron image (Carter, 1972). This is probably an electrical phenomena ("charging") because the amount of distortion is directly proportional to beam current.

Investigation of these patches by means of montages and stereoscopic SEM photographs reveals that they occur on "high" areas on the glass siliceous surface (Figs. 1, 11 and 12), on the surface of minerals that protrude through the siliceous glass surface (Figs. 13 and 14) and on the surface of irregularly-shaped metallic iron mounds that surround the mineral "islands" (Fig. 11). They do not occur on the surface of the intervening siliceous glass. The "high" areas are surface expressions of high points on the rock substrate that were covered by a thin layer of siliceous melt which quenched faster than the thicker areas of melt. Examination of a patch at high magnification (Figs. 15, 16) (see also Carter and Crosthwait, 1973; Carter, 1973) reveals that they are composed of a series of stalks with bulbs on 0.2 μm in diameter, and the stalks vary from less than 0.015 μm to 0.15 μm in diameter. Stalk length varies from 2 to 10 times bulb diameter. The iron stalks are thus either single domain or pseudo-single domain due to shape anisotropy.

From the scanning electron microprobe and energy dispersive X-ray data, the bulbs are probably a mixture of iron and sulfur, whereas the

stalks are metallic iron possibly with Si in solid solution (?). Because of the extremely small size of the whisker structures in a patch, the exact nature of their chemistry could not be determined. Stripping the energy dispersive X-ray sweep data obtained from the silicate host neighboring a patch from the energy dispersive X-ray sweep data obtained on a patch revealed excess Si in a patch.

The chemical data and the morphological relationships are consistent with the stalks and bulbs being the result of a VLS (Vapor-Liquid-Solid)-type of growth mechanism operating in the lunar environment during an impact event. This type of growth mechanism involving vapor, liquid and solid phases was proposed by Wagner and Ellis (1965) to explain many observations on the effect of impurities in crystal growth from a vapor in laboratory experiments. They showed that the role of the impurities is to form a liquid solution with the crystalline material to be grown from the vapor. They also showed that as a liquid has a large surface of accommodation, it will preferentially incorporate elements from the vapor state. When the liquid becomes supersaturated growth would occur at the solid-liquid interface resulting in elevation of the liquid alloy droplet from the substrate atop the growing solid whisker crystal. Material precipitating from the droplet is replenished from the vapor phase during growth of the whisker from the droplet. Whiskers formed in this way are usually of very pure composition and structure. Since metallic iron has no solid solution with sulfur, iron will precipitate from a melt consisting of various proportions of sulfur and iron as metallic iron over a wide range of temperatures.

CONCLUSIONS

The data presented suggest that the following conclusions and inferences may be drawn about the surface of breccia fragment 15015,36.

1) An irregularly-shaped breccia surface was partially coated with siliceous melt of varying thickness. Some minerals protruded through the melt, and thin areas of melt and melt surrounding the mineral "islands" quenched faster than the thicker areas of melt. The siliceous melt contained dissolved gases or it mobilized the gases from the breccia substrate during heating, which resulted in vesiculation of the solidifying siliceous melt. Some gas bubbles broke through the surface spraying minute droplets of siliceous melt onto the already partially solidified crust (still capable of plastic deformation). The surface expression of the collapse of large bubbles is seen as wrinkled areas (Figs. 4 and 5), with relatively small depressions (Figs. 5 and 6).

2) The lack of hypervelocity-type craters suggests that the glass coated surface of breccia 15015,36 was a) exposed when cold for only a very short time, if at all, to either bombardment by micrometeroids or high velocity projectiles in impact-generated debris clouds and b) from the shielded (probably buried) portion of the rock. The presence of low velocity-type impacts (Figs. 1 and 2) that are reminiscent of impacts into heated targets (Carter and McKay, 1971) suggests that this surface was in an impact-generated hot debris cloud.

3) The mounds consisting of metallic iron and mixtures of metallic iron and iron sulfide do not represent splashes but were grown on the liquid siliceous surface, with the larger mounds growing at the expense of the smaller mounds. There were at least four nucleation events resulting in mounds with average diameters of approximately 45, 19, 10 and 0.2 μm. The sulfur was supplied from an external source such as an impact-generated cloud, and the iron was supplied both from an impact-generated cloud and by in situ reduction of the liquid siliceous surface (Figs. 8 to 10; Carter and McKay, 1972).

4) The proposed VLS-type growth (whisker structures) on the surface of lunar rock 15015,36 is the first recognized in nature. Since the metallic iron stalks are either single domain or pseudo-single domain, due to shape anisotropy, they may affect strongly the magnetic properties of this rock and contribute to its hard magnetic component (Dunlop, 1973). VLS-type growth may be very common on fragments in the lunar soil that have been exposed to an impact-generated cloud, and especially common as individual needles in the less than 1 μm size fraction of the soil because micrometeoritic bombardment of the surfaces of materials with VLS-type growth on them would cause dislogement of needles. Low-grade metamorphic breccia produced from this soil would then contain metallic iron needles of single or pseudo-single domain type.

5) Since probable VLS-type growth has occurred in an impact situation on the lunar surface, it may have been an important growth mechanism in the early accretionary history of the Earth especially before it acquired an appreciable oxidizing atmosphere, and in other planetary situations.

ACKNOWLEDGEMENTS

Supported by NASA Grant NGR-44-004-116. I thank J. B. Toney for technical assistance. I thank D. L. Crosthwait, Jr. of Texas Instruments, Inc. of Dallas, Texas for taking the SEM (Cambridge MK IIA) photographs shown in Figs. 3 and 4, for introducing me to the concept of VLS growth and for suggesting that the patches on the surface of breccia 15015,36 could be the result of VLS-type growth. I thank D. S. McKay of the Lyndon Baines Johnson Space Center, Houston, Texas for taking the SEM (JEOLCO U3) photographs shown in Figs. 12 and 16. J. C. Butler and D. S. McKay have contributed to the improvement of the manuscript.

REFERENCES

Apollo 15 Preliminary Science Report (1972) National Aeronautics and Space Administration, Washington, D. C., NASA SP-289, p. 5-49.

Carter, J. L. (1972) Morphology and chemistry of glass surface of breccia 15015,36. In "The Apollo 15 Lunar Samples" (editors J. W. Chamberlain and C. Watkins) pp. 51-53, Lunar Science Institute, Houston.

Carter, J. L. (1973) VLS (Vapor-Liquid-Solid): A newly discovered growth mechanism on the lunar surface? Submitted to Science.

Carter, J. L. and Crosthwait, Jr., D. L. (1973) Vapor-Liquid-Solid whisker growth on lunar breccia 15015 (abstract). Submitted to Electron Microscopy Soc. of America.

Carter, J. L. and MacGregor, I. D. (1970) Mineralogy, petrology and surface features of some Apollo 11 samples. "Proc. Apollo 11 Lunar Sci. Conf., Geochim. Cosmochim. Acta" Suppl. 1, Vol. 1, pp. 247-275. Pergamon.

Carter, J. L. and McKay, D. S. (1971) Influence of target temperature on crater morphology and implications on the origin of craters on lunar glass spheres. "Proc. Second Lunar Sci. Conf., Geochim. Cosmochim Acta" Suppl. 2, Vol. 3, pp. 2653-2670. MIT Press.

Carter, J. L. and McKay, D. S. (1972) Metallic mounds produced by reduction of material of simulated lunar composition and implications on the origin of metallic mounds on lunar glasses. "Proc. Third Lunar Sci. Conf., Geochim. Cosmochim. Acta" Suppl. 3, Vol. 1, pp. 953-970. MIT Press.

Dunlop, D. J. (1973) The metallic iron content of Breccia 14313. In "Lunar Science IV" (editors J. W. Chamberlain and C. Watkins) p. 193, Lunar Science Institute, Houston.

Wagner, R. S. and Ellis, W. C. (1965) The Vapor-Liquid-Solid mechanism of crystal growth and its application to silicon. Trans. Met. Soc. AIME, Vol. 233, pp. 1053-1064.

FIGURE CAPTIONS

Fig. 1. SEM photograph of surface of breccia 15015,36 showing relationship of various types of mounds, dimples and an impact feature (lower right).

Fig. 2. Enlarged SEM view of impact feature in lower right of Fig. 1. Bottom of crater is lined with K-rich siliceous globules.

Fig. 3. Enlarged view of central area of Fig. 2. Surfaces of K-rich globules are covered with FeS spherules from 0.1 μm to 0.3 μm in diameter.

Fig. 4. SEM photograph of a collapsed area on surface of breccia 15015,36.

Fig. 5. Enlarged view of the central area of Fig. 4 showing details of collapsed structure. Droplets in central area of photograph are of same composition as siliceous glass substrate.

Fig. 6. Histogram showing number of depressions (holes) versus depression (hole) diameter in μm on various features.

Fig. 7. Enlarged SEM view of typical metallic iron mound with FeS rim.

Fig. 8. Histogram showing relationship of mound diameter in μm to % of total surface area covered.

Fig. 9. Histogram showing number of mounds versus mound diameter in μm.

Fig. 10. Histogram showing relationship of mound diameter in μm to total volume of mound in μm^3.

Fig. 11. SEM view of irregularly-shaped metallic iron mounds around base of silicate mineral "island". Probable VLS-type whisker growth occurs on surface of irregularly-shaped metallic iron mounds and on "high" areas (upper right). Note absence of small mounds around irregularly-shaped mounds.

Fig. 12. SEM view of high electron emission patches intermingled with iron-rich mounds. Patches are composed of whisker structures of probable VLS-type growth.

Fig. 13. SEM view showing relationship of probable VLS-type of whisker growth on "high" areas and mineral "islands" to larger metallic iron mounds with FeS rims.

Fig. 14. SEM view showing probable VLS-type of whisker growth only on surface of silicate mineral "islands".

Fig. 15. Enlarged SEM view of edge of patch of probable VLS-type of whisker growth showing stalk structure.

Fig. 16. Enlarged SEM view of probable VLS-type of whisker growth showing nature of metallic iron stalks with bulbous tips composed of iron and sulfur.

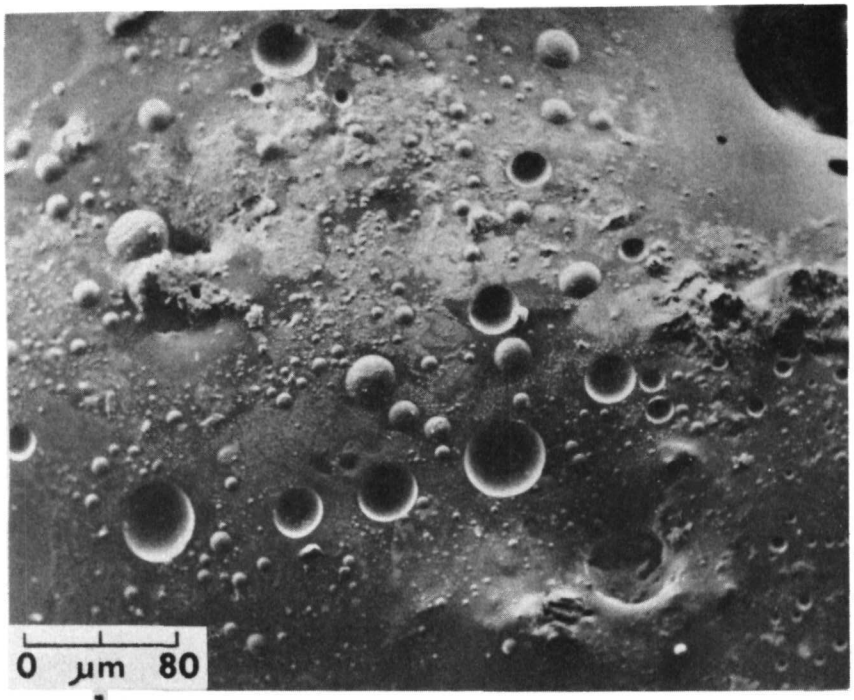

1

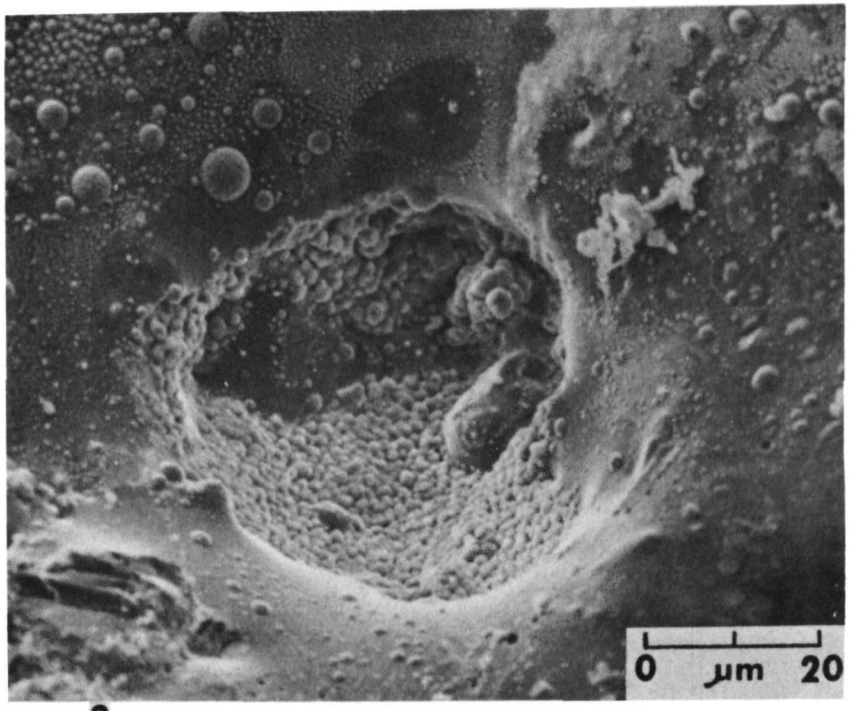

2

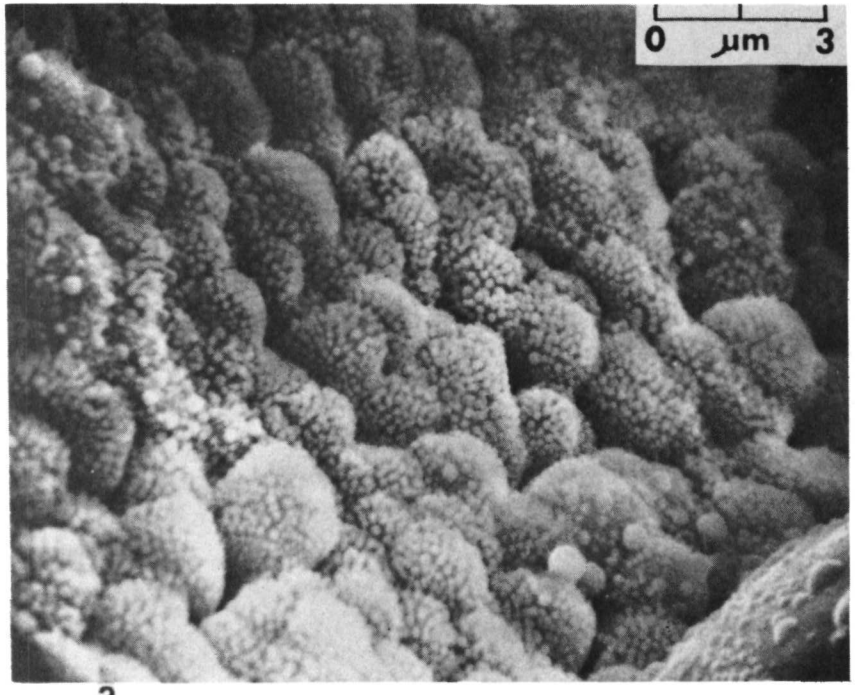

3

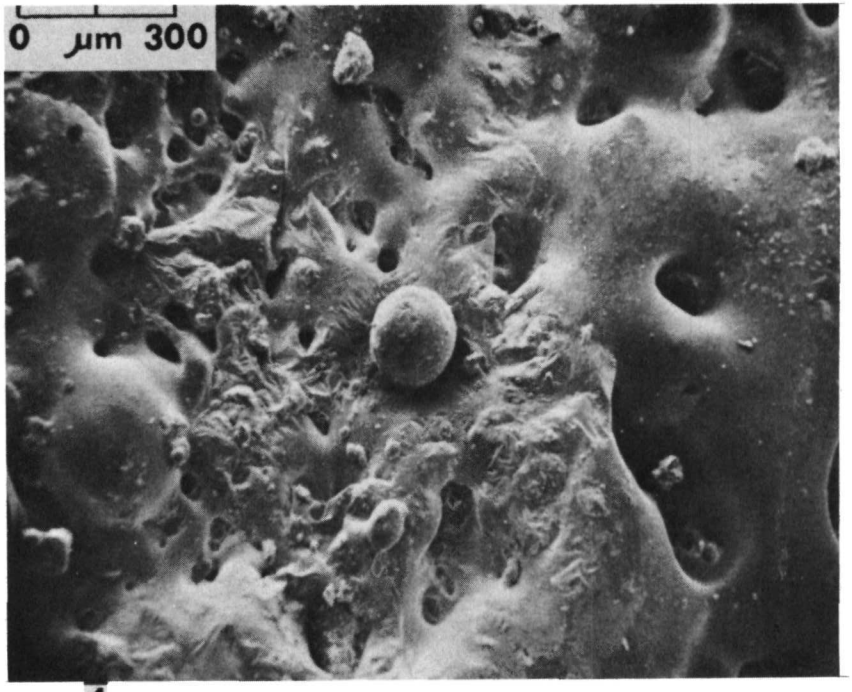

4

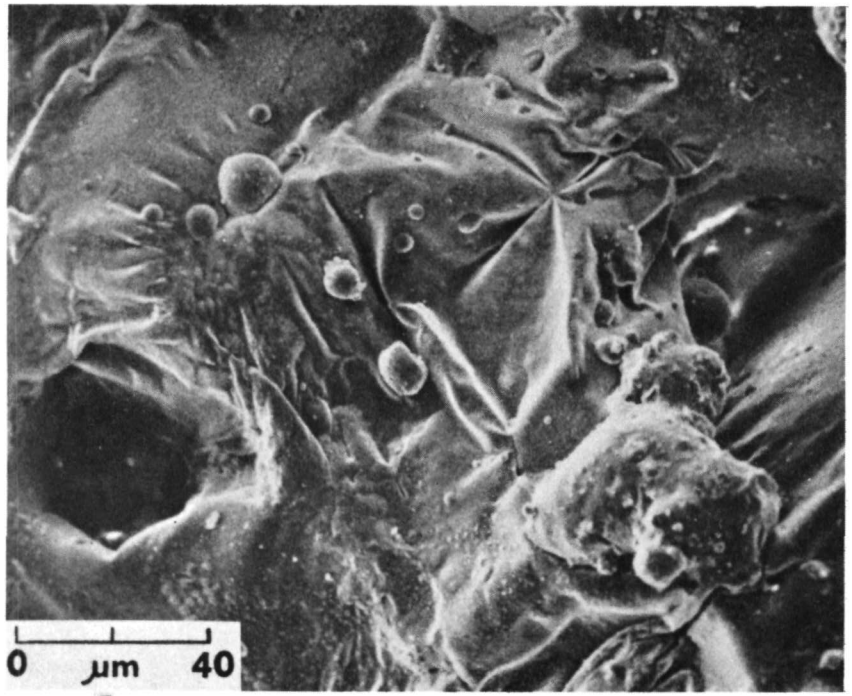
0 μm 40

5

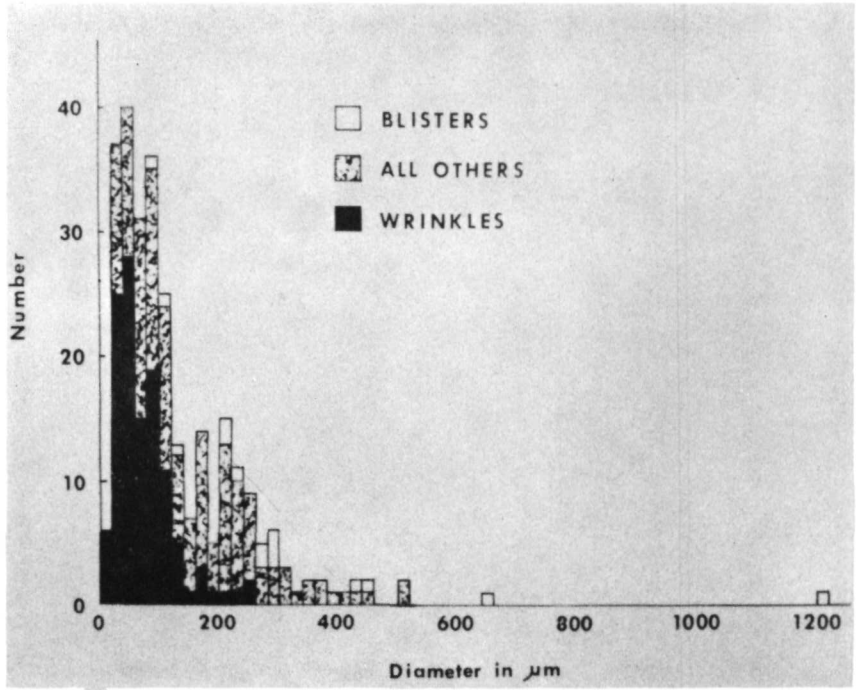
BLISTERS
ALL OTHERS
WRINKLES
Number
0
10
20
30
40
0
200
400
600
800
1000
1200
Diameter in μm

6

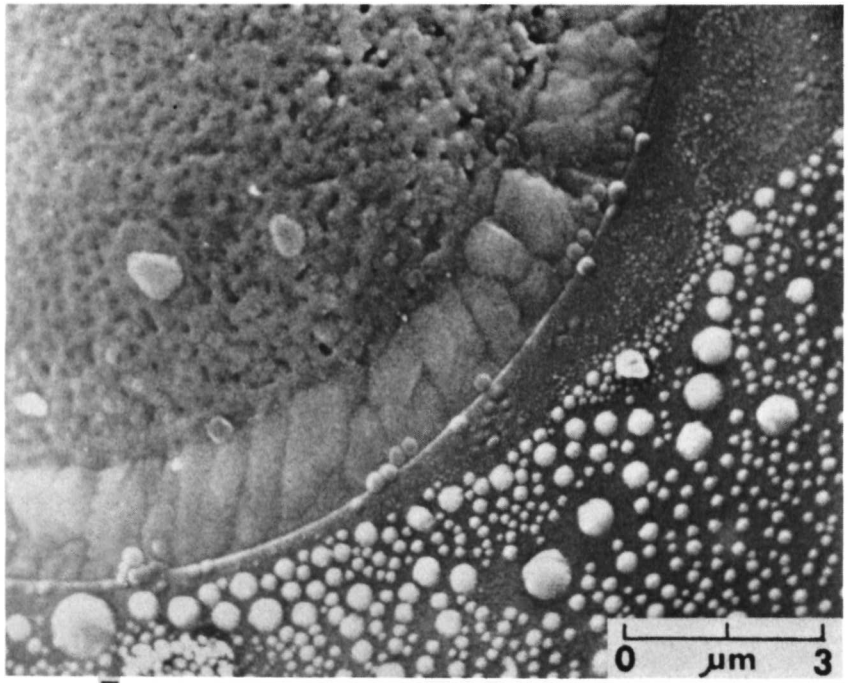
0 μm 3

7

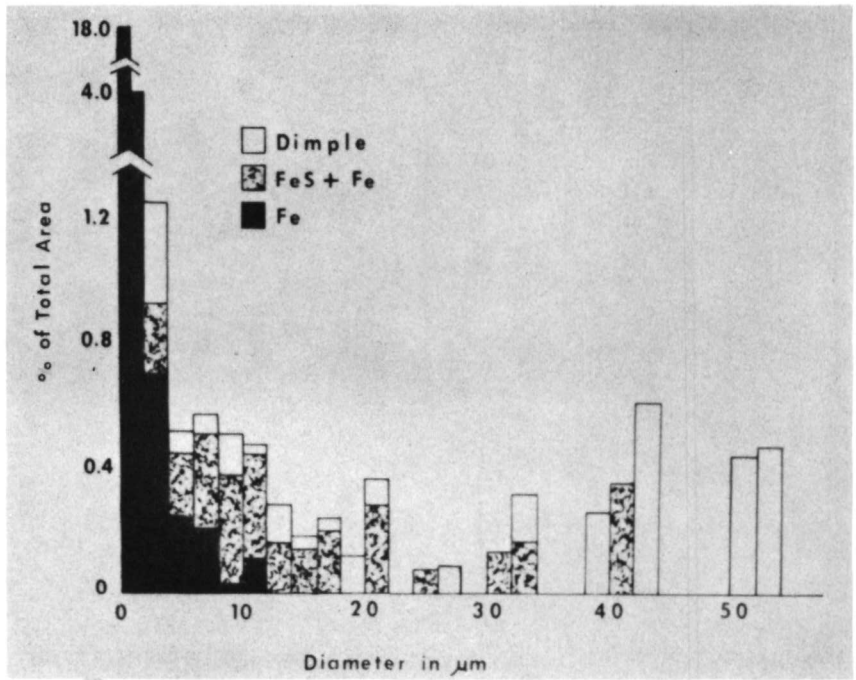
Dimple
FeS + Fe
Fe
% of Total Area
18.0
4.0
1.2
0.8
0.4
0
0
10
20
30
40
50
Diameter in μm

8

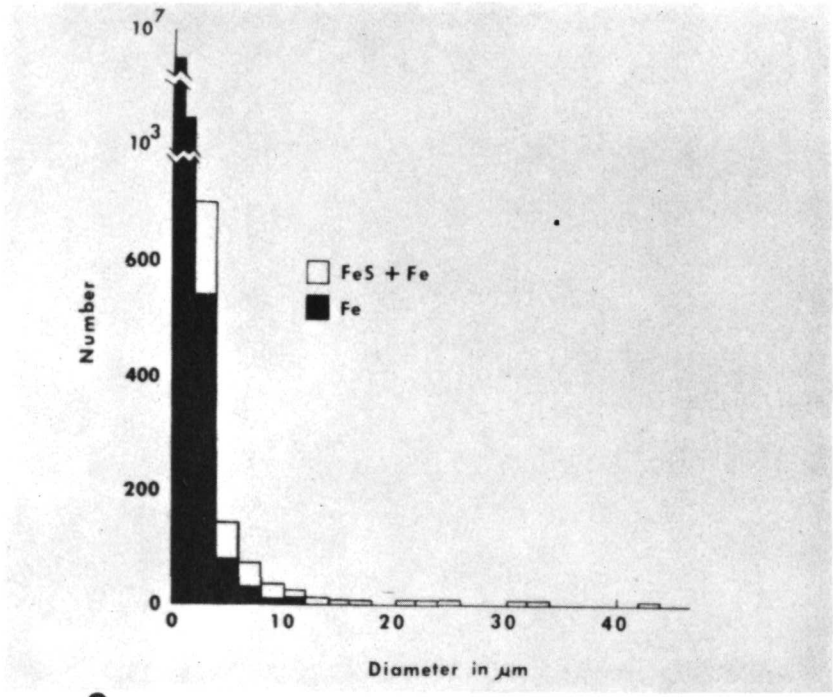
10^7
10^3
600
400
200
0
Number
FeS + Fe
Fe
0
10
20
30
40
Diameter in μm

9

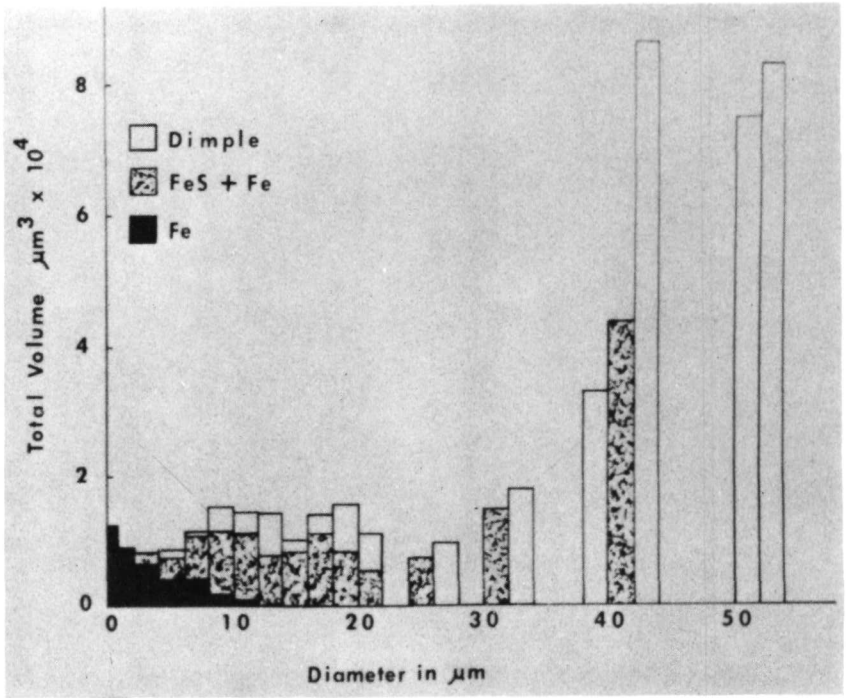
8
6
4
2
0
Total Volume μm^3 x 10^4
Dimple
FeS + Fe
Fe
0
10
20
30
40
50
Diameter in μm

10

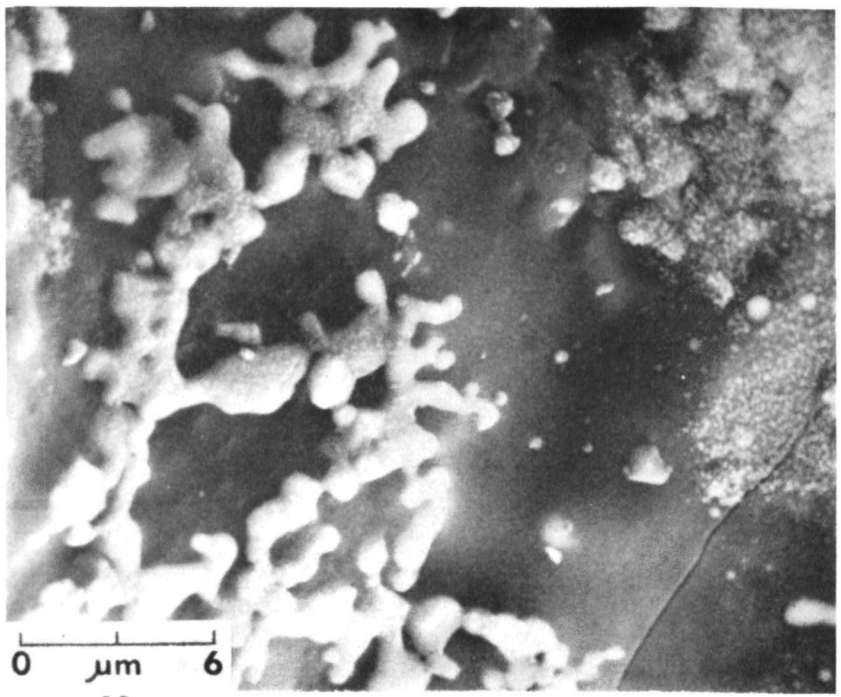
0 μm 6

11

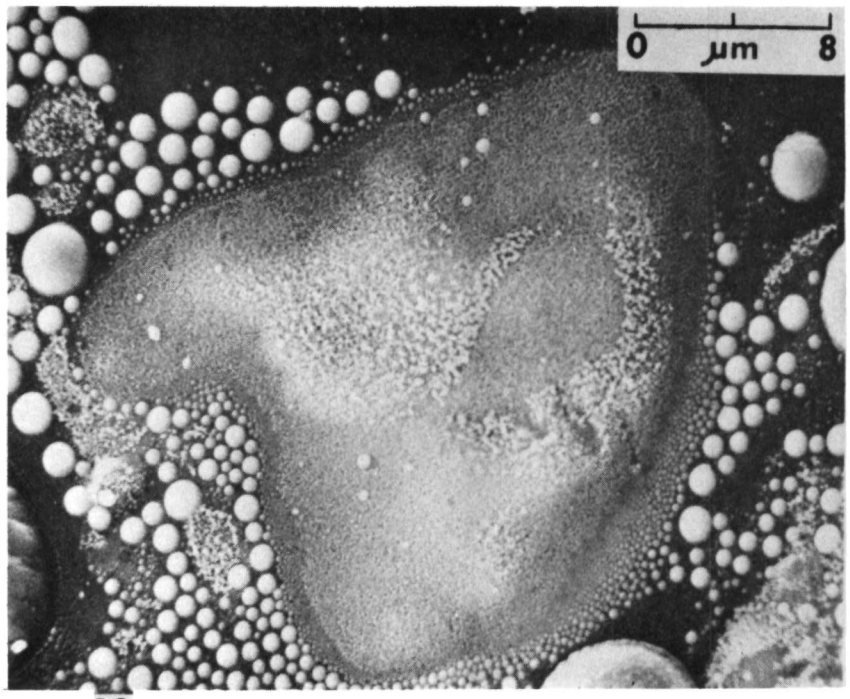
0 μm 8

12

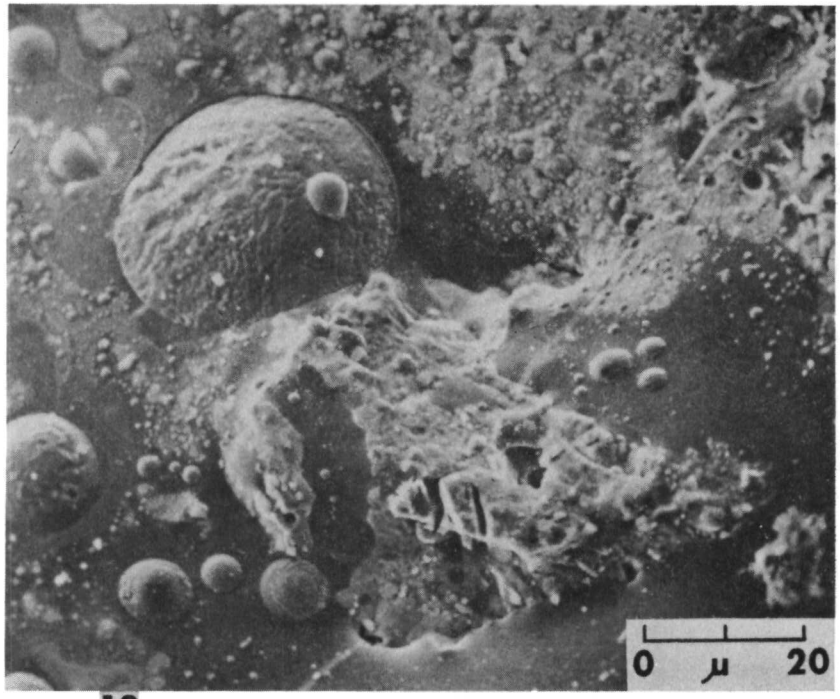

13

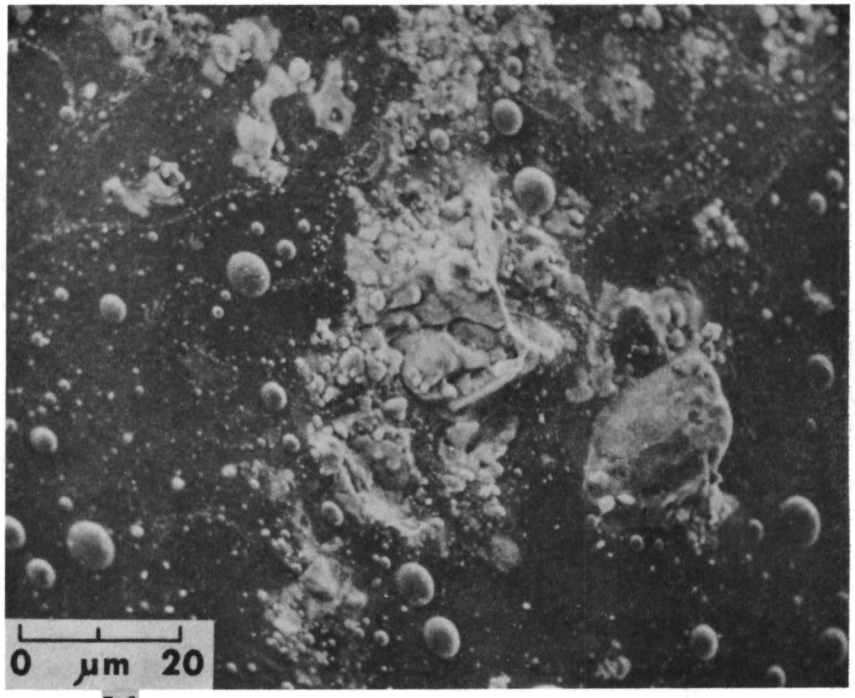

14

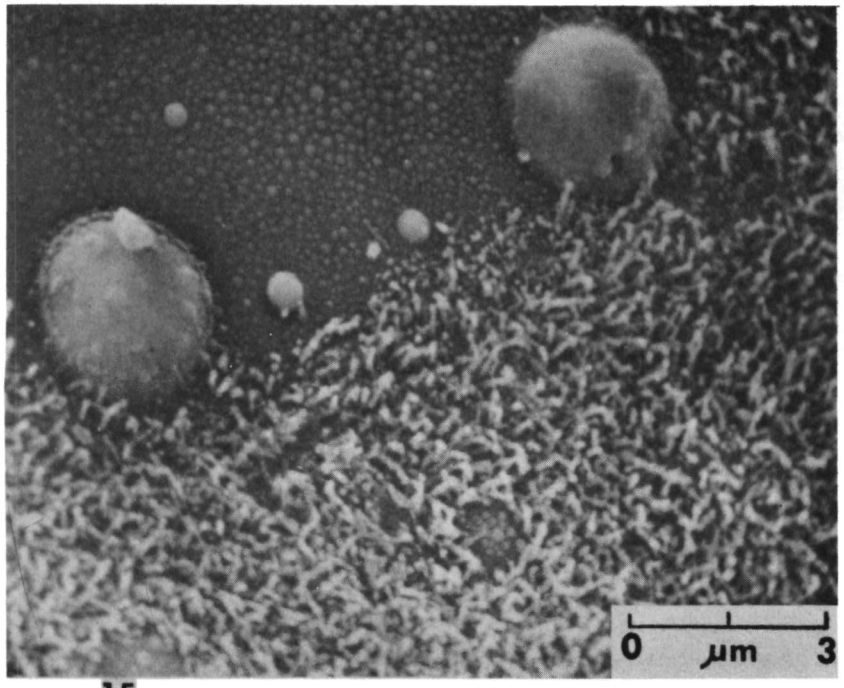

15

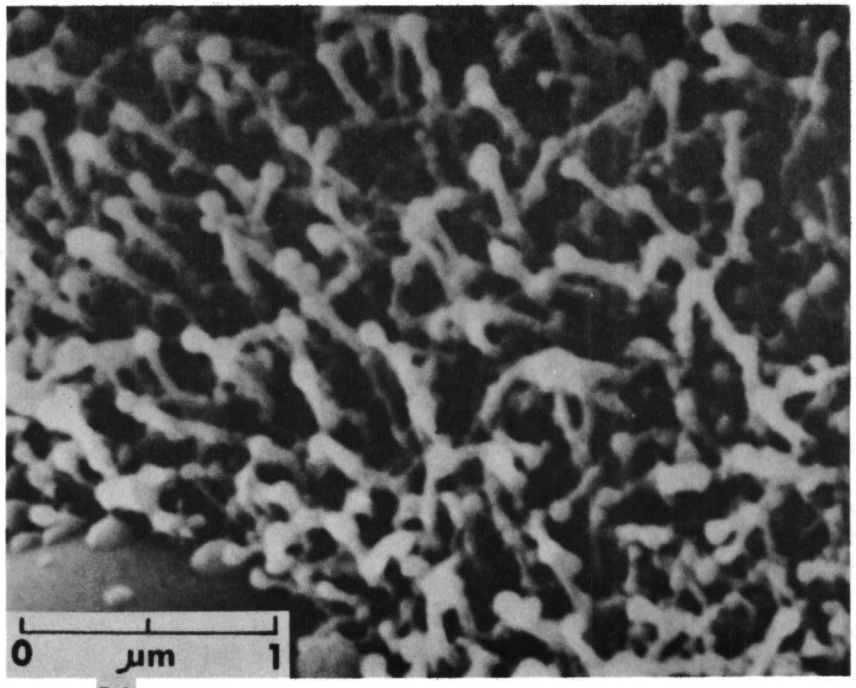

16

American Geophysical Union
2100 Pennsylvania Avenue, N.W.
Washington, D.C. 20037 U.S.A.

Abstract form for Spring 1973 Annual Meeting

Submitted to Section (Sub-Section) of volcanol., geochem., & petrol.

Unusual Particles in Apollo 16 Soils. Particles from four soil localities (62241.14, 66041.11, 68841.11, 69941.13) were examined using optical, scanning electron microscope, electron microprobe and energy dispersive techniques. Dark ray material from South Ray Crater contain two unusual types of particles. One type consists of reddish colored metallic objects in contact with olivine and feldspar. Their surfaces consist of interlocking crystals of iron with 5 wt. % nickel, minor patches of iron sulfide and phosphide. Some of the surfaces contain a crystalline ruby-red, transparent, goethite-like reaction product with minor chlorine. This material also occurs between the metal and silicate contact. The second type consists of silicate spheres with structurally continuous hemispheres or spherules attached to their surfaces, which are composed of a network of interlocking feldspar crystals and iron spherules in glass that is reminiscent of quench textures. A volcanic hypothesis is suggested for these spheres because of the apparent homogeneity of the original silicate melt (approx. ANT in composition), the similarity of composition between individual spheres, the presence of FeS and metallic iron with less than 1 wt. % nickel and the general lack of agglomerated surface debris.

Elaine R. Padovani
James L. Carter
Inst. for Geological Sciences, Univ. Texas at Dallas, P. O. Box 30365, Dallas, Texas 75230

VLS (Vapor-Liquid-Solid) growth on the surface of rock 15015. The surface of glass-coated breccia sample 15015,36 contains numerous metallic iron mounds less than 4 μm in diameter and complex mixtures of metallic iron and iron sulfide mounds up to 60 μm in diameter, and peculiar patches ranging from 0.4 to 400 μm in longest dimension that distort the electron beam as it passes over a patch. This suggests that this is an electrical or magnetic phenomena. The patches occur on "high" areas on the glass silicate surface and especially on the surfaces of minerals that protrude through the glass surface. The patches are composed of a series of stalks with bulbs on their tops. The bulbs vary from less than 0.03 to 0.2 μm in diameter and the stalks vary from less than 0.015 to 0.15 μm in diameter. Stalk length varies from 2 to 10 times bulb diameter. From electron microprobe and energy dispersive X-ray data, the bulbs may be FeS and the stalks metallic Fe. These data suggest that the stalks and bulbs are natural consequences of a VLS growth mechanism operating in the lunar environment. Since a liquid has a large surface of accommodation, it will preferentially incorporate vapor and growth from a supersaturated liquid would occur at the liquid-solid interface resulting in whisker growth. Since the metallic iron stalks are either single domain or pseudo-single domain due to shape anisotropy, they are likely to strongly affect the magnetic properties of this rock.

James L. Carter
The Inst. for Geological Sciences, The Univ. of Texas at Dallas, P. O. Box 30365, Dallas, Texas 75230.